THE SOLUTION OF PARTIAL DIFFERENTIAL EQUATIONS BY MEANS OF ELECTRICAL NETWORKS

Thesis by

Richard H. MacNeal

In Partial Fulfillment of the Requirements

For the Degree of

Doctor of Philosophy

California Institute of Technology

Pasadena, California

1949

ACKNOWLEDGMENTS

The subject to which this thesis is devoted is one for which a large and growing literature exists. For the benefit of those who are unfamiliar with this literature it has been necessary to include a large amount of background material for some of which it has been impossible to give specific acknowledgment.

The author has relied heavily on R. V. Southwell's Relaxation Methods in Theoretical Physics for an exposition of finite difference methods. The publications of Gabriel Kron, particularly his articles on the equivalent circuits of Maxwell's equations, have been very helpful. Specific acknowledgment is given in the footnotes for the ideas of others when these could be attributed to a definite source. The idea for the dynamic beam analogy was originated by G. D. McCann and H. E. Criner.

The experimental data on beam and plate problems was obtained as part of official Analysis Laboratory projects in collaboration with Dr. G. D. McCann, Dr. C. H. Wilts and other members of the Analysis Laboratory staff. The author is deeply indebted for their cooperation and also for the use of the Computor on the electromagnetic field problems, which were not official projects.

The author acknowledges a very great debt to his wife, Carolyn, who assisted him in the preparation of the manuscript and to Dorothy Denhard who prepared all the curves.

ABSTRACT

The material in this thesis is the result of a year's experience in the solution of problems on the Cal Tech Electric Analog Computor. Although much work has been done elsewhere, the solution of partial differential equations is a relatively new field for the Cal Tech Computor. It is natural that such an undertaking should initiate points of view and techniques that differ from those of other investigators. This thesis contains the development of certain ideas that have been useful to the author in the solution of problems on the computor.

In Part I, finite difference methods are treated with reference to problems with one space variable. Techniques are developed for the representation of differential operators by means of electrical networks and the question of unequal lumping is discussed.

The solutions of the fourth order differential equations of a beam are treated in Part II. Such practical considerations as the effects of parasitic impedances and cell size are investigated. Solutions are presented for the normal modes of a cantilever beam, the transient vibration of a cantilever beam and the coupled modes of vibration of an airplane wing.

Problems involving the scalar Laplacian operator are treated in Part III. A general asymmetric network is developed that is useful for problems with irregular boundaries and for problems where it is desired to have variable cell size. These techniques are illustrated with respect to a cavity resonator problem and an electromagnetic radiation problem.

Elastic plate problems are treated in Part IV. The analogy for the elastic plate is an extension of the beam analogy to two dimensions. Here the difficult problems are those relating to the representation of boundary conditions, particularly of boundary conditions along an irregular edge.

Some conclusions regarding the construction of a network analyzer designed specifically for the solution of partial differential equations are given in Part V. The chief conclusion is that such a computor must contain a much larger number of electrical elements than are at present available in the Cal Tech Computor.

TABLE OF CONTENTS

PREFACE

The subject of this thesis is the application of electrical networks to the solution of partial differential equations. There is no intention to imply that all of the important types of partial differential equations of mathematical physics together with their network analogues will be found here. The emphasis is rather upon methods and techniques that have a wider application than the equations that have been chosen for investigation.

Only linear partial differential equations having not more than two space dimensions have been considered in this thesis. This type of equation lends itself more satisfactorily than any other to solution by means of electrical networks.

It is impractical to construct a network analyzer for the solution of problems with three space dimensions because an excessive number of elements would be required. For example, a cubical network with only ten cells on a side would contain 3000 impedance elements. Furthermore it is not practical to solve problems that cannot be represented by bilateral impedance elements (e.g. a third order equation). Such a network would require electronic amplifiers for every cell.

Certain types of nonlinear equations can be solved with a passive bilateral network using iterative methods. In the author's opinion these equations are not well suited to solution by networks and, except for one dimensional problems and problems in which the non-linearities are small, other methods of computation are more satisfactory.

The choice of examples has been influenced by still other considerations. The emphasis on beam and plate problems results from the fact that the Analysis Laboratory has recently been called upon to solve such problems. These are, furthermore, problems that have received little attention in the published literature on analog computors. The emphasis on equations involving the Laplacian operator is a result of the unrivaled importance of this type of equation.

Examples of important equations that have not been considered and for which network analogies exist in the literature are the equations of compressible fluid flow[1,2*], Schroedinger's equation[3,4], and the general equations of elasticity[5,25].

In the usual type of analog computor, time is regarded as the independent variable. The alternative use of position as an independent variable in an analog computor is investigated here. It will be shown that, even for problems with one independent variable, this point of view has certain advantages. An electric analog computor can readily be adapted to this technique.

---

* Numbers refer to items in the bibliography, p 140-142

I PROBLEMS WITH ONE SPACE VARIABLE

1.1 The Finite Difference Approximation

The essential mathematical step in the solution of partial differential equations by networks is the replacing of a differential operation by an equivalent finite difference operation. A dependent variable which is a continuous function of the independent variables is replaced by a set of variables each of which is defined only for a discrete point in the coordinate space. The differential equation is replaced by a large number of algebraic equations relating the new set of variables. This is, in a sense, the inverse of the usual process employed in the derivation of the differential equations of physics, wherein the distance between discrete points is permitted to become infinitesimal. This mathematical step involves an approximation which will determine the attainable accuracy of the final solution.

The development of the method begins with the principle of polynomial representation.* In the finite difference approximation of a function of one independent variable the function is defined only at discrete points and it is necessary for purposes of differentiation, integration and interpolation to define the function in some manner for the intervening points. The function passing through the n+1 defined points y_0, y_1, y_2 - - -y_n which has the least number of derivatives (i.e. the smoothest function) is a polynomial of degree n:

$$y = c_o + c_1x + c_2x^2 + - - + c_nx^n \qquad (1.1)$$

* This treatment summarizes results given in R. V. Southwell, Relaxation Methods in Theoretical Physics, ref. 6, pages 13-20 as well as in books on finite difference methods.

On the basis of this representation the value of the function at $x = 0$ and its first two derivatives are:

$$\begin{aligned} y_o &= c_o \\ \left(\frac{dy}{dx}\right)_o &= c_1 \\ \left(\frac{d^2y}{dx^2}\right)_o &= c_2 \end{aligned} \tag{1.2}$$

The coefficients c_0, c_1, c_2, - - - c_n are functions of y_0, y_1, - - - y_n. Consequently the derivatives of the function may be expressed in terms of its values at n+1 discrete points. In this way tables of three point, four point, or n-point differentiation may be built up.[6] For example, for a range of three points and equal spacing Δx:

$$\begin{aligned} \left(\frac{dy}{dx}\right)_o &= \frac{1}{2\Delta x}(-3y_o + 4y_1 - y_2) \\ \left(\frac{dy}{dx}\right)_1 &= \frac{1}{2\Delta x}(-y_o + y_2) \\ \left(\frac{dy}{dx}\right)_2 &= \frac{1}{2\Delta x}(y_o - 4y_1 + 3y_2) \\ \left(\frac{d^2y}{dx^2}\right)_{o,1,2} &= \frac{1}{\Delta x^2}(y_o - 2y_1 + y_2) \end{aligned} \tag{1.3}$$

The errors in these formulae may be estimated by means of the Mac-Laurin series for the function and its derivatives. For example:

$$\begin{aligned} y_2 &= y_o + 2\Delta x y_o' + \frac{4\Delta x^2}{2!}y_o'' + \frac{8\Delta x^3}{3!}y_o''' + - - - \\ \left(\frac{dy}{dx}\right)_1 &= y_o' + \Delta x y_o'' + \frac{\Delta x^2}{2!}y_o''' + - - - - \end{aligned} \tag{1.4}$$

Hence the remainder-error for the second of eqns(1.3) is

$$\left(\frac{dy}{dx}\right)_1 - \frac{1}{2\Delta x}(-y_o + y_2) = -\frac{\Delta x^2}{6}y_o''' + - - - \tag{1.5}$$

In general, the greater the number of points that are taken, the smaller will be the error in the representation of a derivative, although this will not always be the case. Since these errors

depend on the spacing, Δx, they can also be diminished by making this quantity small. In the representation of these differentiation formulae by electrical networks it is advisable to choose the simplest formula that has a reasonably small error and to make the spacing small, since the accuracy of the solution will be increased more rapidly in this way than by using more complicated formulae that may be difficult to represent electrically. The derivatives that can be represented by electrical networks together with their point differentiation formulae and remainder-errors are given in the following table.

Table I

Derivative	Formula	Error
$(\frac{dy}{dx})_1$	$\frac{1}{2\Delta x}(-y_o + y_2)$	$-\frac{\Delta x^2}{6}y_o'''$
$(\frac{d^2y}{dx^2})_1$	$\frac{1}{\Delta x^2}(y_o - 2y_1 + y_2)$	$-\frac{\Delta x^2}{12}y_o^{iv}$
$(\frac{d^4y}{dx^4})_2$	$\frac{1}{\Delta x^4}(y_o - 4y_1 + 6y_2 - 4y_3 + y_4)$	$-\frac{\Delta x^2}{6}y_o^{vi}$
$(\frac{d^6y}{dx^6})_3$	$\frac{1}{\Delta x^6}(y_o - 6y_1 + 15y_2 - 20y_3 + 15y_4 - 6y_5 + y_6)$	$-\frac{\Delta x^2}{4}y_o^{viii}$

Note that in all of these formulae the errors are proportional to the square of the spacing and the second higher derivative. The third, fifth and all higher odd order derivatives cannot be represented by bilateral electrical networks.

1.2 An Electrical Network for a Linear Second Order Differential Equation

The general expression for a linear second order differential equation is:

$$\frac{d^2y}{dx^2} + f_1(x)\frac{dy}{dx} + f_2(x)\cdot y = f_3(x) \tag{1.6}$$

A form of this equation that is more convenient for solution by electrical network is:

$$\frac{d}{dx}\left(g(x)\frac{dy}{dx}\right) = g(x)\left[f_3(x) - f_2(x)\, y\right] \tag{1.7}$$

where

$$g(x) = e^{\int f_1(x)dx} \tag{1.8}$$

as may be verified by expanding eqn.(1.7). We shall now replace eqn.(1.7) by its finite difference equivalent. In Fig. 1 y is represented as a single valued function of x continuous together with its first two derivatives. The values, y_k, that will be used in the finite difference representation are marked on the curve. The spacing, $x_k - x_{k-1} = \Delta x$, is constant.

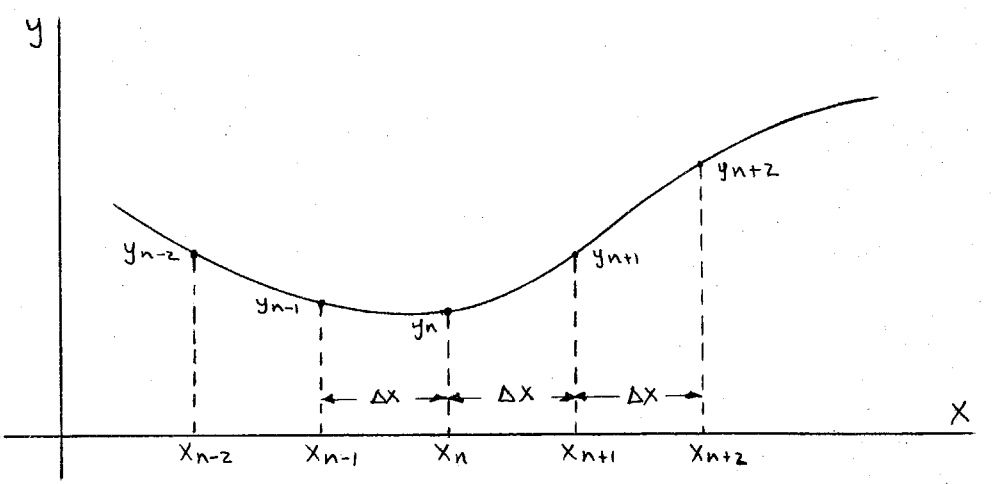

Fig. 1.

Define $x_{n+\frac{1}{2}} = x_n + \frac{\Delta x}{2}$. Then, by the differentiation formulae of Table I,

$$\left(\frac{dy}{dx}\right)_{n+\frac{1}{2}} \simeq \frac{y_{n+1} - y_n}{\Delta x} \tag{1.9}$$

is an approximation with an error proportional to the square of the increment, Δx. Furthermore

$$\left[g(x)\frac{dy}{dx}\right]_{n+\frac{1}{2}} \simeq g(x_{n+\frac{1}{2}})\ \frac{y_{n+1} - y_n}{\Delta x} \tag{1.10}$$

and

$$\left[\frac{d}{dx}\left(g(x)\frac{dy}{dx}\right)\right]_n \simeq \frac{\left(g(x)\frac{dy}{dx}\right)_{n+\frac{1}{2}} - \left(g(x)\frac{dy}{dx}\right)_{n-\frac{1}{2}}}{\Delta x}$$

$$\simeq \frac{g(x_{n+\frac{1}{2}})(y_{n+1} - y_n) - g(x_{n-\frac{1}{2}})(y_n - y_{n-1})}{\Delta x^2} \tag{1.11}$$

Hence, the finite difference equivalent of eqn.(1.7) is, for the n^{th} node:

$$\frac{g(x_{n+\frac{1}{2}})}{\Delta x}\left[y_{n+1} - y_n\right] + \frac{g(x_{n-\frac{1}{2}})}{\Delta x}\left[y_{n-1} - y_n\right]$$

$$= \Delta x g(x_n)\left[f_3(x_n) - f_2(x_n)y_n\right] \tag{1.12}$$

for the $n + 1^{st}$ node:

$$\frac{g(x_{n+3/2})}{\Delta x}\left[y_{n+2} - y_{n+1}\right] + \frac{g(x_{n+\frac{1}{2}})}{\Delta x}\left[y_n - y_{n+1}\right]$$

$$= \Delta x\ g(x_{n+1})\left[f_3(x_{n+1}) - f_2(x_{n+1})y_{n+1}\right] \tag{1.13}$$

We now turn to the representation of these equations by an electrical network. In the network of Fig. 2., the Y's are the admittances of the impedance branches, and the I's are currents inserted by an external source. The V's are the potentials at the nodes.

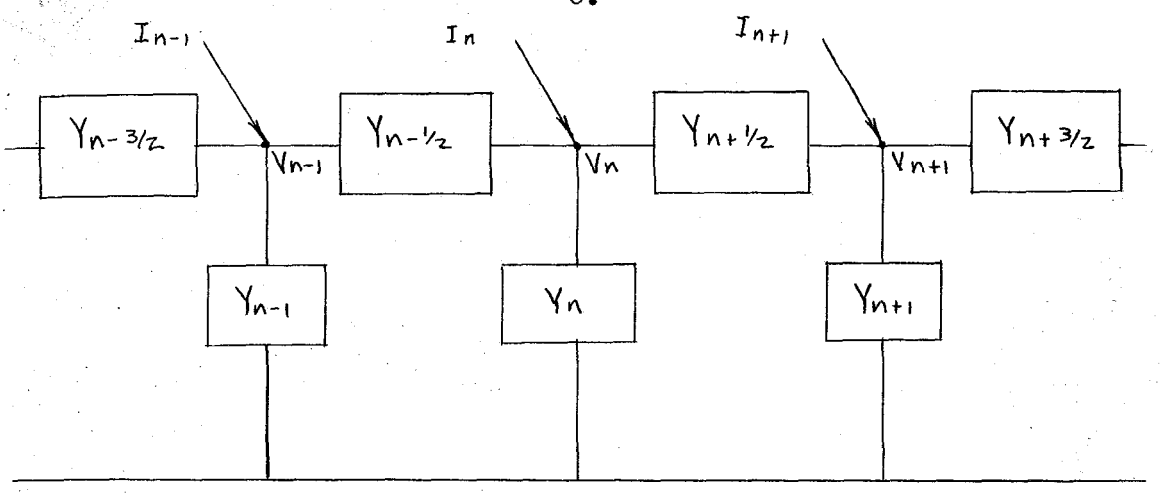

Fig. 2.

Electrical Network for a Second Order Differential Equation

Kirchoff's Current Law for the n^{th} node is:

$$Y_{n+\frac{1}{2}}(V_{n+1} - V_n) + Y_{n-\frac{1}{2}}(V_{n-1} - V_n) = -I_n + Y_n V_n \qquad (1.14)$$

Eqns.(1.12) and (1.14) are similar in form. They will be identical if

$$V_k = s\, y_k \qquad k = n-1,\ n,\ n+1$$

$$Y_{n+\frac{1}{2}} = \frac{g(x_{n+\frac{1}{2}})}{a\Delta x}$$

$$Y_{n-\frac{1}{2}} = \frac{g(x_{n-\frac{1}{2}})}{a\Delta x} \qquad (1.15)$$

$$Y_n = \frac{-g(x_n)\, f_2(x_n)\, \Delta x}{a}$$

$$I_n = \frac{-s\Delta x\, g(x_n)\, f_3(x_n)}{a}$$

where s and a are two arbitrary constants and are called the scale change and the impedance base change respectively. Kirchoff's law for the $n+1^{st}$ node can similarly be made identical with eqn.(1.13). Observe that the coefficient of y_{n+1} in eqn.(1.12) is the same as the coefficient of y_n in eqn.(1.13). This symmetrical property per-

mits the representation of these terms by a bilateral admittance. Since n may be considered as a running index every admittance is bilateral.

It has been shown that eqn.(1.7) can be represented by a simple bilateral electrical lattice. The admittances of this network may be either positive or negative. If they are all positive or all negative a network of resistances can represent the equation. If some are positive and some negative a network containing inductances and capacitances must be used. The conditions under which a resistive network may be used will now be determined.

By eqn.(1.8) $g(x)$ is positive for all values of x provided that $f_1(x)$ is a real function of x (which we shall assume is true). Consequently $Y_{k+\frac{1}{2}}$ is positive for all values of x. Y_k will be positive if $f_2(x)$ is negative. Consequently the necessary and sufficient conditions for eqn.(1.6) to be represented by a network of resistances is that $f_1(x)$ be real and $f_2(x)$ be real and negative for all values of x. If $f_2(x)$ is real and positive, $Y_{k+\frac{1}{2}}$ can be represented by an inductance which has a constant positive reactive impedance for a fixed frequency and Y_k can be represented by a capacitor which has a negative reactive impedance.

The continuity of the electrical network requires that $Y_{k+\frac{1}{2}}$ not vanish at any point. Points where $Y_{k+\frac{1}{2}} = 0$ will be singular points and cannot be represented. For example, in Bessel's equation

$$\frac{d^2y}{dx^2} + \frac{1}{x}\frac{dy}{dx} - \left(1 - \frac{n^2}{x^2}\right) y = 0 \qquad (1.16)$$

$$g(x) = e^{\int 1/x\, dx} = x \qquad (1.17)$$

which vanishes for $x = 0$. Hence $x = 0$ is a singular point and can-

not be represented. Incidentally Bessel's equation cannot be represented by a resistance network but the modified Bessel equation can be so represented.

1.3 A Theory of Unequal Lumping

In the derivations of the previous section it has been assumed that the cell size or spacing, Δx, is equal for all finite difference intervals. For many problems it is desirable to have unequal lumping, particularly where the independent variable extends to infinity. A convenient method of introducing unequal lumping is by means of a transformation of the independent variable.

Let $\bar{x}$ be a new variable defined by

$$\bar{x} = F(x) \tag{1.18}$$

where $F(x)$ and its first derivative are smooth continuous functions. Then eqn.(1.7) can be written:

$$\frac{d}{d\bar{x}}\left(g(x)\, F'(x)\frac{dy}{d\bar{x}}\right) = \frac{g(x)}{F'(x)}\left[f_3(x) - f_2(x)\, y\right] \tag{1.19}$$

Allow the new variable to have equal finite difference increments, $\Delta\bar{x}$, and define x_n to be the value of x corresponding to $\bar{x} = n\Delta\bar{x}$. Then the finite difference equivalent of eqn.(1.19) for the n^{th} discrete value of $\bar{x}$ is:

$$\frac{g(x_{n+\frac{1}{2}})F'(x_{n+\frac{1}{2}})}{\Delta\bar{x}}(y_{n+1} - y_n) + \frac{g(x_{n-\frac{1}{2}})F'(x_{n-\frac{1}{2}})}{\Delta\bar{x}}(y_{n-1} - y_n)$$

$$= \frac{g(x_n)\Delta\bar{x}}{F'(x_n)}\left[f_3(x_n) - f_2(x_n)\, y_n\right] \tag{1.20}$$

x rather than $\bar{x}$ may be regarded as the independent variable of eqn. (1.20). This may be emphasized by defining

$$(\Delta x)_n = \frac{\Delta \bar{x}}{F'(x_n)}$$

$$(\Delta x)_{n+\frac{1}{2}} = \frac{\Delta \bar{x}}{F'(x_{n+\frac{1}{2}})} \qquad (1.21)$$

By comparison with eqn.(1.15) we see that the admittances and currents of the network of Fig. 2. become:

$$Y_{n+\frac{1}{2}} = \frac{g(x_{n+\frac{1}{2}})}{a(\Delta x)_{n+\frac{1}{2}}}$$

$$Y_n = \frac{-g(x_n)\, f_2(x_n)}{a} \quad (\Delta x)_n \qquad (1.22)$$

$$I_n = \frac{s(\Delta x)_n\, g(x_n)\, f_3(x_n)}{a}$$

As an example consider a transformation appropriate to a semi-infinite medium which it is desired to represent by a limited number of electrical elements. Such a transformation is

$$\bar{x} = F(x) = 1 - e^{-x} \qquad (1.23)$$

since when $x = 0$, $\bar{x} = 0$ and when $x = \infty$, $\bar{x} = 1$. The lumping constants are given by

$$(\Delta x)_n = \Delta \bar{x}\, e^{x_n}$$

$$(\Delta x)_{n+\frac{1}{2}} = \Delta \bar{x}\, e^{x_{n+\frac{1}{2}}} \qquad (1.24)$$

The admittance and current values may be obtained from eqn.(1.22). The point $x = \infty$, cannot actually be represented because $Y_{n+\frac{1}{2}}$ becomes zero there. However x may be allowed to become very large with only a few cells.

The condition that $F'(x)$ must be continuous is an undesirable restriction in view of the fact that finite differences are being used. It is desirable to be able to represent y for any set of values

of x that we please. Later on, in connection with a wing vibration problem, we shall see that it would be extremely inconvenient not to be able to do so.

In the finite difference equation, eqn.(1.20), F(x) appears only in differentiated form. Now F(x) need only be defined for discrete values of x, that is at the points that it is desired to represent in the network. There are no restrictions on F'(x) at these points or in between except that

$$\int_{x_n}^{x_{n+1}} F'(x)dx = \bar{x}_{n+1} - \bar{x}_n = \Delta\bar{x} \tag{1.25}$$

and

$$\int_{x_{n-\frac{1}{2}}}^{x_{n+\frac{1}{2}}} F'(x)dx = \Delta\bar{x} \tag{1.26}$$

In finite difference form these integrals can be replaced by the value of the integrand at the midpoint of the interval multiplied by the length of the interval. Hence

$$F'(x_{n+\frac{1}{2}})\cdot(x_{n+1} - x_n) = \Delta\bar{x} \tag{1.27}$$

and

$$F'(x_n)\cdot(x_{n+\frac{1}{2}} - x_{n-\frac{1}{2}}) = \Delta\bar{x}$$

so that

$$F'(x_{n+\frac{1}{2}}) = \frac{\Delta\bar{x}}{x_{n+1} - x_n}$$

$$F'(x_n) = \frac{\Delta\bar{x}}{x_{n+\frac{1}{2}} - x_{n-\frac{1}{2}}} \tag{1.28}$$

Substituting these expressions into eqn.(1.21) we find that

$$\begin{aligned}(\Delta x)_n &= x_{n+\frac{1}{2}} - x_{n-\frac{1}{2}} \\ (\Delta x)_{n+\frac{1}{2}} &= x_{n+1} - x_n\end{aligned} \tag{1.29}$$

Hence the quantity $(\Delta x)_{n+\frac{1}{2}}$ is actually the distance between two adjacent nodal points and $(\Delta x)_n$ is the width of the cell associated

with the n^{th} node. Any definition of $x_{n+\frac{1}{2}}$ is satisfactory provided only that the cells do not overlap or underlap. Specifically the n^{th} node need not be at the center of its cell.

1.4 Representation of the Boundary Condition for a Second Order Equation.

Two boundary conditions must be supplied with a second order differential equation. If the independent variable is a space coordinate these will ordinarily be conditions on the function or its first derivative at two different points. Boundary conditions of the type, $y + A\frac{dy}{dx} = B$, will also be encountered. If time is the independent variable both the function and its derivative are frequently specified at the instant, $t = 0$. All of these conditions can be represented in an electrical network as well as the conditions at the boundary between regions of an inhomogeneous medium.

The boundary condition $y = y_1$ at $x = a$ may be satisfied in the network of Fig. 2 by maintaining the voltage equal to sy_1 at that point. $x = a$ need not necessarily be a node of the network.

The boundary condition $\frac{dy}{dx} = C$ at $x = a$ may be easily imposed at the midpoint between two nodes since

$$\left(\frac{dy}{dx}\right)_{n+\frac{1}{2}} \simeq \frac{y_{n+1} - y_n}{\Delta x} \tag{1.30}$$

This is equivalent to specifying the current flowing at this point since

$$\begin{aligned} I_{n+\frac{1}{2}} &= Y_{n+\frac{1}{2}} (V_{n+1} - V_n) \\ &= \frac{g(x_{n+\frac{1}{2}})}{a\Delta x} s(y_{n+1} - y_n) \end{aligned} \tag{1.31}$$

Boundary conditions of this type may also be imposed at nodes of the

network. The condition $\frac{dy}{dx} = 0$ at $x = x_n$ is equivalent to the statement

$$y_{n+1} - y_{n-1} = 0 \tag{1.32}$$

By substituting this into eqn.(1.12), the finite difference equation for the n^{th} node, the fictitious node at n+1 can be eliminated. If g(x) is a constant, this substitution indicates that Y_n and I_n should be given half of their normal value.

Boundary conditions of the form $y + A\frac{dy}{dx} = B$ may be imposed at the midpoint between two nodes. In finite difference form,

$$\left[y + A\frac{dy}{dx}\right]_{n+\frac{1}{2}} \simeq \frac{1}{s}\left[V_{n+\frac{1}{2}} + A\frac{aI_{n+\frac{1}{2}}}{g(x_{n+\frac{1}{2}})}\right] \tag{1.33}$$

so that

$$sB - V_{n+\frac{1}{2}} = I_{n+\frac{1}{2}} \frac{Aa}{g(x_{n+\frac{1}{2}})} = \frac{A}{\Delta x} \frac{I_{n+\frac{1}{2}}}{Y_{n+\frac{1}{2}}} \tag{1.34}$$

The electrical circuit for this condition is shown in Fig. 3.

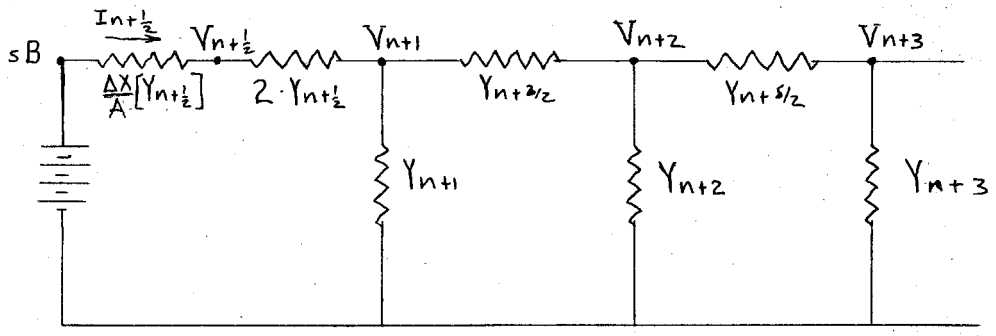

Fig. 3. Network to Represent $y + A\frac{dy}{dx} = B$ at $x = x_{n+\frac{1}{2}}$

For problems in which the solution is known to be periodic with a definite period, the network can be connected back upon itself. The advantage of this type of network over the usual one in which time is the independent variable is that the coefficients in the

differential equation may be made to depend on the independent variable without the need for complicated electrical devices.

1.5 Other Ordinary Differential Equations

The equivalent finite difference equations of a differential equation are a set of simultaneous algebraic equations. An examination of the matrix of the coefficients of these equations will reveal whether or not they can be represented by an electrical network since the impedance matrix of a bilateral electrical network must be symmetrical. For example consider the equation

$$\frac{dy}{dx} + f_2(x)\, y = f_3(x) \tag{1.35}$$

The finite difference equivalent of this equation is

$$\frac{y_{n+1} - y_{n-1}}{2\Delta x} + f_2(x_n)\, y_n = f_3(x_n) \tag{1.36}$$

In matrix form:

$$f_3(x_k) - f_2(x_k)\, y_k = a_{kj}\, y_j \tag{1.37}$$

where

$$a_{kj} = \frac{1}{2\Delta x} \begin{vmatrix} 0 & +1 & 0 & 0 & 0 & - & - \\ -1 & 0 & +1 & 0 & 0 & - & - \\ 0 & -1 & 0 & +1 & 0 & - & - \\ 0 & 0 & -1 & 0 & +1 & - & - \\ 0 & 0 & 0 & -1 & 0 & - & - \\ - & - & - & - & - & - & - \\ - & - & - & - & - & - & - \end{vmatrix} \tag{1.38}$$

This matrix is not symmetrical. It can be made symmetrical, however, by multiplying every other row of coefficients by -1. This is permissible if at the same time the left side of eqn.(1.37) is also

multiplied by -1 for the same rows. Hence

$$(-1)^k \left[f_3(x_k) - f_2(x_k)\, y_k \right] = (-1)^k\, a_{kj}\, y_j \qquad (1.39)$$

The network of admittances that will represent this equation is shown in Fig. 4.

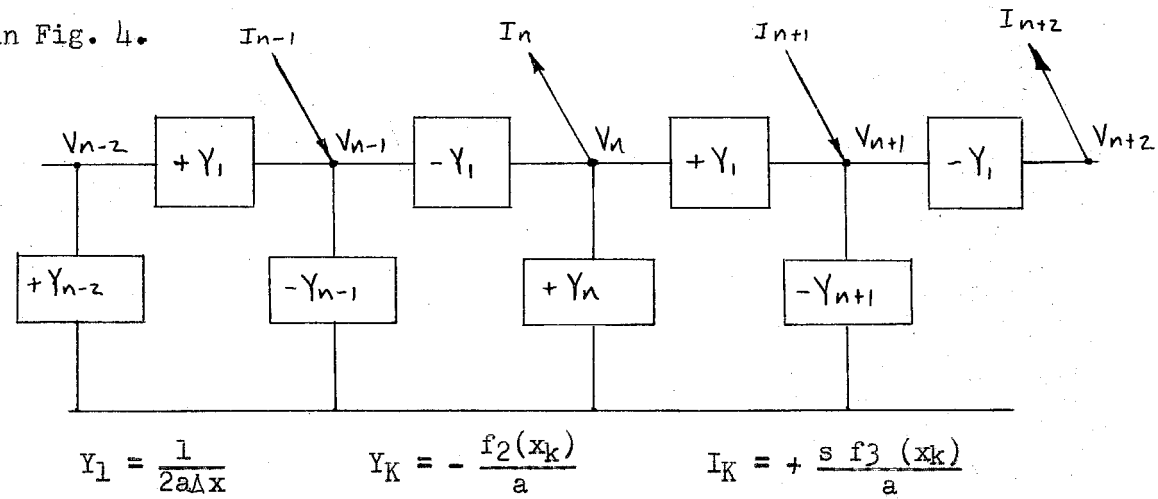

Fig. 4. Network for Equation (1.35)

A third order differential equation cannot be represented by a bilateral electrical network. As an example consider the equation

$$\frac{d^3y}{dx^3} + f_2(x)\, y = f_3(x) \qquad (1.40)$$

The finite difference equivalent of this equation is

$$\frac{1}{2\Delta x^3}(2y_{n+2} - 4y_{n+1} + 4y_{n-1} - 2y_{n-2}) + f_2(x_n)\, y_n = f_3(x_n) \qquad (1.41)$$

The matrix of this equation is:

$$a_{kj} = \frac{1}{2\Delta x^3} \left| \begin{array}{cccccccc} 0 & -4 & +2 & 0 & 0 & 0 & - \\ +4 & 0 & -4 & +2 & 0 & 0 & - \\ -2 & +4 & 0 & -4 & +2 & 0 & - \\ 0 & -2 & +4 & 0 & -4 & +2 & - \\ 0 & 0 & -2 & +4 & 0 & -4 & - \\ 0 & 0 & 0 & -2 & +4 & 0 & - \\ - & - & - & - & - & - & - \end{array} \right| \qquad (1.42)$$

This matrix is not symmetrical and cannot be made symmetrical by multiplying each row by a constant. Consequently it cannot be represented by a network of bilateral impedance elements.

The matrix for every odd ordered derivative is unsymmetrical and except for that of the first order cannot be represented by an electrical network. The matrix for every even ordered derivative is symmetrical.

Non-linear differential equations can be solved by electrical networks but the process involves the manual adjustment of the network parameters. In eqn.(1.7) either $g(x)$ or $f_3(x)$ may be functions of y also. If $g(x)$ is a function of y the network admittances must be adjusted until the equation is satisfied. If only $f_3(x)$ is a function of y then only the current fed into each node must be adjusted. The small computor constructed at Princeton University by Johnson and Alley[7] has been used principally for the solution of this type of problem.

Systems of ordinary differential equations can also be solved by passive bilateral networks provided that the coupling terms are symmetrical.

Eigenvalue problems will be discussed in the next section.

1.6 Partial Differential Equations Involving Time and One Space Coordinate

The equation of heat flow and the wave equation may be solved by the ladder-type network by making use of the transient properties of electrical impedances. In such networks time is represented as actual time. The equation of one dimensional heat

flow is

$$\frac{\partial}{\partial x}\left(g(x)\frac{\partial y}{\partial x}\right) = f(x)\frac{\partial y}{\partial t} \tag{1.43}$$

The finite difference equivalent of this equation is:

$$\frac{g(x_{n+\frac{1}{2}})}{\Delta x}\left[y_{n+1} - y_n\right] + \frac{g(x_{n-\frac{1}{2}})}{\Delta x}(y_{n-1} - y_n) = \Delta x\, f(x_n)\frac{\partial y_n}{\partial t} \tag{1.44}$$

If this equation is regarded as a statement of Kirchoff's current law for the n^{th} node, the right hand side represents the flow of current through a capacitor to ground. The network for the solution of eqn. (1.44) is shown in Fig. 5.

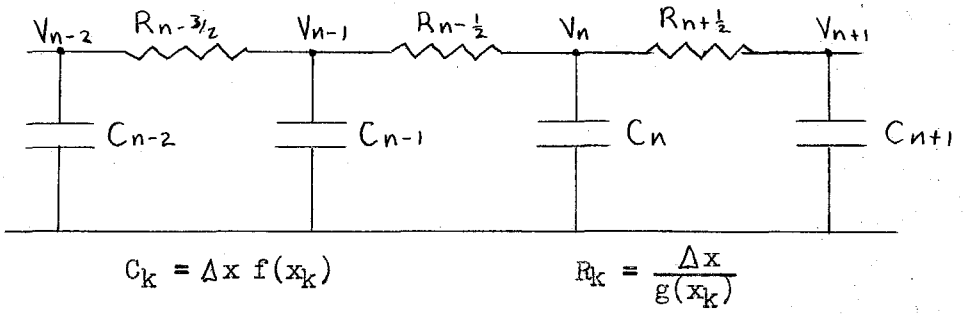

Fig. 5. Network for the Solution of Eqn.(1.44)

The one-dimensional wave equation which may be solved in a similar way is:

$$\frac{\partial}{\partial x}\left(g(x)\frac{\partial y}{\partial x}\right) = f(x)\frac{\partial^2 y}{\partial t^2} \tag{1.45}$$

The finite difference equivalent of this equation is:

$$\frac{g(x_{n+\frac{1}{2}})}{\Delta x}\left[y_{n+1} - y_n\right] + \frac{g(x_{n-\frac{1}{2}})}{\Delta x}\left[y_{n-1} - y_n\right] = \Delta x\, f(x)\frac{\partial^2 y_n}{\partial t^2} \tag{1.46}$$

If this equation is regarded as a statement of Kirchoff's law for the n^{th} node, the left side represents the flow of the time derivative of current through inductors and the right side represents the flow

of the time derivative of current through a capacitor to ground. In Fig. 5 the resistances are replaced by inductors with the same numerical value. For the steady state $\frac{\partial^2}{\partial t^2}$ is replaced by $-\omega^2$. With this substitution eqn.(1.45) may be regarded as an eigenvalue problem. The resonant frequencies of the electrical network give the proper values of ω^2.

1.7 Two Examples of Ordinary Differential Equations

The first example is the determination of the resonant frequencies of a transmission line. The problem is such that the network solution can easily be calculated analytically for any number of cells. This example is studied in order to show how the error in the network solution depends upon cell size. The way in which the errors depend on cell size will determine the minimum number of cells that can be used in the solution of a problem. This is a matter of considerable practical importance.

The mathematical problem is the solution of the equation

$$\frac{1}{L_s}\frac{d^2y}{dx^2} + \omega^2 C_s y = 0 \tag{1.47}$$

where C_s and L_s are the capacitance and inductance per unit length of line subject to the conditions

$$\begin{aligned} y &= \xi \sin\omega t \quad \text{at } x = \ell \\ \frac{dy}{dx} &= 0 \qquad \text{at } x = \ell \\ y &= 0 \qquad \text{at } x = 0 \end{aligned} \tag{1.48}$$

The line and its lumped electrical equivalent are shown in Fig. 6. The values of the electrical elements and the boundary conditions have been selected according to the analysis of the previous sections.

The exact solution of eqn.(1.47) is

$$y = \mathcal{E}\sin(\omega_d\sqrt{L_sC_s}\,x)\,\sin\omega_d t \tag{1.49}$$

where

$$\omega_d\sqrt{L_sC_s}\,\ell = (2n+1)\frac{\pi}{2} \qquad n = 0, 1, 2 - - - \tag{1.50}$$

The exact solution[8] of the difference equations for the lumped network may also be obtained for any number of cells, N. It is:

$$y_K = \mathcal{E}\sin(K\Gamma)\,\sin(\omega_\ell t) \qquad K = 0, 1, 2 - - N \tag{1.51}$$

where $$N\Gamma = (2n+1)\frac{\pi}{2} \qquad n = 0, 1, 2 - - - \tag{1.52}$$

and $$\cos\Gamma = \left[1 - \frac{\omega_\ell^2\ell^2L_sC_s}{2N^2}\right] \tag{1.53}$$

The criterion of resonance in the lumped electrical network has been taken to be that the imput current is zero. Note that the dependence of the solution on x is identical in the two cases and hence that the r.m.s. values of the voltages in the lumped electrical network are exactly correct. However, the values of the frequencies in the two cases are different. Solving for the ratio $\frac{\omega_\ell}{\omega_d}$ from eqns. (1.50), (1.52) and (1.53):

$$\frac{\omega_\ell}{\omega_d} = \frac{\sin\frac{\Gamma}{2}}{\frac{\Gamma}{2}} \tag{1.54}$$

where $\Gamma = \frac{2n+1}{N}\frac{\pi}{2}$. Table II gives the value of the ratio $\frac{\omega_\ell}{\omega_d}$ for $n = 0$ and different numbers of cells, N. The table shows that for $N \geqslant 4$, the error in the network frequency of a quarter wave length transmission line is less than 1%. This result will be approximately true for many other problems involving the wave equation such as radiation problems and cavity resonator problems. It will be an important guide in setting up networks to solve these problems.

As a second example* consider the solution of the equation

$$\frac{d^2y}{dx^2} + \frac{1}{x}\frac{dy}{dx} + \frac{1}{2} - \frac{1}{2}y = 0 \tag{1.55}$$

subject to the boundary conditions

$$\begin{aligned} \frac{dy}{dx} &= 0 \qquad \text{at } x = 0 \\ y &= 0 \qquad \text{at } x = 5.5 \end{aligned} \tag{1.56}$$

The exact solution of this problem in terms of modified Bessel function is:

$$y = 1 - \frac{I_o(x)}{I_o(5.5)} \tag{1.57}$$

As a preliminary to the network solution, convert eqn.(1.55) into the following equivalent form

$$\frac{d}{dx}\left(4x\frac{dy}{dx}\right) + 2x(1-y) = 0 \tag{1.58}$$

The network values for the solution of this problem are, from eqn. (1.15), where we let $a = s = 1$:

$$\begin{aligned} Y_{n+\frac{1}{2}} &= \frac{4(x_{n+\frac{1}{2}})}{\Delta x} \\ Y_n &= 2\Delta x \cdot x_n \\ I_n &= 2\Delta x \cdot x_n \end{aligned} \tag{1.59}$$

In addition, let $\Delta x = 1$. In Fig. 7, which is the electrical representation of the problem, the numerical value of the admittances and currents are shown. The numerical solution of the network equations is not difficult and has been carried out. A comparison between the numerical network solution and the exact solution of eqn.(1.57) is

---

* The network solution of this problem has been carried out for slightly different values of parameters by Johnson and Alley in ref. 7.

shown in Table III. This comparison shows that an accurate solution of this problem may be obtained with only five cells even though the values of the admittances and currents are sharply graded for small values of x.

Table II

Comparison of the Exact and Network Frequencies for the Transmission Line Problem, Eqn.(1.47)

No. of Cells, N	$\frac{\omega_\ell}{\omega_\delta}$
1	0.900
2	0.974
3	0.989
4	0.994
6	0.997
8	0.9984

Table III

Comparison of the Analytical and Network Solutions of Eqn.(1.56)

x	Analytical Solution	Network Solution	percent difference
0.5	0.8996	0.8923	0.81
1.5	0.8729	0.8654	0.86
2.5	0.8104	0.8015	1.10
3.5	0.6859	0.6761	1.43
4.5	0.4488	0.4404	1.87

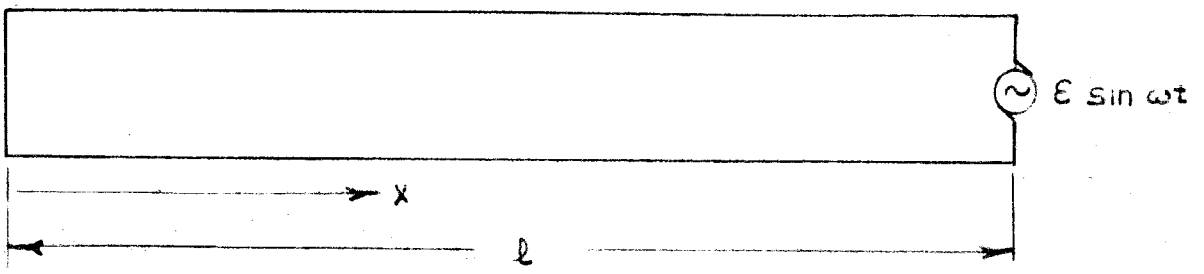

6(a) DISTRIBUTED TRANSMISSION LINE:

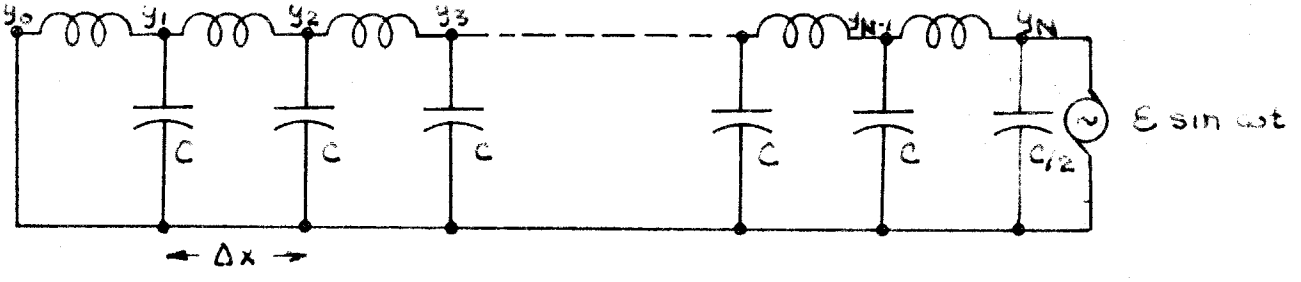

6(b) LUMPED EQUIVALENT NETWORK

FIG. 6 TRANSMISSION LINE PROBLEM

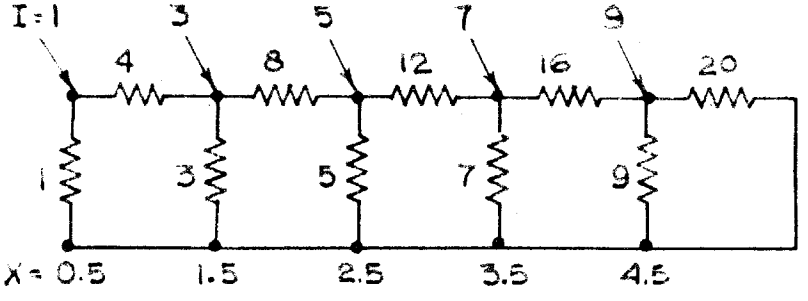

FIG. 7 NETWORK FOR THE SOLUTION OF

$$\frac{d}{dx}\left(4x\frac{dy}{dx}\right) + 2x(1-y) = 0$$

II THE SOLUTION OF BEAM PROBLEMS BY MEANS OF ELECTRICAL NETWORKS*

In the first part of this thesis methods were developed for solving problems with one space coordinate. Particular emphasis was placed upon second order differential equations. In this part these methods are extended to the solution of the equations of a beam which are fourth order differential equations with one space coordinate. Electrical analogies for an elastic beam have previously been described in the literature[10,11] but the dynamic analogy described here seems to be superior both in the range of problems that it can be used to solve and the speed and accuracy with which it can solve them. It has been found to be well suited to the study of beams having several coupled degrees of freedom including torsion and bending in two directions. Damping and other complicating factors such as the effect of rotational inertia about a transverse axis can readily be handled.

2.1 Differential Equations for the Vibration of Beams

This section comprises a tabulation of the beam equations for which electrical analogies will be derived. The equation for uncoupled torsional vibration is

$$\frac{\partial}{\partial x}\left(K\frac{\partial \alpha}{\partial x}\right) = I_\alpha \frac{\partial^2 \alpha}{\partial t^2} \qquad (2.1)$$

where α is the angular displacement, I_α is the moment of inertia per

---

* The results of this investigation are also given in ref. 9. The basic dynamic analogy for a beam in bending was derived by H. E. Criner and G. D. McCann in 1946 while both were associated with the Westinghouse Electric Corporation.

unit length and K is the torsional rigidity. Both K and I_α may be functions of x.

The equation for uncoupled bending vibration is

$$\frac{\partial^2}{\partial x^2}\left(EI\frac{\partial^2 y}{\partial x^2}\right) + m\frac{\partial^2 y}{\partial t^2} = 0 \tag{2.2}$$

where y is the bending deflection, m is the mass per unit length, E is Young's modulus, and I is the areal moment of inertia with respect to the neutral plane.

If bending and torsional oscillations are coupled through an unsymmetric load distribution, equations (2.1) and (2.2) become, for the coupled motion:

$$\frac{\partial^2}{\partial x^2}\left(EI\frac{\partial^2 y}{\partial x^2}\right) + m\frac{\partial^2 y}{\partial t^2} \pm S_\alpha\frac{\partial^2 \alpha}{\partial t^2} = 0 \tag{2.3}$$

$$-\frac{\partial}{\partial x}\left(K\frac{\partial \alpha}{\partial x}\right) \pm S_\alpha\frac{\partial^2 y}{\partial t^2} + I_\alpha\frac{\partial^2 \alpha}{\partial t^2} = 0 \tag{2.4}$$

where S_α is the first moment per unit length. The choice of sign depends on the choice of the positive sense of rotation.

If bending deflections in two perpendicular directions are considered, an additional equation is introduced, as well as coupling between the bending modes through the product of inertia, I_{yz}. The following equations are valid only if α is small.

$$\frac{\partial^2}{\partial x^2}\left(EI_z\frac{\partial^2 y}{\partial x^2} + EI_{yz}\frac{\partial^2 z}{\partial x^2}\right) + m\frac{\partial^2 y}{\partial t^2} \pm S_{\alpha y}\frac{\partial^2 \alpha}{\partial t^2} = 0 \tag{2.5}$$

$$\frac{\partial^2}{\partial x^2}\left(EI_y\frac{\partial^2 z}{\partial x^2} + EI_{yz}\frac{\partial^2 y}{\partial x^2}\right) + m\frac{\partial^2 z}{\partial t^2} \pm S_{\alpha z}\frac{\partial^2 \alpha}{\partial t^2} = 0 \tag{2.6}$$

$$-\frac{\partial}{\partial x}\left(K\frac{\partial \alpha}{\partial x}\right) \pm S_{\alpha y}\frac{\partial^2 y}{\partial t^2} \pm S_{\alpha z}\frac{\partial^2 z}{\partial t^2} + I_\alpha\frac{\partial^2 \alpha}{\partial t^2} = 0 \tag{2.7}$$

Besides these principal types of vibration certain other effects

can be included in the electrical analogy. In eqn.(2.2) the effect of rotational inertia about a transverse axis has been omitted. For slender beams this effect is negligible. When this effect cannot be neglected the differential equation for bending is:

$$\frac{\partial^2}{\partial x^2}\left(EI\frac{\partial^2 y}{\partial x^2}\right) - \frac{\partial}{\partial x}\left(\rho I'\frac{\partial^3 y}{\partial x \partial t^2}\right) + m\frac{\partial^2 y}{\partial t^2} = 0 \qquad (2.8)$$

where ρ is the volumetric mass density and I' includes, besides the areal moment of inertia of the shaft, I, the areal moment of inertia of parts that do not contribute to the stiffness. Eqn.(2.8) is developed in ref. 12.

If the beam is subjected to a tension, T, the differential equation of bending becomes:

$$\frac{\partial^2}{\partial x^2}\left(EI\frac{\partial^2 y}{\partial x^2}\right) - \frac{T}{\rho}\frac{\partial^2 y}{\partial x^2} + m\frac{\partial^2 y}{\partial t^2} = 0 \qquad (2.9)$$

Eqn.(2.9) is also developed in ref. 12.

No satisfactory simple theory of the internal damping of elastic bodies is known to the author. An approximation that gives fair agreement with experimental results and yet is simple to represent is obtained by replacing E by $E + c\frac{\partial}{\partial t}$. In this case eqn.(2.2) becomes:

$$\frac{\partial^2}{\partial x^2}\left(EI\frac{\partial^2 y}{\partial x^2} + Ic\,\frac{\partial^3 y}{\partial t \partial x^2}\right) + m\frac{\partial^2 y}{\partial t^2} = 0 \qquad (2.10)$$

where c is an experimental constant. For an account of this and other theories of damping see ref. 13.

2.2 The Electrical Circuit for Uncoupled Bending

Eqn.(2.2) above applies to the uncoupled bending vibration of a non-uniform beam.

If we define the slope, $$\theta = \frac{\partial y}{\partial x} \tag{2.11}$$

and the shear, $$S = \frac{\partial}{\partial x}\left(EI \frac{\partial \theta}{\partial x}\right) \tag{2.12}$$

then eqn.(2.2) becomes, $$\frac{\partial}{\partial x}(S) + m \frac{\partial^2 y}{\partial t^2} = 0 \tag{2.13}$$

It is simpler to write the finite difference equation corresponding to eqns.(2.11), (2.12), and (2.13) than to write the finite difference equation corresponding to eqn.(2.2).* This method has the advantage that it immediately reveals the correct form of the electrical network for the solution of transient problems. It also gives simple expressions for the case of unequal lumping. The finite difference equations equivalent to eqns.(2.11), (2.12) and (2.13) are:

$$\theta_{n+\frac{1}{2}} = \frac{y_{n+1} - y_n}{\Delta x} \tag{2.14}$$

$$\Delta x \cdot S_{n+\frac{1}{2}} = (\theta_{n+3/2} - \theta_{n+\frac{1}{2}}) \frac{EI_{n+1}}{\Delta x} + (\theta_{n-\frac{1}{2}} - \theta_{n+\frac{1}{2}}) \frac{EI_n}{\Delta x} \tag{2.15}$$

$$(S_{n+\frac{1}{2}} - S_{n-\frac{1}{2}}) + \Delta x \cdot m_n \frac{\partial^2 y_n}{\partial t^2} = 0 \tag{2.16}$$

If eqns.(2.15) and (2.16) are to be regarded as statements of Kirchhoff's laws for either current or voltage, S and θ must be quantities of different type (one current, one voltage) and also S and y must be quantities of different type. Consequently θ and y must be quantities of the same type and Δx in eqn.(2.14) must be a dimensionless ratio in the electrical analogy. The circuit of Fig. 8a satisfies all three of these equations if θ and y are regarded

---

* See Table I, page 5.

as voltages. Eqn.(2.14) expresses the relationship between the primary and secondary voltages of the transformers where the turns ratio is Δx. Eqn.(2.15) is Kirchhoff's law for the sum of the currents entering the node $\theta_{n+\frac{1}{2}}$. The current flowing in the secondary of the transformer is the turns ratio times the current in the primary i.e. $\Delta x \cdot S_{n+\frac{1}{2}}$. Eqn.(2.16) is Kirchhoff's law for the sum of the currents entering the node y_n.

Because of the presence of the second derivative with respect to time in eqn.(2.16), S must be the time derivative of current in the electrical network. By comparison with eqn.(1.47) the network inductance $L_n = \frac{\Delta x}{EI_n}$ and the network capacitance $C_n = \Delta x\, m_n$. The moment, $M = EI\frac{\partial^2 y}{\partial x^2}$, is the time derivative of the current flowing in the inductive branches.

The variables θ and y in eqns.(2.14), (2.15) and (2.16) can also be regarded as circulating electrical charges, and the equations can be regarded as Kirchhoff's laws for the voltages around the loops. The network so obtained is the same as before. The analogies are shown in Fig. 8b where the shears and moments become the voltages at the nodes. The inductance $L_n = \Delta x\, m_n$ while the capacitance $C_n = \frac{\Delta x}{EI_n}$.

In setting up an actual beam problem the value of inductance given by $L_n = \frac{\Delta x}{EI_n}$ may be too large as might also be the case for the capacitors. Also the turns ratio of the transformers and the unit of time or frequency may be inconvenient. To meet this difficulty arbitrary dimensional scale factors and other constants are introduced into the original equations which are later chosen to give practical values of the electrical components.* This feature has been elimin-

* See section 2.7.

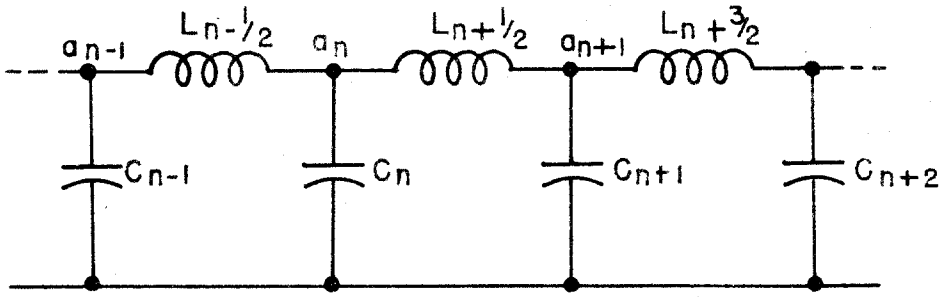

$$C_n = (I_\alpha)_n \cdot \Delta x \; ; \qquad L_{n+1/2} = \frac{\Delta x}{K_{n+1/2}}$$

EQUIVALENT CIRCUIT FOR TORSIONAL VIBRATION

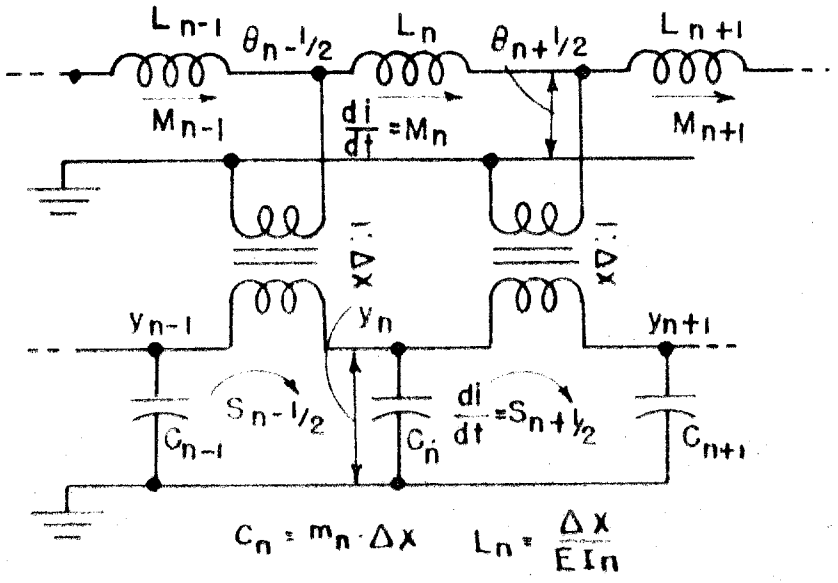

$$C_n = m_n \cdot \Delta x \qquad L_n = \frac{\Delta x}{EI_n}$$

a. MASS-CAPACITANCE ANALOGY

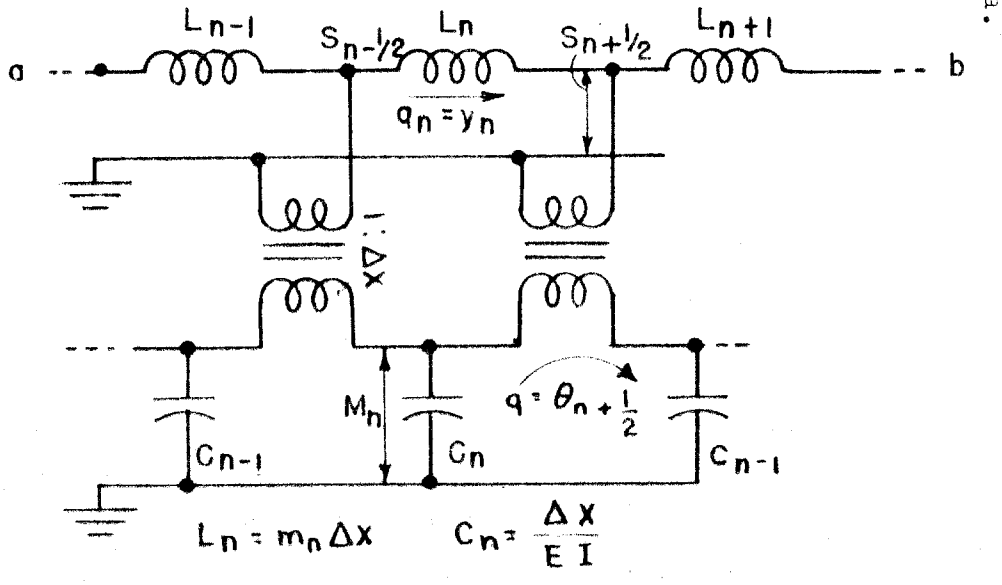

$$L_n = m_n \Delta x \qquad C_n = \frac{\Delta x}{EI}$$

b .MASS- INDUCTANCE

FIG 8 EQUIVALENT CIRCUITS FOR UNCOUPLED BENDING

ated here to simplify the analysis.

2.3 Boundary Conditions for a Beam in Bending

The three principal terminations for a beam are a clamped end, a pinned end and a free end. The analytical expression of these conditions, together with their electrical representations are listed in Fig. 9 for the mass-capacitance analogy alone.

In each case the end of the beam is chosen to coincide with a node of the θ circuit (n ≡ half-integer). The end could as easily have been made to coincide with integral values of n. In the circuit for the clamped end (Fig. 9a) θ should be grounded at $x = \frac{1}{2}$, and the center-tap of the primary of the transformer for cell number $\frac{1}{2}$ should be grounded at $x = \frac{1}{2}$. Since the secondary is also grounded, y is zero at x = 1, and the transformer may be left out. Consequently in the electrical analogy, the deflection y is zero at the center of the first section of a clamped beam. The effect of this approximation will be discussed later.

In the circuit for the free end (Fig. 9b) the current analogous to the shear force, S, and the current analogous to the moment, M, are both zero at $x = N+\frac{1}{2}$. By virtue of the first condition the current in the secondary of the transformer is zero so that $M_N - M_{N+1} = 0$ Also $M_{N+\frac{1}{2}} = \frac{1}{2}(M_N + M_{N+1}) = 0$ by the second condition. The only way that both of these conditions can be satisfied is to set $M_N = M_{N+1} = 0$

In the circuit for the pinned end (Fig. 9c) y is zero at $x = \frac{1}{2}$ and the center tap of the transformer is consequently grounded. M is also zero at $x = \frac{1}{2}$ which means that $M_0 - M_1 = 0$ or that the current in the secondary of the transformer should be twice as great as

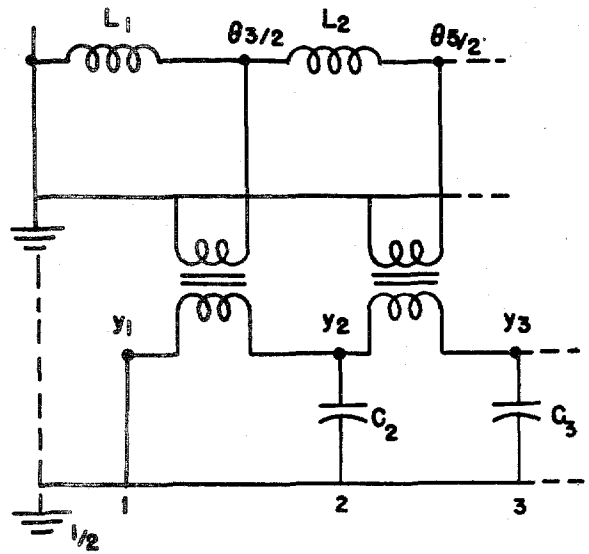

$y=0;\ \frac{\partial y}{\partial x}=\theta=0$

(a) END CLAMPED AT $X=1/2$

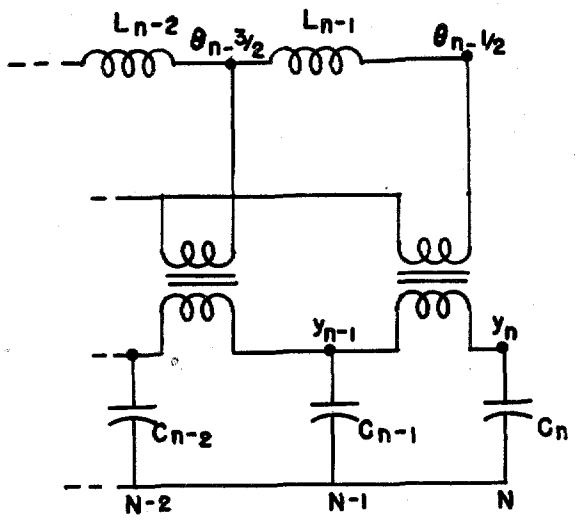

$\frac{\partial}{\partial x}\left(EI\frac{\partial^2 y}{\partial x^2}\right)=S=0;\quad EI\frac{\partial^2 y}{\partial x^2}=M=0$

(b) END FREE AT $X=N+1/2$

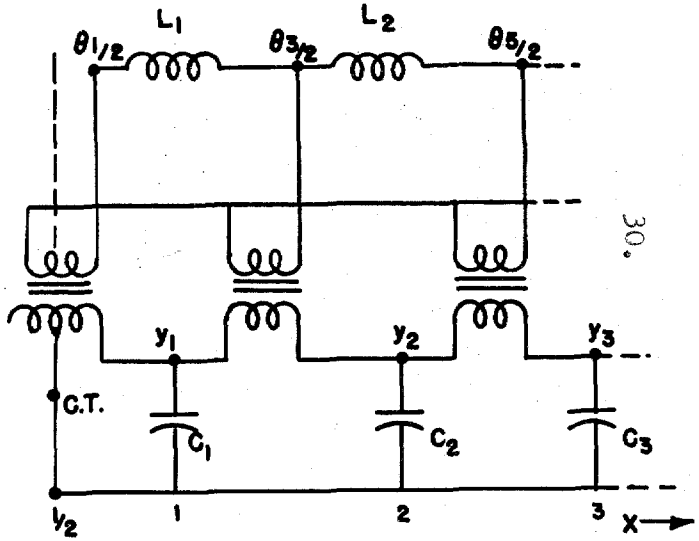

$y=0;\ EI\frac{\partial^2 y}{\partial x^2}=M=0$

(c) END PINNED AT $X=1/2$

FIG. 9 BOUNDARY CONDITIONS FOR A VIBRATING BEAM

the current in L_1. But since only half of the primary winding is used, the same effect can be produced in the primary circuit if the current in the secondary equals M_1, instead of twice M_1. Consequently the Θ circuit to the left of $x = \frac{1}{2}$ may be omitted. In a similar manner the circuit boundary conditions for the mass-inductance analogy can readily be determined.

An electrical network can also be developed for a beam with elastic supports. In fact, the beam (or several beams) may be integrated into a complete mechanical or electro-mechanical system.

2.4 The Normal Modes of a Uniform Cantilever Beam

The electrical analogy described in the two preceding sections was applied first to the calculation of the normal modes of a uniform cantilever beam. Since this problem can easily be solved analytically it provided a very satisfactory means for determining the effect of the different sources of error on the accuracy of the computor solution. The possible sources of error include the effects of transformer impedances, cell size, parasitic resistance and capacitance and the methods of imposing terminal conditions.

In the Cal Tech Electric Analog Computor[14] all capacitors and resistors are essentially perfect in the frequency range used. The inductors have "Q's" of 100 or better and thus are representative of low loss mechanical systems. All elements can be set to one percent of the desired value. Frequency and circuit impedance bases are so chosen that stray capacitance effects are negligible. The only elements with appreciable imperfections are the transformers. Although they are designed for a high ratio of magnetizing to leakage

impedance this ratio is not high enough to eliminate the transformers as a source of error.

The complete circuit for a cantilever beam with eight cells is shown in Fig. 10 on page 44. The methods of imposing the boundary conditions at the clamped and at the free ends are discussed in section 2.3. The network was driven by a voltage source connected through a small resistor to the free end section. The presence of a resonant mode was indicated by a minimum current flowing in the network at the proper frequency. These minima were always very sharp and resonant frequencies were reproducible to within 0.2 percent, on consecutive trials.

The mode shape data from the steady state tests are compared with theoretical curves in Fig. 11. The first, second, third and fifth modes are presented using analogies with eight, sixteen and twenty-four cells. Since only relative amplitudes are given by the theoretical curves, one point for each set of data can arbitrarily be placed on the curve. The points so chosen are indicated in Fig. 11.

In the analogy used the displacement of the midpoint of the first cell must be zero. It may be seen from the curves that this does not seriously affect the displacement at the second and third cells. An important conclusion that can be drawn from these curves is that, except as just mentioned, cell size has little effect on the accuracy of the mode shapes. Eight cells are sufficient for the first two modes and are nearly sufficient for the third mode. As a consequence it is possible to represent a uniform beam which, for instance, is part of a larger engineering structure by a small

number of cells. This should also be true to a limited extent for non-uniform beams. These conclusions also imply that the boundary conditions have been correctly imposed, for if they were not, marked improvement should have been obtained as the number of cells was increased.

In addition to calculating mode shapes, the normal mode frequencies were measured for a large number of combinations of cell size, mode number, and the network components L and C. The difference between the measured frequency and the theoretical frequency was calculated. The percent error is plotted in Fig. 12 as a function of network frequency. In this figure it will be noticed that for a given value of the ratio $\frac{L}{C}$ the percent error lies close to a mean curve so that cell size and mode number have little effect on the error. In the next section it will be shown that these errors are due principally to the leakage and magnetizing inductances of the transformers.

2.5 The Effects of Transformer Impedances

In the network of Fig. 13, L_{1y} and L_{2y} represent respectively the leakage and magnetizing inductances of the transformers. The method that will be used here will be to write the circuit equations for the network for Fig. 13; then to replace them by the equivalent expressions for a continuous system (differential equations); then to identify the circuit elements by reference to the equations of a beam.

In Fig. 13 the arrows indicate the direction of assumed current flow. Summing the currents at node y_n we obtain

$$S_{n+\frac{1}{2}} - S_{n-\frac{1}{2}} = C\omega^2 y \tag{2.17}$$

The voltage in the slope circuit is given by:

$$\theta_{n+\frac{1}{2}} = \frac{y_{n+1} - y_n}{\Delta x} + L_{1y}\Delta x\left[S_{n+\frac{1}{2}} - (y_n - y_{n+1})\frac{1}{L_{2y}}\right] \tag{2.18}$$

or, ignoring $(y_n - y_{n+1})/L_{2y}$ compared with $S_{n+\frac{1}{2}}$:

$$\theta_{n+\frac{1}{2}} = \frac{y_{n+1} - y_n}{\Delta x} + L_{1y}\Delta x\, S_{n+\frac{1}{2}} \tag{2.19}$$

Sum the currents at the node $\theta_{n+\frac{1}{2}}$:

$$\frac{1}{L_y}(\theta_{n+3/2} - 2\theta_{n+\frac{1}{2}} + \theta_{n-\frac{1}{2}}) = \Delta x\left[S_{n+\frac{1}{2}} - (y_n - y_{n+1})\frac{1}{L_{2y}}\right] \tag{2.20}$$

In these equations replace the difference expressions by the corresponding differential expressions. Then

$$\frac{\partial S}{\partial x} = \frac{C\omega^2 y}{\Delta x} = -\frac{C}{\Delta x}\frac{\partial^2 y}{\partial t^2} \tag{2.21}$$

$$\theta = \frac{\partial y}{\partial x} + \Delta x\, L_{1y} S \tag{2.22}$$

$$\frac{1}{L_y}\frac{\partial^2\theta}{\partial x^2} = \frac{1}{\Delta x} S + \frac{\partial y}{\partial x}\frac{1}{L_{2y}} \tag{2.23}$$

Differentiate eqn.(2.23)

$$\frac{1}{L_y}\frac{\partial^3\theta}{\partial x^3} = \frac{1}{\Delta x}\frac{\partial S}{\partial x} + \frac{\partial^2 y}{\partial x^2}\frac{1}{L_{2y}} \tag{2.24}$$

Substitute for θ from eqn.(2.22)

$$\frac{1}{L_y}\frac{\partial^4 y}{\partial x^4} + \frac{L_{1y}}{L_y}\Delta x\frac{\partial^3 S}{\partial x^3} = \frac{1}{\Delta x}\frac{\partial S}{\partial x} + \frac{\partial^2 y}{\partial x^2}\frac{1}{L_{2y}} \tag{2.25}$$

Substitute for $\frac{\partial S}{\partial x}$ from eqn.(2.21)

$$\frac{1}{L_y}\frac{\partial^4 y}{\partial x^4} - \frac{L_{1y}C}{L_y}\frac{\partial^4 y}{\partial x^2\partial t^2} + \frac{C}{\Delta x^2}\frac{\partial^2 y}{\partial t^2} - \frac{\partial^2 y}{\partial x^2}\frac{1}{L_{2y}} = 0 \tag{2.26}$$

If we let

$$C = m\Delta x \qquad L_{2y} = \Delta x \frac{\rho}{T}$$

$$L_y = \frac{\Delta x}{EI} \qquad L_{1y} = \frac{\rho I'}{EI\, m \Delta x}$$

we see that eqn.(2.26) is equivalent to eqns.(2.8) and (2.9). Thus the effects of rotary inertia and tension can be included in the network analogy of a vibrating beam, and will always be present in small amounts due to the presence of the transformer impedances.

If $\frac{\partial^2}{\partial t^2}$ is replaced by $-\omega^2$ in eqn.(2.26) there results

$$\frac{1}{L_y}\frac{\partial^4 y}{\partial x^4} + \frac{C}{\Delta x^2}\frac{\partial^2 y}{\partial t^2} + \frac{\partial^2 y}{\partial x^2}\left[\frac{\omega^2 L_{1y} C}{L_y} - \frac{1}{L_{2y}}\right] = 0 \qquad (2.27)$$

The term involving leakage and magnetizing inductance will vanish if

$$f_c = \frac{\omega}{2\pi} = \frac{1}{2\pi}\sqrt{\frac{L_y}{C}}\sqrt{\frac{1}{L_{1y}L_{2y}}} \qquad (2.28)$$

For the transformers in use with the Cal Tech Electric Analog Computor $L_{1y} = .025$ henry and $L_{2y} = 60$ henries. For $\frac{L_y}{C} = 10^6$, $f_c = 131$ cps. The values of f_c for the different ratios $\frac{L_y}{C}$ are indicated in Fig. 12 along the axis of zero error. The observed errors cross the axis at approximately these points.

The effect of magnetizing and leakage inductances can be eliminated by tuning the transformers. At low frequencies magnetizing impedance is tuned with parallel condensers across the terminals of one winding and at high frequencies leakage impedance is tuned with condensers in series with one winding. The values of these condensers depends on frequency but if the resonant frequency is first obtained without them, only a single adjustment has been found to be necessary. In Table IV the effect of tuning is illustrated for typical cases.

It is seen that the errors in natural frequency plotted in Fig. 12 can be considerably improved, even for extreme values of network frequency.

For a transient study, where all frequency components are present, it is impossible to tune the transformers, but in this case the accuracy requirements on frequency will usually be less strict.

TABLE IV

TRANSFORMER IMPEDANCES AND EFFECT OF TUNING ON ACCURACY OF MODE FREQUENCIES

(a) Impedances

Leakage inductance = 0.025 henries, leakage resistance = 5 ohms. Magnetizing inductance ranges from 55 to 80 henries for range of frequency between 50 and 800 cps and 1 to 10 volts.

(b) Effect of Tuning out Transformer Inductances

Type of Tuning	Mode	Theoretical Freq. cps	Cross over Freq.[3]	Computer Percent Error
None	First	43.75	131	+4.0
Magnetizing[1]	First	43.75	131	+1.2
None	First	21.875	131	+6.0
Magnetizing	First	21.875	131	+2.4
None	Third	767	131	-7.7
Leakage[2]	Third	767	131	-2.0
None	Second	547	262	-2.2
Leakage	Second	547	262	+0.4

1. Tuning capacitors across one winding for 60 henries.
2. Tuning capacitors in series with one winding for 0.025 henries.
3. Frequency at which effects of magnetizing and leakage cancel each other.

2.6 Response of a Cantilever Beam to an Impulsive Motion of the Base

The transformer beam analogy is suited to the study of the transient behavior of beams because the values of the electrical components are not functions of frequency. This is in sharp contrast with the other beam analogies mentioned.[10,11] As an example of transient behavior, the following problem was selected for investigation: a long homogeneous beam has a large mass concentrated at its base. The base may not rotate, but otherwise there are no constraints or supports. The large mass is given an impulse at t = 0 so that it moves with nearly constant velocity in a direction perpendicular to the axis of the beam. The subsequent motion of points along the beam is required.

The mechanical problem and its electrical analogy are illustrated in Fig. 14. In the electrical network, time rate of change of current is the analog of force. Consequently, the analog of an impulse is a step-current. Closing switch No. 1 of Fig. 14 allows C_{01} to charge up at a constant rate through R_1. A cyclic repetition process of applying the transient[14] is used so that the solution is displayed as a standing wave on the screen of a cathode ray oscilloscope. Switches 2, 3, 4 and 5 remove the energy from the system while switch 1 is open. For more complex beams a single application would usually be made of the transient forcing function to eliminate the switching circuit necessary to remove energy.

Oscillograms showing the response of the system are given in Figs. 15 and 16. In Fig. 15 the solution is given for a beam with a lowest natural frequency of 14.78 cps. The base has a mass 2.5 times

the mass of the beam. From Fig. 15 (the solution for $x = \frac{15}{16}$) it may be seen that there is no appreciable motion of the end of the beam until the arrival of the initial surge and that initially the end moves in a direction opposite to the direction of motion of the base.

The electrical solution is compared with an analytical solution for $x = \frac{15}{16}$ in Fig. 17. The analytical solution is for a beam whose base has an infinite mass, which accounts for part of the discrepancy between the two curves.

In the oscillograms of Fig. 16 the lowest mode frequency of the cantilever beam has been changed to 43.75 cps and the mass of the base is 8.75 times the mass of the beam. Figs. 16a, 16b and 16c show the deflections for $x = \frac{7}{16}$, $\frac{11}{16}$ and $\frac{15}{16}$ respectively. These solutions are similar to those for the corresponding positions of the first beam except that more cycles of oscillation are shown. Figs. 16d, 16e, and 16f show the slope $(\frac{dy}{dx})$ of the beam at $x = \frac{1}{8}$, $\frac{3}{8}$ and $\frac{7}{8}$ respectively. The importance of higher modes is more evident in these oscillograms than in those of deflection. The second mode, whose frequency is 6.25 times the frequency of the lowest mode, does not appear in Fig. 16 for $x = \frac{3}{8}$. The reason for this is that at $x = \frac{3}{8}$ the slope of the second normal mode is small (see Fig. 11b)

Moment and shear could have been measured in the network had that been desired. The stresses in the beam could have been obtained from the network solution with only a small amount of additional computation. This is important because maximum stress is often the desired result in a transient beam study. All of these measurements can be extended without difficulty to the study of non-uniform beams, beams with coupled bending and torsion, and to beams with

linear internal damping. In all of these cases numerical calculation is very difficult.

2.7 An Airplane Wing Vibration Study*

The elastic properties of an airplane wing can, in many cases, be approximated by a beam of variable cross section. Besides the simple bending modes already discussed, torsional modes will be present. There will also be some coupling between bending and torsion due to masses that are not symmetrical with respect to the elastic axis.

Eqns.(2.3) and (2.4) must be used to describe the vibrations of the wing. Except for the terms involving the first moment, S_α, analogies for these equations have already been derived, the second equation having been discussed in section 1.6. The points along the beam where the nodes of the bending and torsion circuits are placed should coincide. Then the coupling terms in these equations can be represented by a mutual admittance between corresponding nodes. If the sign of the coupling term does not change along the length of the beam this mutual admittance can be represented by a capacitor as is illustrated in Fig. 18. If the sign of the coupling term does change some of the mutual admittances can be represented by inductances in a steady state analysis. For a transient analysis these mutual admittances must be converted into mutual inductances and represented by transformers in the manner of section 4.3.

---

* The problem for which results are given in this section was submitted for solution by the Engineering Department of the El Segundo Branch of the Douglas Aircraft Co. The results are given in dimensionless form in the interest of security.

The finite difference intervals shown in Fig. 18 are not constant along the span. In the calculation of the elastic and loading constants the wing was divided into sections by the aircraft engineers in the way that was most convenient for them. When the problem was submitted by them for solution, it did not seem advisable to redistribute the constants of the wing into cells of equal length. Instead use was made of the theory of unequal lumping developed in section 1.3. If a new independent variable is defined by the transformation

$$\bar{x} = F(x) \tag{2.29}$$

then eqns.(2.11), (2.12) and (2.13) become:

$$\theta = \frac{\partial y}{\partial \bar{x}} F'(x) \tag{2.30}$$

$$\frac{S}{F'(x)} = \frac{\partial}{\partial \bar{x}} \left(EI\, F'(x) \frac{\partial \theta}{\partial \bar{x}}\right) \tag{2.31}$$

$$\frac{\partial S}{\partial \bar{x}} + \frac{1}{F'(x)} m \frac{\partial^2 y}{\partial t^2} = 0 \tag{2.32}$$

The finite difference expressions equivalent to these equations are:

$$\theta_{n+\frac{1}{2}} = \frac{y_{n+1} - y_n}{(\Delta x)_{n+\frac{1}{2}}} \tag{2.33}$$

$$(\Delta x)_{n+\frac{1}{2}} S_{n+\frac{1}{2}} = (\theta_{n+3/2} - \theta_{n+\frac{1}{2}}) \frac{EI_{n+1}}{(\Delta x)_{n+1}} + (\theta_{n-\frac{1}{2}} - \theta_{n+\frac{1}{2}}) \frac{EI_n}{(\Delta x)_n} \tag{2.34}$$

$$(S_{n+\frac{1}{2}} - S_{n-\frac{1}{2}}) + (\Delta x)_n \cdot m_n \frac{\partial^2 y_n}{\partial t^2} = 0 \tag{2.35}$$

where $(\Delta x)_n$ and $(\Delta x)_{n+\frac{1}{2}}$ have the same meaning as in eqns.(1.21) and (1.29). The physical elements of the bending network are given by

$$C_n = m_n \cdot (\Delta x)_n \qquad L_n = \frac{(\Delta x)_n}{EI_n} \tag{2.36}$$

and the transformer turns ratio, T, is $(\Delta x)_{n+\frac{1}{2}}$.

According to eqn.(1.22) the network elements of the torsion circuit are given by:

$$C'_n = (I_\alpha)_n \cdot (\Delta x)_n \qquad L_{n+\frac{1}{2}} = \frac{(\Delta x)_{n+\frac{1}{2}}}{K_{n+\frac{1}{2}}} \tag{2.37}$$

With these formulae for the network elements the wing may be divided into sections in any convenient manner since $(\Delta x)_n$ is the width of the n^{th} cell and $(\Delta x)_{n+\frac{1}{2}}$ is the distance between the n^{th} and the $n+1^{st}$ cells.

In order to allow the widest possible freedom in the choice of network elements several dimensionless parameters are inserted into the differential equations. In eqns.(2.3) and (2.4) the following changes should be made:

Replace t by $N\bar{t}$	(N = time base change)
Replace x by $P\bar{x}$	(P = metric scale change)
Replace α by α'/b	(b = dependent variable scale change)
Divide through by a	(a = impedance base change)

Then eqns.(2.3) and (2.4) become

$$\frac{\partial^2}{\partial \bar{x}^2}\left(\frac{EI}{aP^4}\frac{\partial^2 y}{\partial \bar{x}^2}\right) + \frac{m}{aN^2}\frac{\partial^2 y}{\partial \bar{t}^2} - \frac{S_\alpha}{abN^2}\frac{\partial^2 \alpha'}{\partial \bar{t}^2} = 0 \tag{2.38}$$

$$-\frac{\partial}{\partial \bar{x}}\left(\frac{K}{ab^2P^2}\frac{\partial \alpha'}{\partial \bar{x}}\right) - \frac{S_\alpha}{abN^2}\frac{\partial^2 y}{\partial t^2} + \frac{I_\alpha}{ab^2N^2}\frac{\partial^2 \alpha'}{\partial \bar{t}^2} = 0 \tag{2.39}$$

The values of the physical elements in Fig. 18 become:

$$C_{1n} = \frac{(\Delta \bar{x})_n}{aN^2}\left(m - \frac{S_\alpha}{b}\right) \qquad C_{2n} = \frac{(\Delta \bar{x})_n}{aN^2}\frac{S_\alpha}{b} \qquad C_{3n} = \frac{(\Delta \bar{x})_n}{a\,N^2}\left(\frac{I_\alpha}{b^2} - \frac{S_\alpha}{b}\right)$$

$$L_{1n} = aP^4\frac{(\Delta \bar{x})_n}{EI} \qquad L_{4n} = \frac{ab^2P^2(\Delta \bar{x})_{n-\frac{1}{2}}}{K} \qquad \bar{T}_{n+\frac{1}{2}} = (\Delta \bar{x})_{n+\frac{1}{2}}$$

The four factors a, b, P and N permit these electrical parameters to be chosen in such a way that they fit the range of available physical elements. In Fig. 18 the wing constants are given in dimen-

sionless form in terms of the actual electrical parameters set into the computor.

The problem for which solution was desired was the determination of the first and second torsional and bending mode frequencies and shapes for both symmetrical and unsymmetrical displacements. The correct boundary conditions for all cases are listed in Fig. 18. The unsymmetrical cases correspond to a simple support along the center line of the airplane with no constraint on the slopes at that point. In the symmetrical cases the slopes, θ and $\frac{\partial \alpha}{\partial x}$, are constrained to zero value at the center. As indicated S_α is negative for the first two cells requiring negative capacitors for C_{2n}. Since these terms were found to have little effect it was convenient to use inductors that were adjusted for the final setting at each mode frequency.

Figs. 19 and 20 give the bending and torsional displacements and frequencies for the bending modes. To show the effect of coupling with the torsional system the bending modes without coupling are also plotted.

2.8 Internal Damping and Bending in Two Directions

For simple bending $\frac{EI}{\Delta x}$ is the admittance between nodes of the slope circuit. For internal damping we see from eqn.(2.10) that $\frac{I_c}{\Delta x} \frac{\partial}{\partial t}$ represents an additional admittance (to rate of change of current) caused by the internal damping. Consequently in Fig. 13:

$$R_y = \frac{\Delta x}{I_y \cdot c} \qquad \text{and} \qquad R_z = \frac{\Delta x}{I_z \cdot c}$$

For bending deflections in two perpendicular directions we see from eqns.(2.5) and (2.6) that $\frac{EI_{yz}}{\Delta x}$ can be represented by a mutual admittance between the slope circuits. In practice a mutual

admittance must be expressed as a mutual impedance so that in Fig. 13:

$$Z_y = \frac{\Delta x}{E}\left[I_y - \frac{I_{yz}^2}{I_z}\right]^{-1} \tag{2.40}$$

$$Z_z = \frac{\Delta x}{E}\left[I_z - \frac{I_{yz}^2}{I_y}\right]^{-1} \tag{2.41}$$

$$Z_{yz} = \frac{\Delta x}{E}\left[I_{yz} - \frac{I_y I_z}{I_{yz}}\right]^{-1} \tag{2.42}$$

In eqn.(2.7) we see that it is possible for both bending circuits to be coupled to the torsional circuit, through unsymmetrical loading.

The static loading of beams has not been discussed. For static loading the capacitors representing the mass of the beam are replaced by currents from an external source representing the load. The inductors in the slope circuit may also be replaced by resistors which is advantageous since it reduces the effects of transformer leakage and magnetizing impedances.

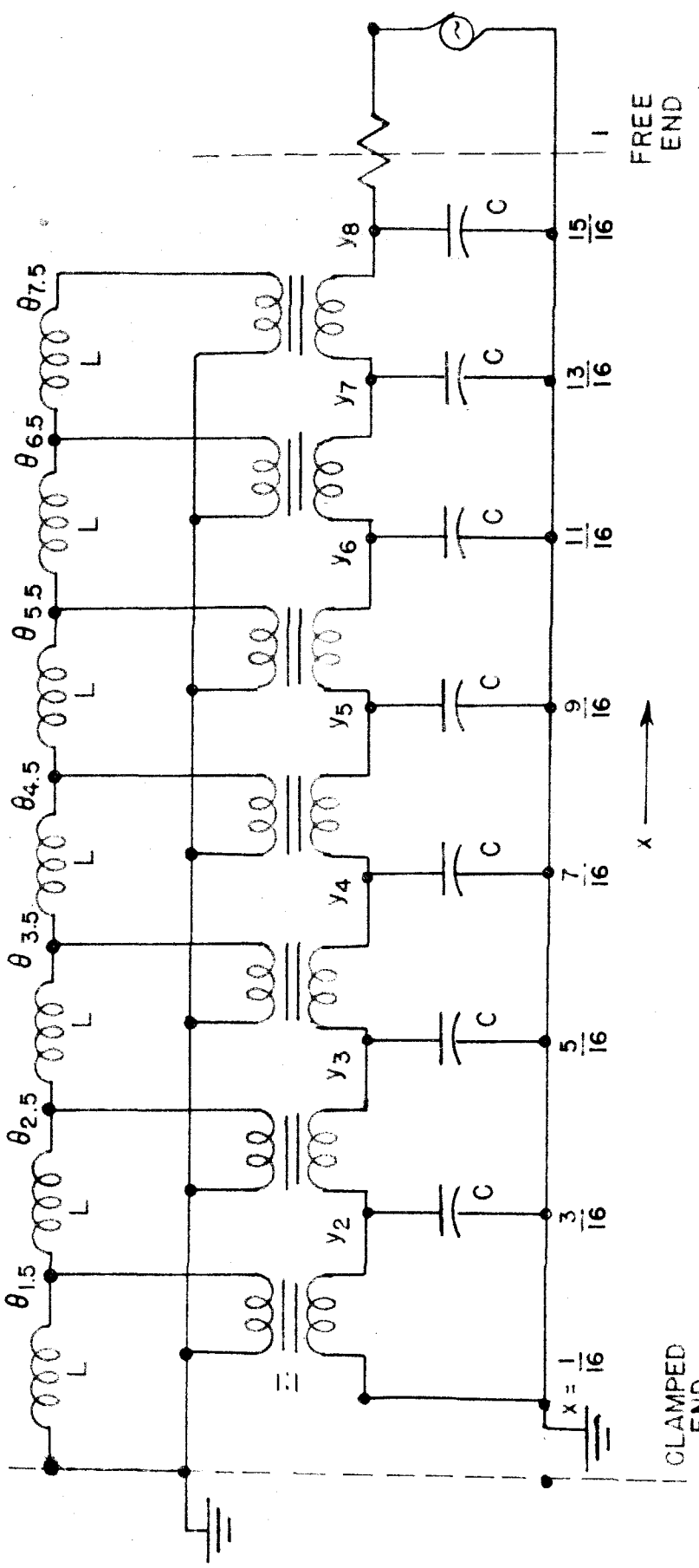

FIG.10 COMPLETE CIRCUIT FOR THE STEADY STATE VIBRATION OF A UNIFORM CANTILEVER BEAM WITH EIGHT CELLS

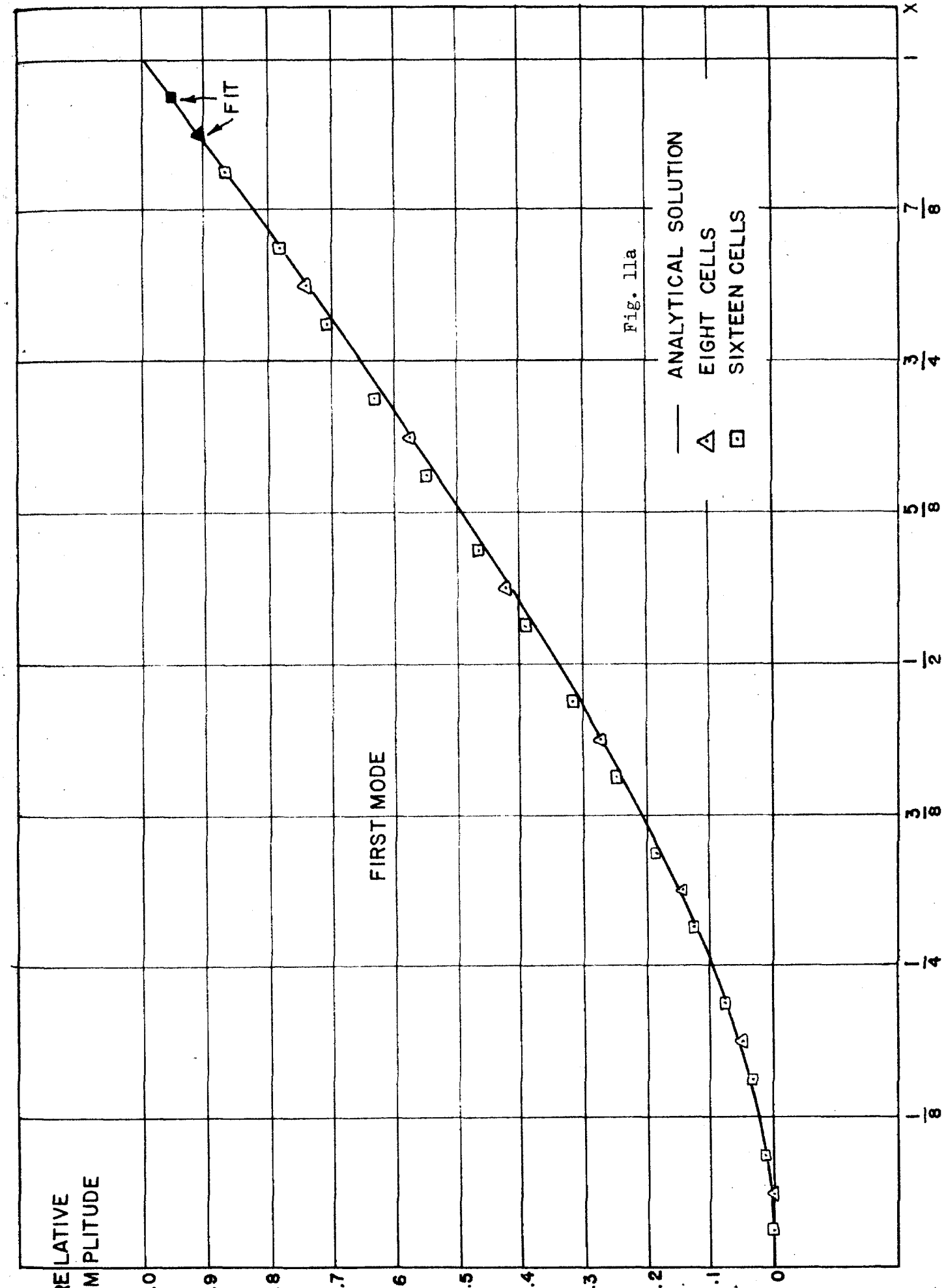
RELATIVE AMPLITUDE
1.0
.9
.8
.7
.6
.5
.4
.3
.2
.1
0
FIRST MODE
FIT
ANALYTICAL SOLUTION
EIGHT CELLS
SIXTEEN CELLS
X
1
7/8
3/4
5/8
1/2
3/8
1/4
1/8

Fig. 11a

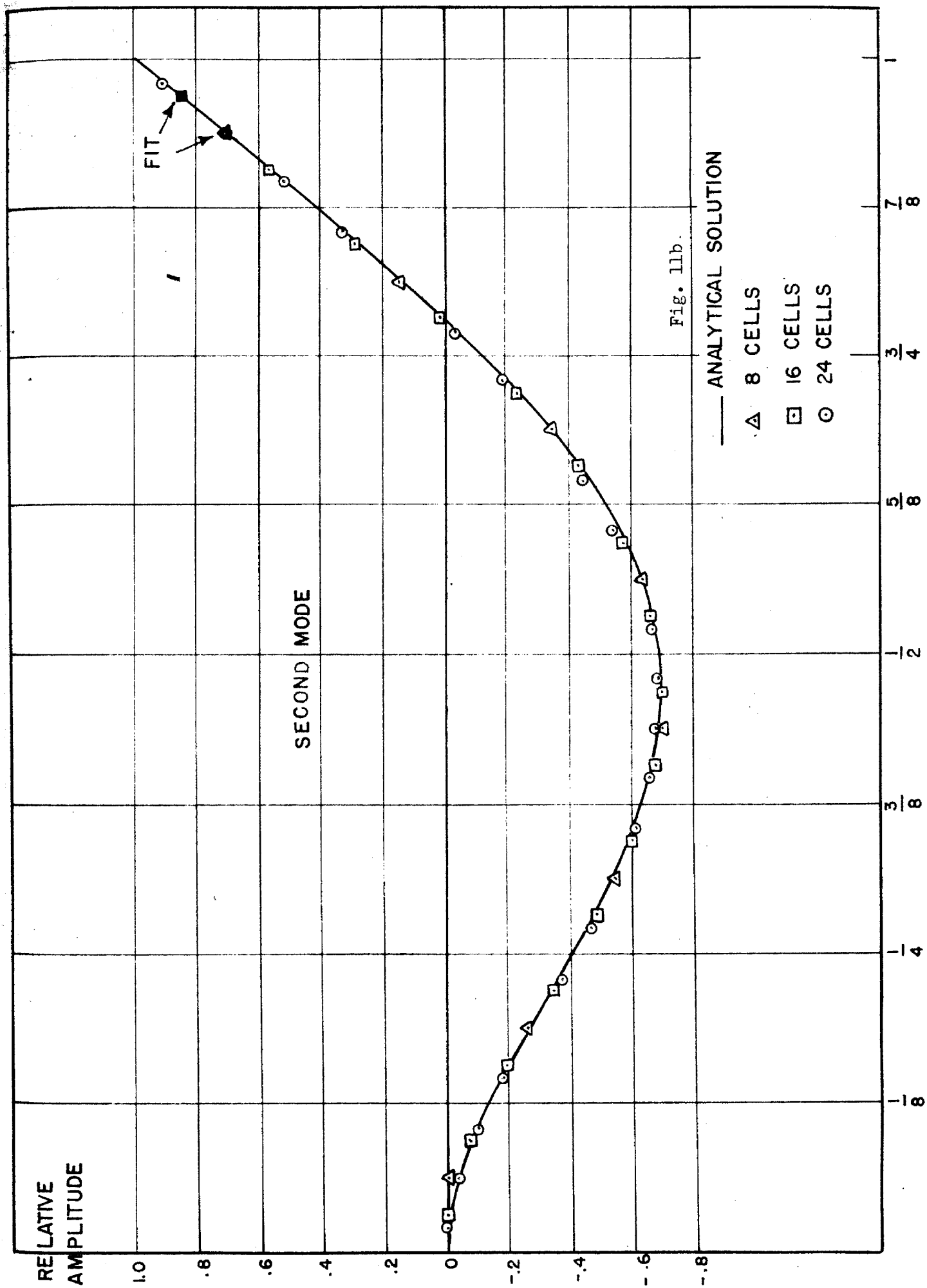
RELATIVE AMPLITUDE
1.0
.8
.6
.4
.2
0
-.2
-.4
-.6
-.8
1/8
1/4
3/8
1/2
5/8
3/4
7/8
1
SECOND MODE
FIT
ANALYTICAL SOLUTION
8 CELLS
16 CELLS
24 CELLS

Fig. 11b.

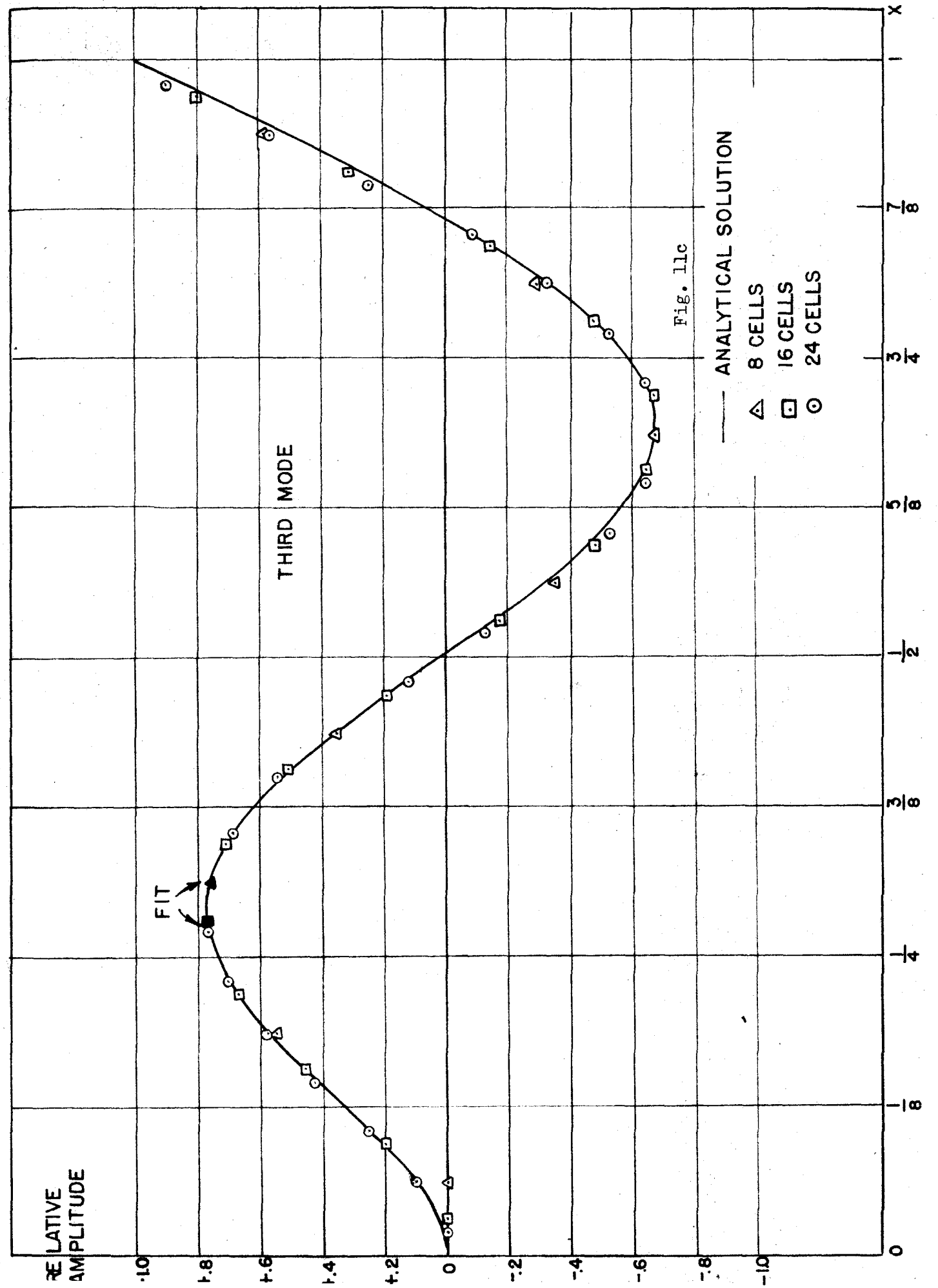
RELATIVE AMPLITUDE
+1.0
+.8
+.6
+.4
+.2
0
-.2
-.4
-.6
-.8
-1.0
0
1/8
1/4
3/8
1/2
5/8
3/4
7/8
1
X
THIRD MODE
FIT
ANALYTICAL SOLUTION
8 CELLS
16 CELLS
24 CELLS

Fig. 11c

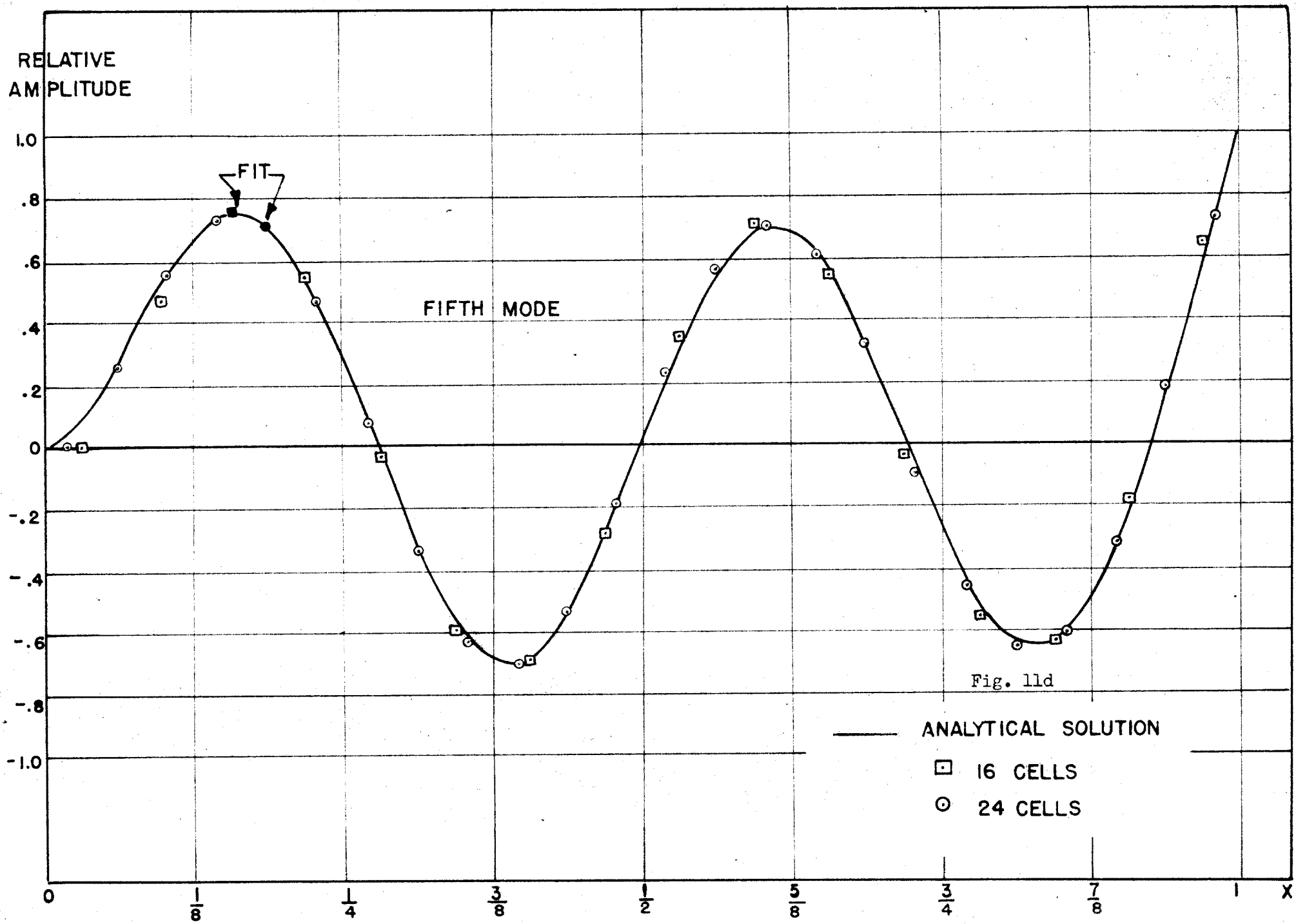
RELATIVE
AMPLITUDE
1.0
.8
.6
.4
.2
0
-.2
-.4
-.6
-.8
-1.0
FIT
FIFTH MODE
0
1/8
1/4
3/8
1/2
5/8
3/4
7/8
1
X
ANALYTICAL SOLUTION
16 CELLS
24 CELLS

Fig. 11d

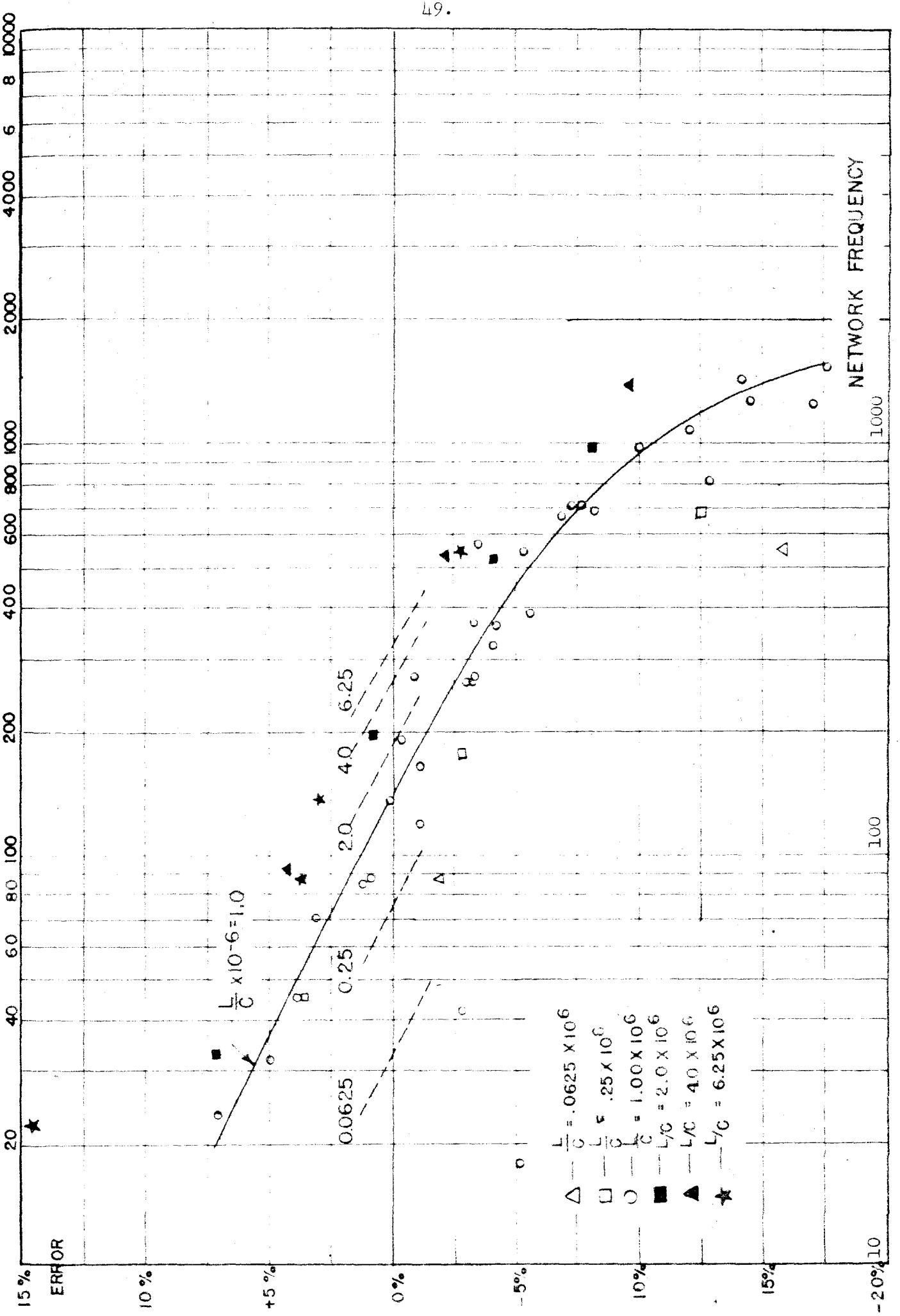

FIG. 12 ERROR IN MODE FREQUENCY OF CANTILEVER BEAM

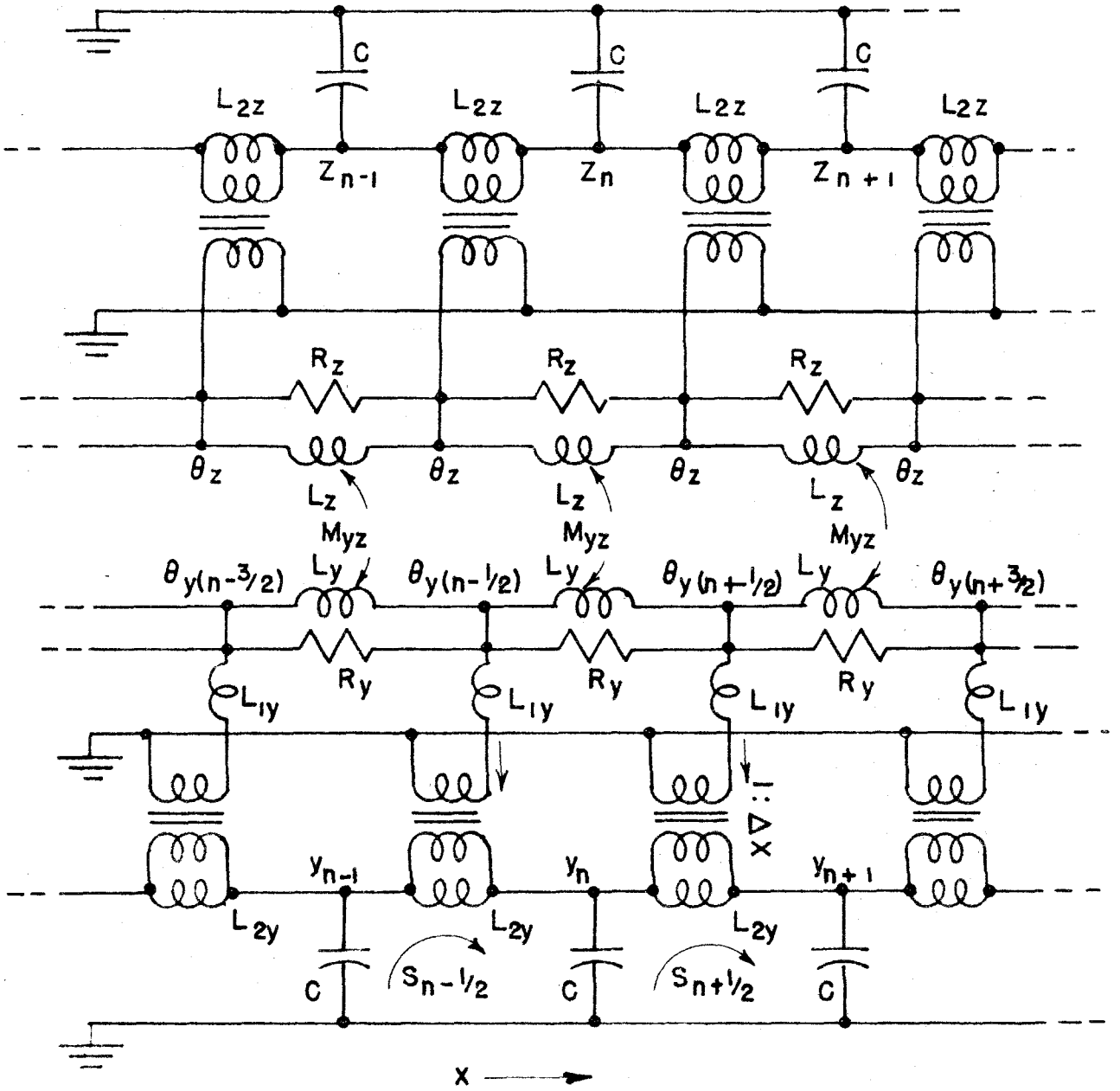

FIG.13 ELECTRIC NETWORK FOR BENDING IN TWO DIMENSIONS INCLUDING THE EFFECTS OF INTERNAL DAMPING, ROTARY INERTIA AND TENSION.

$$C = m\Delta X, \qquad L_y = \frac{\Delta X}{E}\left[I_y - \frac{(I_{yz})^2}{I_z}\right]^{-1} \qquad L_z = \frac{\Delta X}{E}\left[I_z - \frac{(I_{yz})^2}{I_y}\right]^{-1}$$

$$M_{yz} = \frac{\Delta X}{E}\left[I_{yz} - \frac{I_y I_z}{I_{yz}}\right]^{-1} \qquad L_{1y} = \frac{\rho I'}{EI_m \Delta X} \qquad L_{zy} = \frac{\Delta X \rho}{T}$$

$$L_{2z} = \frac{\Delta X \rho}{T} \qquad R_y = \frac{\Delta X}{I_y . c} \qquad R_z = \frac{\Delta X}{I_z . c}$$

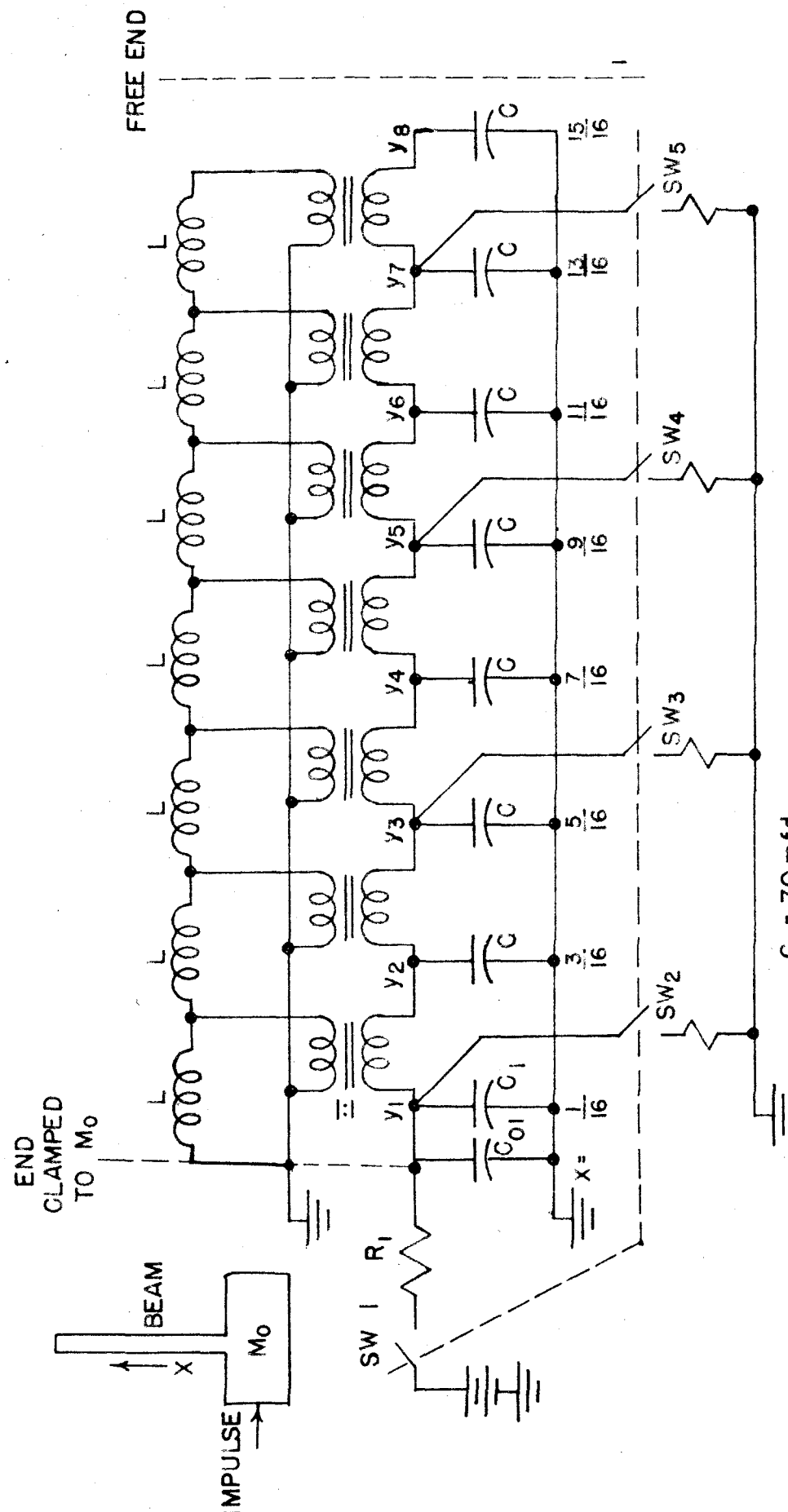

FIG. 14 COMPLETE CIRCUIT FOR TRANSIENT OSCILLATION OF A UNIFORM CANTILEVER BEAM WITH EIGHT CELLS

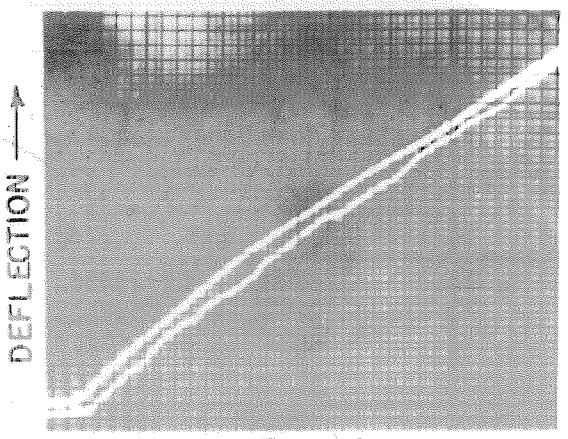

(a) $X = \frac{3}{16}$

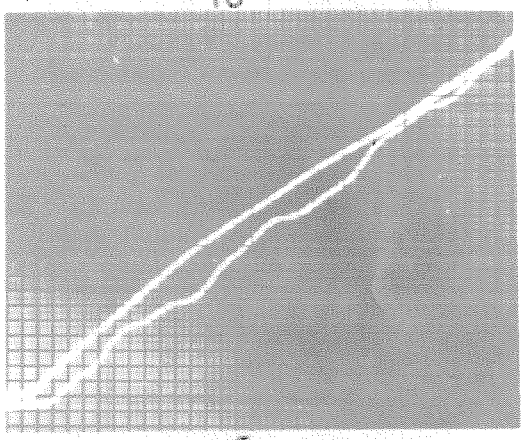

(b) $X = \frac{5}{16}$

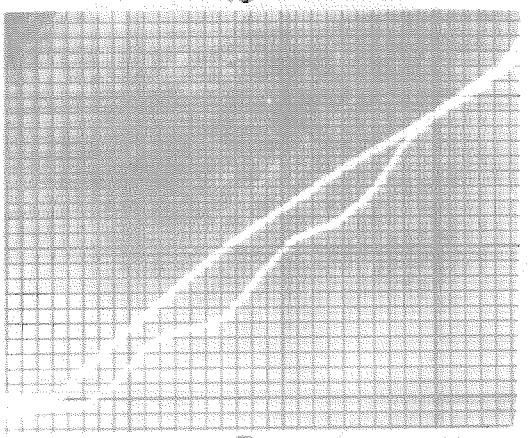

(c) $X = \frac{7}{16}$

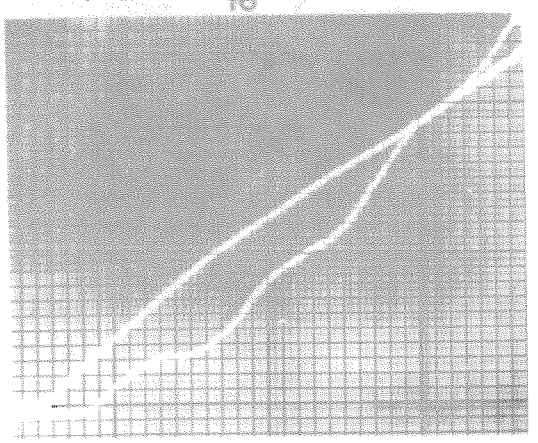

(d) $X = \frac{9}{16}$

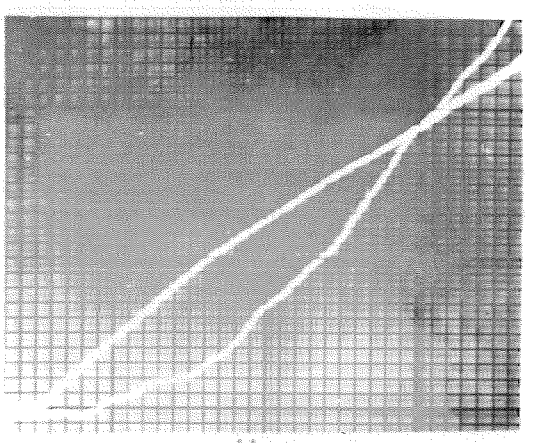

(e) $X = \frac{11}{16}$

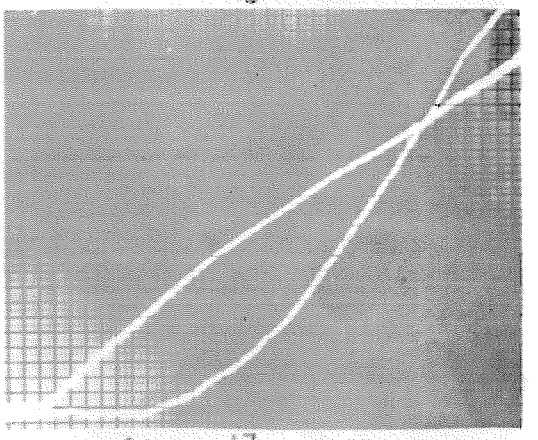

(f) $X = \frac{13}{16}$

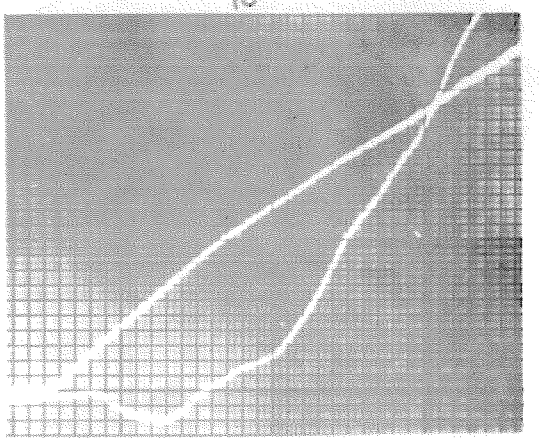

(g) $X = \frac{15}{16}$

FIG. 15

DEFLECTION OF A CANTILEVER BEAM IN RESPONSE TO AN IMPULSIVE MOTION OF THE BASE

$f_1 = 14.78$ cps

10 DIV. = .0116 SEC.

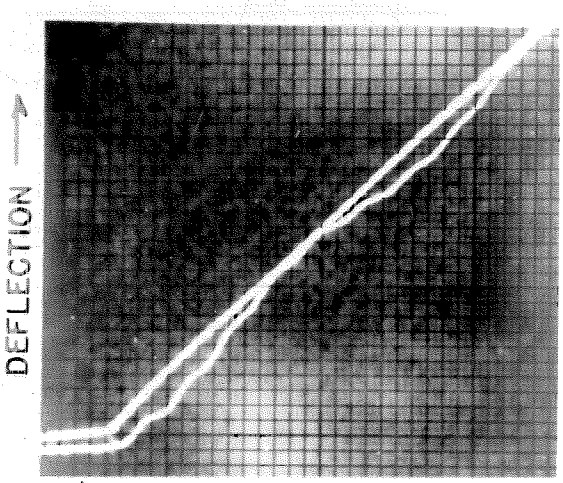

(a) DEFLECTION AT $X = \frac{7}{15}$

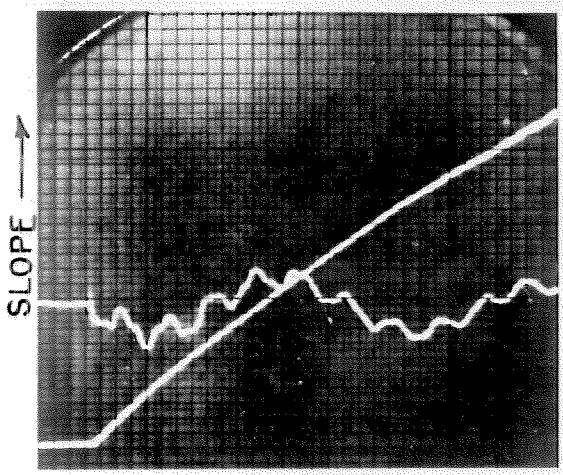

(d) SLOPE A $X = \frac{1}{8}$

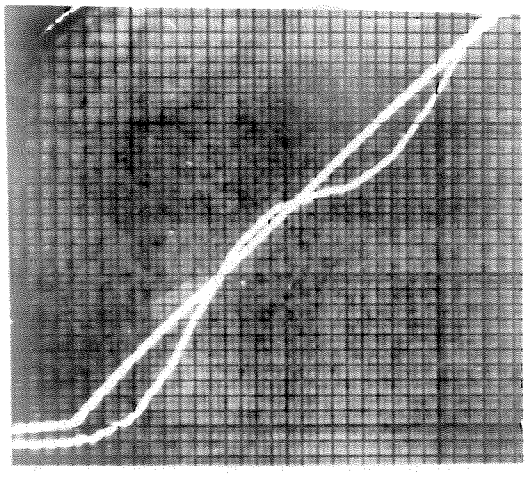

(b) DEFLECTION AT $X = \frac{11}{16}$

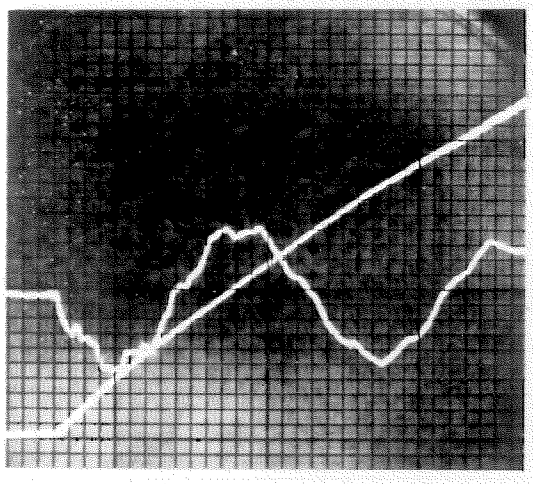

(e) SLOPE AT $X = \frac{3}{8}$

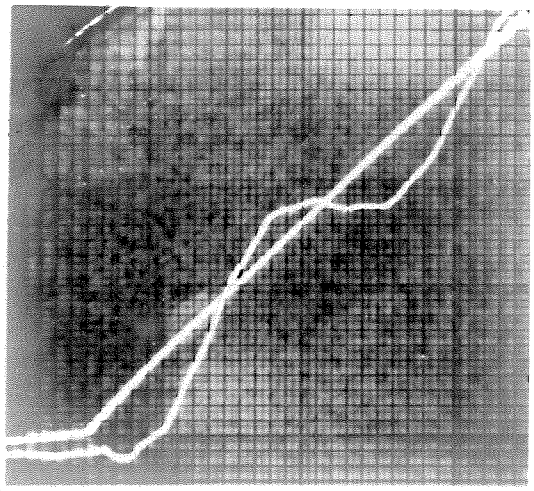

(c) DEFLECTION AT $X = \frac{15}{16}$

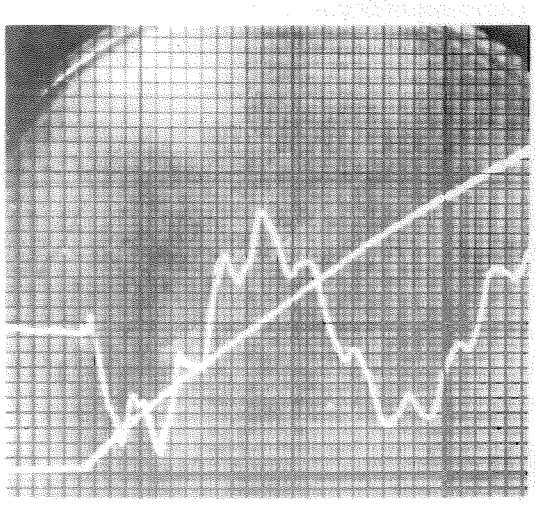

(f) SLOPE AT $X = \frac{7}{8}$

FIG. 16 RESPONSE OF A CANTILEVER BEAM TO AN IMPULSIVE MOTION OF THE BASE

$f_1 = 43.75$ cps 10 DIV. = .0124 SEC.

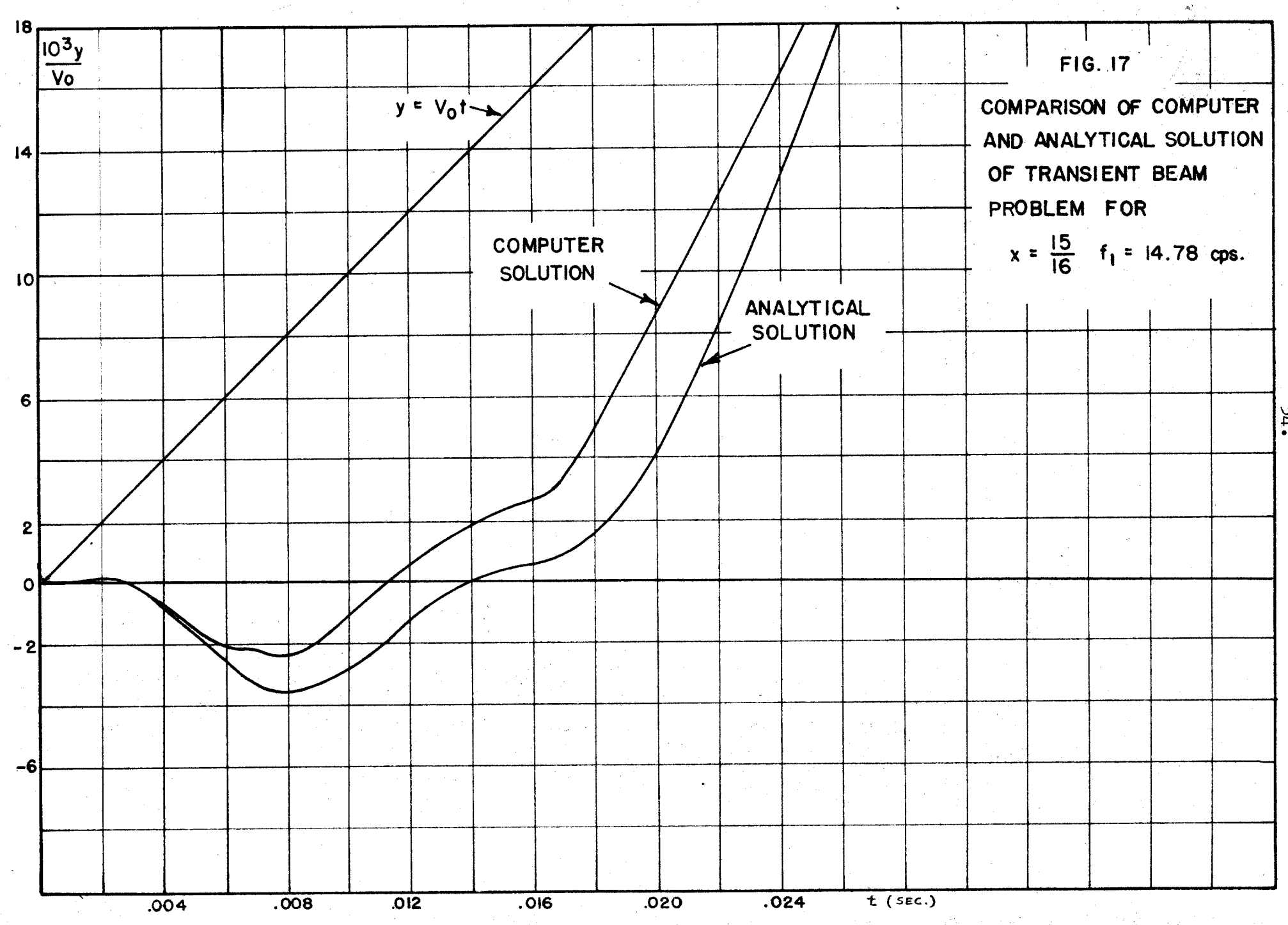

FIG. 17

COMPARISON OF COMPUTER AND ANALYTICAL SOLUTION OF TRANSIENT BEAM PROBLEM FOR

$x = \frac{15}{16}$ $f_1 = 14.78$ cps.

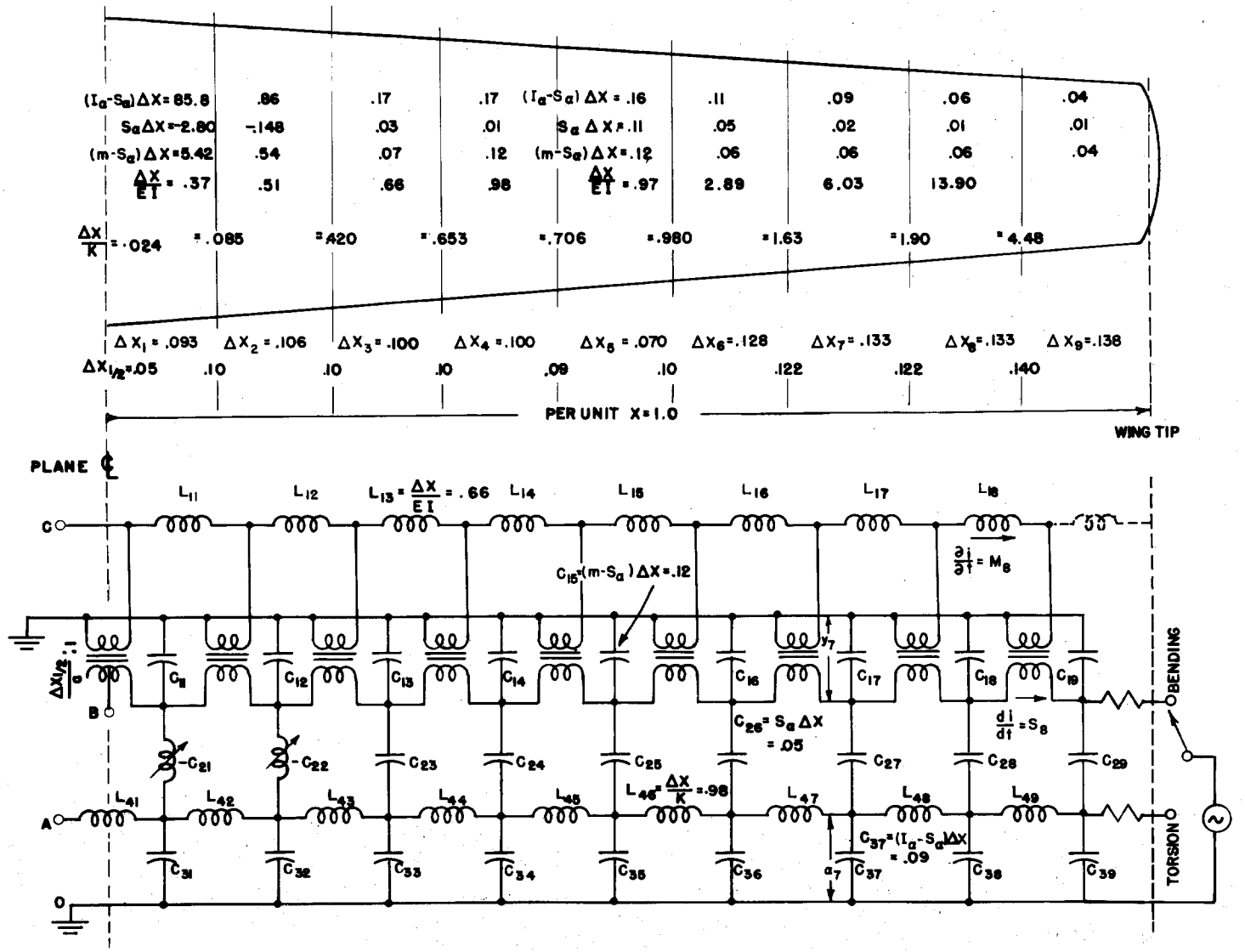

FIG. 16 EQUIVALENT CIRCUIT OF AIRPLANE WING IN TORSION AND BENDING

BOUNDARY CONDITIONS. FOR SYMMETRIC MODES OPEN A AND B, SHORT C TO GROUND. . FOR UNSYMMETRIC MODES SHORT A AND B TO GROUND, OPEN C .

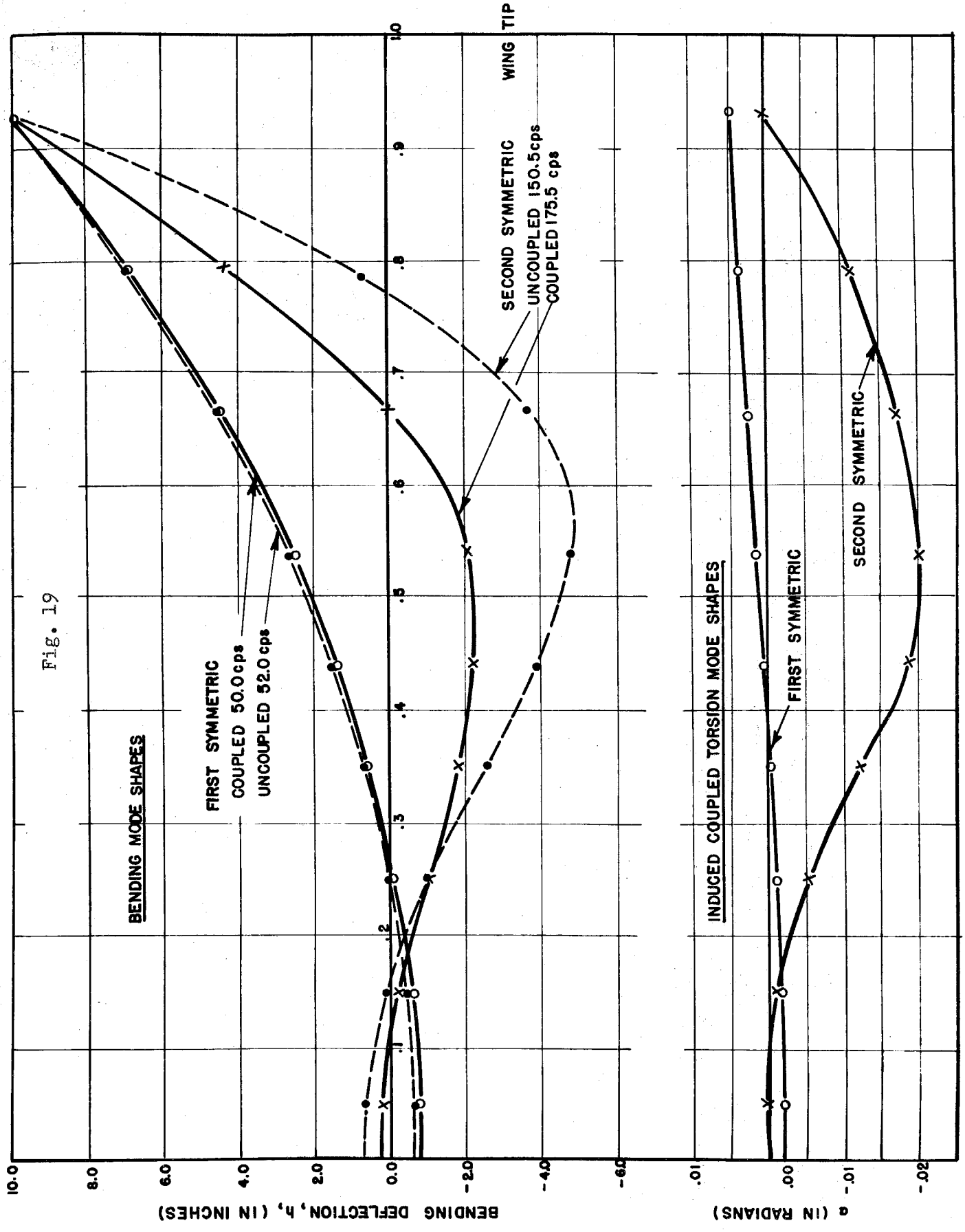
BENDING MODE SHAPES
FIRST SYMMETRIC
COUPLED 50.0 cps
UNCOUPLED 52.0 cps
SECOND SYMMETRIC
UNCOUPLED 150.5cps
COUPLED 175.5 cps
WING TIP
BENDING DEFLECTION, h, (IN INCHES)
INDUCED COUPLED TORSION MODE SHAPES
FIRST SYMMETRIC
SECOND SYMMETRIC
α (IN RADIANS)

Fig. 19

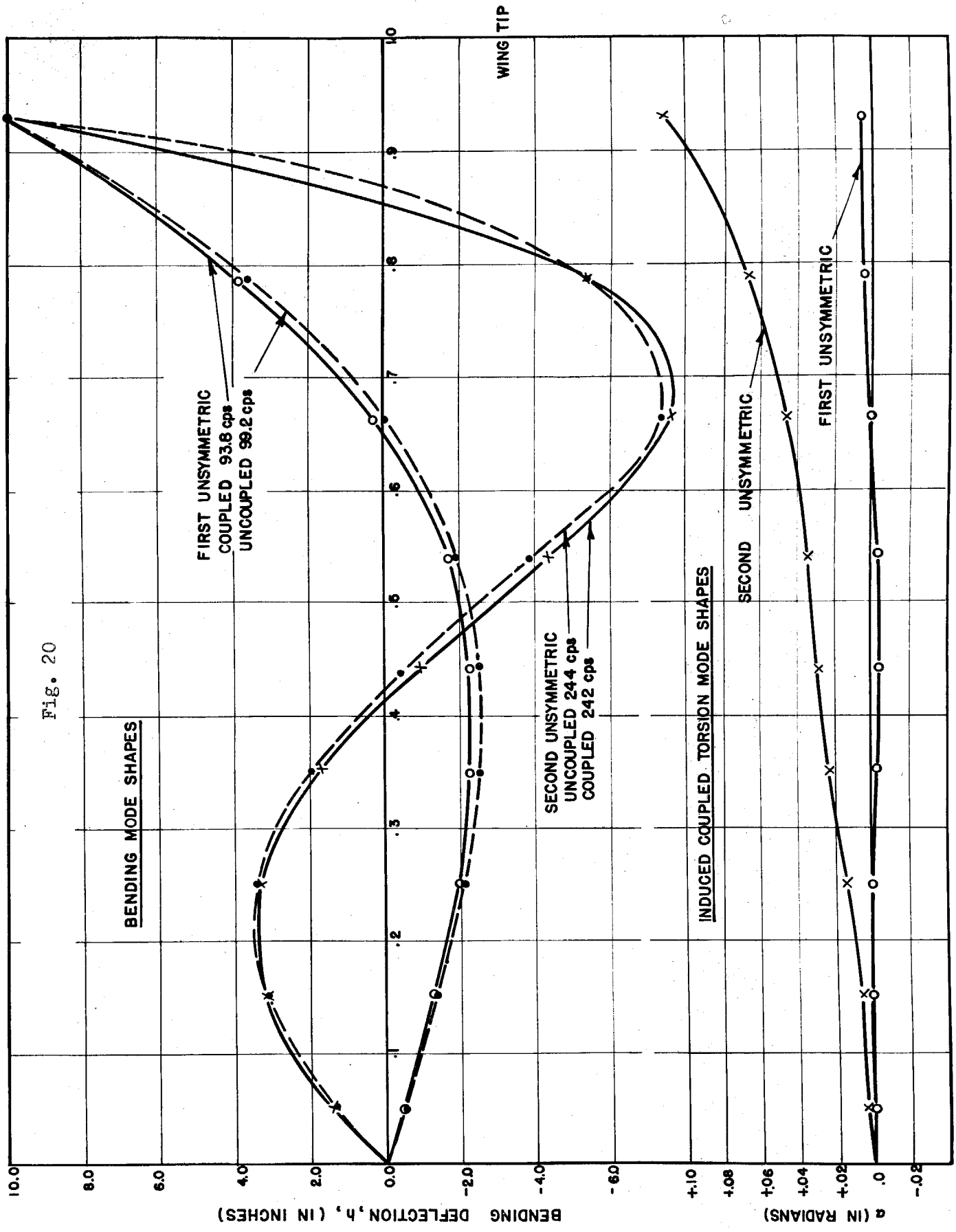
BENDING MODE SHAPES
FIRST UNSYMMETRIC
COUPLED 93.8 cps
UNCOUPLED 99.2 cps
SECOND UNSYMMETRIC
UNCOUPLED 244 cps
COUPLED 242 cps
INDUCED COUPLED TORSION MODE SHAPES
SECOND UNSYMMETRIC
FIRST UNSYMMETRIC
WING TIP
BENDING DEFLECTION, h, (IN INCHES)
α (IN RADIANS)
10.0
8.0
6.0
4.0
2.0
0.0
-2.0
-4.0
-6.0
+.10
+.08
+.06
+.04
+.02
0.
-.02
.1
.2
.3
.4
.5
.6
.7
.8
.9
1.0

Fig. 20

III PROBLEMS INVOLVING THE SCALAR LAPLACIAN OPERATOR

It is difficult to exaggerate the importance of the Laplacian operator. A branch of mathematics, potential theory, is devoted to its study and in every branch of physics numerous examples will be found of its application. The numerical and network solutions of two dimensional problems involving the Laplacian operator has also received considerable attention. In his book, Relaxation Methods in Theoretical Physics, R. V. Southwell has applied finite difference methods with very great success to a large number of problems all of which involve the two dimensional Laplacian operator. Southwell used a network of strings under tension as an analogy for the finite difference net. He could as easily have used a net of electrical resistances[15,16] to give a physical interpretation to his ideas. The electrical analogy has an advantage in that the concept of reactive impedance can be used to extend the technique to time-dependent problems.

Many problems whose general equations are written in vector or tensor form reduce to the solution of a scalar Laplacian in important special cases. For example, the equations of elasticity are simplified in this way when only plane shearing stresses need be considered. Maxwell's equations reduce to a two dimensional scalar Laplacian form whenever variations with respect to one of the three orthogonal space coordinates is eliminated. Since it is not considered practical to construct an analog computor for the solution of equations with three space coordinates, only two-dimensional problems will be considered.

In the analytical solution of plane potential problems great

difficulty is usually encountered when the medium is inhomogeneous, or anisotropic. For the relaxation and network methods of solution, inhomogeneity makes little difference whereas anisotropy, unless it be constant in direction, can be troublesome. Fortunately anisotropy can often be removed by a transformation of coordinates.

The decisive advantage of finite-difference methods lies in the treatment of irregular boundaries. Whereas such boundaries pose very great difficulties for analytical methods of solution, the generality of the finite-difference technique is such that the shape of the boundaries is a matter of indifference.

3.1 The Rectangular Net

By using the methods of Part I a network analogy can be constructed for a linear second order partial differential equation with two space coordinates. Consider the equation:

$$\frac{\partial}{\partial x}\left(f_1(x,y)\frac{\partial \phi}{\partial x}\right) + \frac{\partial}{\partial y}\left(f_2(x,y)\frac{\partial \phi}{\partial y}\right) + f_3(x,y)\phi + f_4(x,y) = 0 \qquad (3.1)$$

The finite difference equivalent of this equation for the node m,n is:

$$\begin{aligned} &\frac{\Delta y}{\Delta x}\left\{\left[\phi_{m+1,n} - \phi_{m,n}\right]\cdot f_1(m+\tfrac{1}{2},n) + \left[\phi_{m-1,n} - \phi_{m,n}\right]\cdot f_1(m-\tfrac{1}{2},n)\right\} \\ &+ \frac{\Delta x}{\Delta y}\left\{\left[\phi_{m,n+1} - \phi_{m,n}\right]\cdot f_2(m,n+\tfrac{1}{2}) + \left[\phi_{m,n-1} - \phi_{m,n}\right]\cdot f_2(m,n-\tfrac{1}{2})\right\} \\ &+ \Delta x \Delta y\left\{f_3(m,n)\,\phi_{m,n} + f_4(m,n)\right\} = 0 \end{aligned} \qquad (3.2)$$

where the f's are written as functions of the node indices rather than of x and y. The electrical network representation of this equation for the node m,n is shown in Fig. 21.

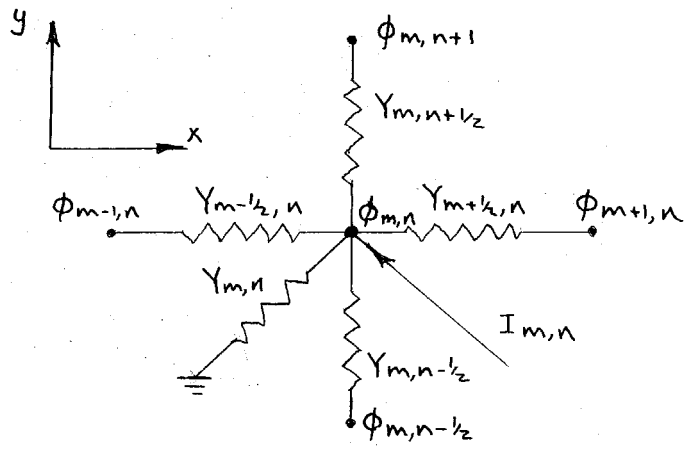

Fig. 21. Electrical Network for Eqn.(3.2)

The values of the electrical elements of Fig. 21 are:

$$
\begin{aligned}
Y_{m+\frac{1}{2},n} &= \frac{\Delta y}{\Delta x} f_1(m+\tfrac{1}{2},n) \\
Y_{m-\frac{1}{2},n} &= \frac{\Delta y}{\Delta x} f_1(m-\tfrac{1}{2},n) \\
Y_{m,n+\frac{1}{2}} &= \frac{\Delta x}{\Delta y} f_2(m,n+\tfrac{1}{2}) \\
Y_{m,n-\frac{1}{2}} &= \frac{\Delta x}{\Delta y} f_2(m,n-\tfrac{1}{2}) \\
Y_{m,n} &= -\Delta x \Delta y \cdot f_3(m,n) \\
I_{m,n} &= \Delta x \Delta y \cdot f_4(m,n)
\end{aligned}
\qquad (3.3)
$$

Scale and impedance base changing factors may be introduced into these formulae if it is so desired. The completed network for the solution of eqn.(3.1) will be a grid of horizontal and vertical elements connecting neighboring nodes.

For most problems of practical interest f_1 and f_2 will be positive functions of x and y. We then see that if f_3 is negative for all values of x and y, that the network of Fig. 21 may be constructed entirely of resistances. If f_3 is positive, then, for a fixed network frequency, $Y_{m,n}$ can be represented by a capacitor while the other admittances will be represented by inductors. This arrangement is also applicable when $f_3(x,y)\cdot\phi$ in eqn.(3.1) is replaced by

$-f_3(x,y)\frac{\partial^2\phi}{\partial t^2}$: i.e. when eqn.(3.1) is the wave equation. In this case a capacitor whose value is

$$C_{m,n} = \Delta x \Delta y \, f_3(m,n) \tag{3.4}$$

replaces $Y_{m,n}$.

When $f_3(x,y)\cdot\phi$ is replaced by $-f_3(x,y)\frac{\partial\phi}{\partial t}$ eqn.(3.1) becomes the equation of transient heat flow. In this case $Y_{m,n}$ can be represented by a capacitor whose value is given by eqn.(3.4). The other admittances can be represented by resistive elements, the value of whose conductances are given by eqn.(3.3).

The question of unequal lumping is one of considerable importance for two dimensional electrical nets. There may be regions in the plane which require considerably more detail than other regions. All that can be done if the rectangular character of the network is to be preserved is to transform each of the space coordinates separately according to the procedure outlined in section 1.3. A more general transformation will involve diagonal branches in the network.

The question of unequal lumping is connected with the problem of the representation of boundary points. In contrast with the problems of one space variable it is not always possible to allow the boundaries of the space to coincide with nodes of the network. Unless the boundaries are natural for the coordinate system being used (rectangular for Cartesian coordinates) the boundary will cross some network branches at intermediate points. Two general approaches are possible in the representation of such points. The regular character of the network may be retained and the treatment of "irregular stars" may proceed on the basis of physical reasoning and ficticious nodes.*

* See section 4.6 or ref. 6, pages 67-78

On the other hand the nodes may be placed on the boundary and interconnected with interior points by an asymmetrical network, as will be explained in the next section. This asymmetrical network, being perfectly general, can also be used for varying the cell size, and obtaining increased detail in critical regions.

Eqn.(3.1) can represent Poisson's equation for an anisotropic medium since $f_1(x,y)$ and $f_2(x,y)$ can be different functions. The principal axes of the anisotropy, however, are necessarily parallel to the coordinate axes. A more general equation than eqn.(3.1) is

$$\frac{\partial}{\partial x}\left(f_1(x,y)\frac{\partial \phi}{\partial x}\right) + \frac{\partial}{\partial y}\left(f_2(x,y)\frac{\partial \phi}{\partial y}\right) + \frac{\partial}{\partial x}\left(f_5(x,y)\frac{\partial \phi}{\partial y}\right) + \frac{\partial}{\partial y}\left(f_6(x,y)\frac{\partial \phi}{\partial x}\right) + f_3(x,y)\cdot\phi + f_4(x,y) = 0 \qquad (3.5)$$

The additional terms can be represented by diagonal admittance branches if f_5 and f_6 are constants. When f_5 and f_6 are slowly varying functions the method to be described may be adequate if the finite difference cells are small. The finite difference equivalent of such a term is given by

$$\left(K\frac{\partial^2 \phi}{\partial x \partial y}\right)_{m,n} \simeq \frac{K}{4\Delta x \Delta y}\left[\phi_{m+1,n+1} - \phi_{m+1,n-1} - \phi_{m-1,n+1} + \phi_{m-1,n-1}\right] \qquad (3.6)$$

The network branches to represent these terms are shown in Fig. 22a. This circuit has the disadvantage that two of the four admittances must be negative. An alternative form of eqn.(3.6) useful when K is positive, is:

$$\left(K\frac{\partial^2 \phi}{\partial x \partial y}\right)_{m,n} \simeq \frac{K}{2\Delta x \Delta y}\left[\phi_{m+1,n+1} - \phi_{m+1,n} - \phi_{m,n+1} + \phi_{m,n}\right] + \frac{K}{2\Delta x \Delta y}\left[\phi_{m,n} - \phi_{m,n-1} - \phi_{m-1,n} + \phi_{m-1,n-1}\right] \qquad (3.7)$$

The network to represent these terms is shown in Fig. 22b. If K is small compared with the coefficients of the other terms of the differential equation, the resultant value of the horizontal and vertical admittances will still be positive. Fig. 22c shows the appropriate network for the case when K is negative.

It will be shown in section 3.4 that under certain conditions eqn.(3.5) represents Poisson's equation for an isotropic medium in which the coordinates x and y are not orthogonal and that an electrical network can be constructed that will solve the problem in this coordinate system.

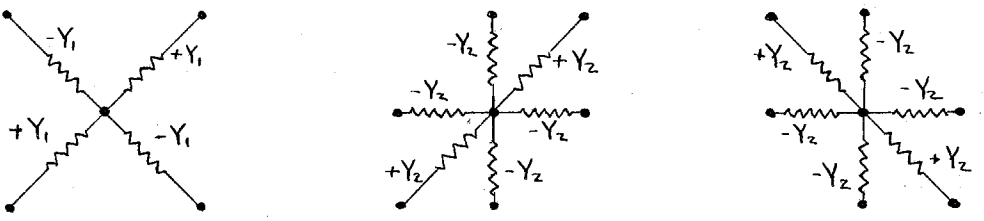

(a) K positive (b) K positive (c) K negative

$$Y_1 = \frac{K}{4\Delta x \Delta y} \qquad Y_2 = \frac{K}{2\Delta x \Delta y}$$

Fig. 22. Networks to Represent $K\left[\frac{\partial^2 \phi}{\partial x \partial y}\right]_n$

3.2 The Asymmetric Net

In this section we shall derive a very general two dimensional network for the representation of the Laplacian operator. Since current flow in a conducting sheet satisfies Laplace's equation, it is convenient to use this analogy in discussing the problem. The problem may be stated as follows. "Imagine an isotropic region, R, in which Laplace's equation is known to apply and a large number of points, p, in R chosen at random. In what way should the points be

interconnected with electrical resistances in order that the voltages at the nodes shall be as nearly as possible the correct solutions of Laplace's equation?"

The first step in the solution of this problem is to connect the points, p, by a net of triangles. The resulting configuration is shown in Fig. 23. Branches of the net should not cross each other and none of the triangles should be obtuse. It may be necessary in order to fulfil the second condition to insert additional points.

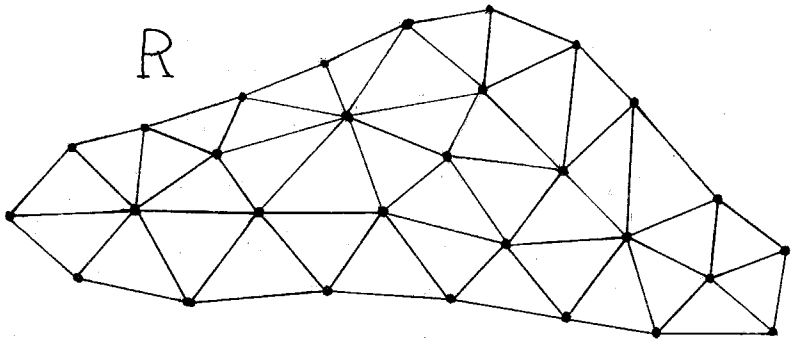

Fig. 23. An Asymmetric Net

Consider a portion of this net shown in Fig. 24. Drawing the perpendicular bisectors of the sides of the triangles divides the region into polygons surrounding each point, p. We shall consider the interior of the polygons as the cells into which the region is divided and the dotted lines as the boundaries across which current flows from one cell to another. This distributed flux will be replaced by current flowing in a single conductor connecting the centers of adjacent cells. The problem is to calculate the resistance of these conductors.

In two dimensions the solution of Laplace's equation may be written as $W = \phi + j\psi$, where ϕ and ψ are orthogonal potential functions. We shall identify ϕ with the scalar potential and ψ with the flux.

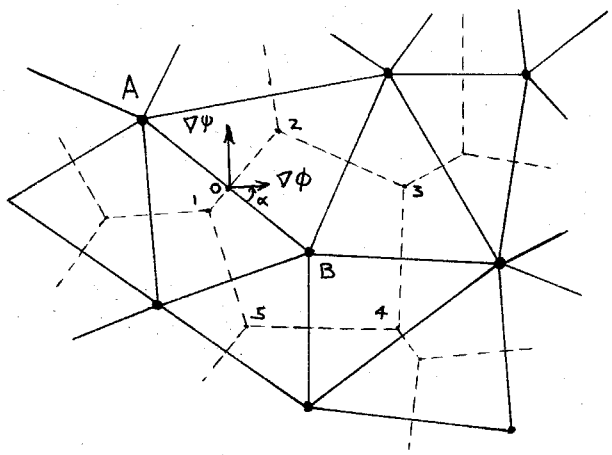

Fig. 24.

If the voltage across the junction pair $\overline{AB}$ is $\phi_A - \phi_B$ then the current in the branch $\overline{AB}$ may be identified with the normal flux crossing the boundary 1-2.

The potential difference between the points A and B is

$$\phi_B - \phi_A = \int_A^B \nabla\phi \cdot d\underset{\sim}{S} \tag{3.8}$$

where any path may be taken in going from A to B. This, incidentally, says that the net change in potential around a completed loop is zero which is, of course, satisfied by a lumped electrical network.

The normal flux crossing the boundary 1-2 is:

$$\psi_2 - \psi_1 = \int_1^2 \nabla\psi \cdot d\underset{\sim}{\ell} \tag{3.9}$$

The region is assumed to be isotropic so that the lines of current flow are parallel to the potential gradient:

$$\underset{\sim}{i} = -\sigma \nabla \phi \tag{3.10}$$

The surface conductivity, σ, can be a function of position i.e. the conducting sheet may be inhomogeneous.

The gradient of the flux is given by

$$\nabla\psi = \underset{\sim}{k} \times \underset{\sim}{i} = -\sigma(\underset{\sim}{k} \times \nabla\phi) \tag{3.11}$$

where k is a unit vector normal to the surface. Then

$$\psi_2 - \psi_1 = -\sigma \int_1^2 (\underset{\sim}{k} \times \nabla\phi) \cdot d\underset{\sim}{\ell} \tag{3.12}$$

Approximations will now be made to the integrals in eqns.(3.8) and (3.12). It is assumed that the mesh is sufficiently fine that the magnitude and direction of $\nabla\phi$ change slowly in the region shown in Fig. 24. If in eqn.(3.8) the path of integration is chosen as the straight line $\overline{AB}$ then a good approximation is:

$$\phi_B - \phi_A \simeq \nabla\phi_o \, \overline{AB} \cos\alpha \tag{3.13}$$

where $(\nabla\phi)_0$ is the absolute magnitude of the gradient measured at O, the intersection of $\overline{AB}$ and 1-2. This point is halfway between A and B. α is the angle between the gradient and the line $\overline{AB}$ at the point O.

A good approximation to eqn.(3.12) is:

$$\psi_2 - \psi_1 \simeq -\sigma_o \, \nabla\phi_o \ell_{12} \cos\alpha \tag{3.14}$$

where ℓ_{12} is the distance between 1 and 2. The point O is not necessarily at the midpoint of ℓ_{12}. Consequently the approximation for the flux is not as accurate as that for the voltage. If the mesh is sufficiently fine, this will not lead to a large error. It indicates, however, that an attempt should be made to keep the triangles as nearly regular as possible. From eqns.(3.13) and (3.14) we see that

$$\frac{\phi_A - \phi_B}{\psi_2 - \psi_1} = \frac{\overline{AB}}{\sigma_o \ell_{12}} \tag{3.15}$$

where $\psi_2 - \psi_1$ is the total current crossing the boundary 1-2. If this current flows in a single wire then the appropriate value of the resistance of the wire is:

$$R_{AB} = \frac{\overline{AB}}{\sigma_o l_{12}} \tag{3.16}$$

We now have a simple formula for calculating the value of resistance for every branch in Fig. 24. This network can immediately be applied to Poisson's equation. The additional terms in Poisson's equation represent current density while the currents in the network of Fig. 24 represent total flux. Consequently the additional terms in Poisson's equation should be multiplied by an appropriate area if they are to be included in the network. The appropriate area for the point B of Fig. 24 is that of the polygon 1-2-3-4-5.

A construction will now be described* that makes it unnecessary to draw the dotted polygons of Fig. 24. An enlarged view of a portion of Fig. 24 is shown in Fig. 25.

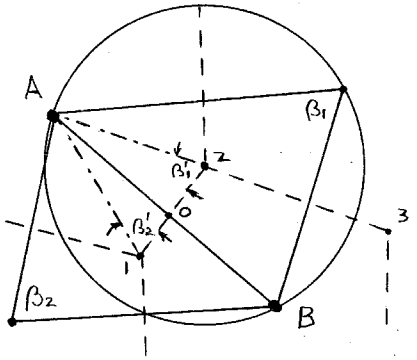

Fig. 25.

By a theorem in geometry we know that the point where the perpendicular bisectors of the sides of a triangle meet is the center of the circumscribed circle. By another theorem the angles β_1 and β_1' of Fig. 25 are equal. Hence

$$\frac{l_{o2}}{\overline{AB}} = \frac{1}{2} \operatorname{ctn} \beta_1' = \frac{1}{2} \operatorname{ctn} \beta_1 \tag{3.17}$$

---

* This construction was suggested by Dr. Stanley Frankel of the Analysis Laboratory.

and similarly

$$\frac{\ell_{10}}{\overline{AB}} = \frac{1}{2}\,\mathrm{ctn}\beta_2 \tag{3.18}$$

The value of the admittance inserted in the branch $\overline{AB}$ is, from eqn.(3.16):

$$Y_{AB} = \frac{\sigma_o \ell_{12}}{\overline{AB}} = \frac{\sigma_o}{2}\,(\mathrm{ctn}\beta_1 + \mathrm{ctn}\beta_2) \tag{3.19}$$

For Poisson's equation the area appropriate to the point A can be divided into triangles of which the triangle A-1-2 will be one. The area of this triangle is

$$\frac{1}{4}\,\overline{AB}\,\ell_{12} = \frac{(\overline{AB})^2}{8}\,(\mathrm{ctn}\beta_1 + \mathrm{ctn}\beta_2) \tag{3.20}$$

The total area of the polygon is a sum of such terms, one for each neighboring point. For the calculation of admittances and areas, the function $(\mathrm{ctn}\beta_1 + \mathrm{ctn}\beta_2)$ and the distances $\overline{AB}$ must be calculated for every branch in the network. If the network is first laid out on a large sheet of drawing paper, the angles can be measured with a protractor and the distances scaled off with sufficient accuracy in a short time.

The method described in this section will work for any network configuration in which the perpendicular bisectors of the branches meet at a point. Thus, besides for triangles, the method will work for rectangles, regular hexagons and isosceles trapezoids. Southwell[6] has derived the relaxation patterns for equilateral triangles and regular hexagons by entirely different methods. For the limiting case of an equilateral triangle the constants of the asymmetric net are identical with his results.

3.3 Boundary Conditions for the Asymmetric Net

A portion of an asymmetric net near a boundary of the region is shown in Fig. 26. Some of the points of the net have been chosen to lie on the boundary.

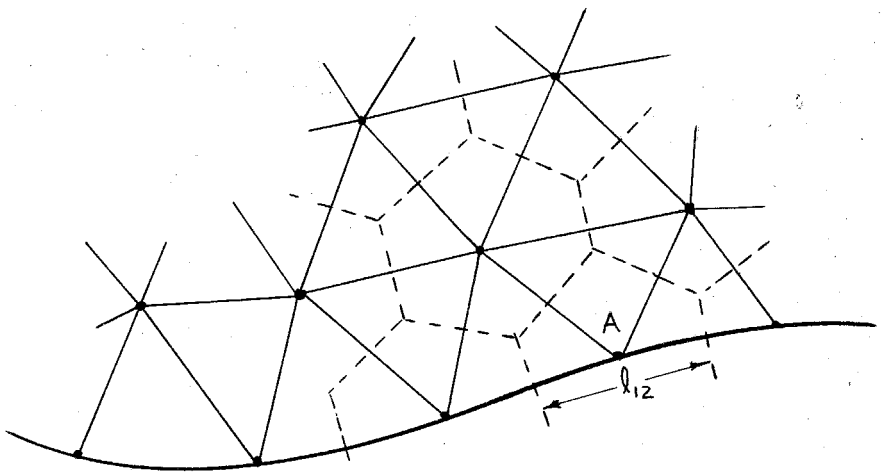

Fig. 26. Asymmetric Net at a Boundary

Three types of boundary conditions will be considered with respect to Fig. 26.

1. The potential ϕ specified at the boundary: In this case the voltages at the nodes on the boundary are set equal to the specified values. For most problems this value will be zero or a constant value.

2. The normal gradient, $\frac{\partial \phi}{\partial n}$, specified at the boundary: In this case currents that are equal to the total flux crossing the boundary into the corresponding polygon are fed into the boundary points. The current fed into node A is equal to $\sigma_A \left(\frac{\partial \phi}{\partial n}\right)_A \cdot \ell_{12}$. For Poisson's equation additional currents must be fed into every node of the network including the boundary points. These currents are proportional to the portion of the area of the surrounding polygon that is interior to the region.

3. The quantity, $\phi + K\sigma\frac{\partial\phi}{\partial n}$, specified at the boundary: This type of boundary condition is encountered, for example, in connection with the cooling of metal rods. If

$$\phi_A + K\sigma_A \left(\frac{\partial\phi}{\partial n}\right)_A = \phi_o \tag{3.21}$$

then the total current entering the node A is

$$I_A = \sigma_A \ell_{12} \left(\frac{\partial\phi}{\partial n}\right)_A = \frac{\ell_{12}}{K}(\phi_o - \phi_A) \tag{3.22}$$

To satisfy this condition, A is connected to a source of potential, ϕ_0, through an admittance whose value is $\frac{\ell_{12}}{K}$.

3.4 Poisson's Equation in Tensor Form

The purpose of this section is to show that a space which is anisotropic can, under certain conditions, be transformed into a space which is isotropic and, if it is desired, also homogeneous. With the anisotropy removed, the asymmetric net can be used to full advantage. Using tensor notation eqn.(3.5) of section 3.1 can be written in the following form:

$$\frac{\partial}{\partial x^\alpha}\left(f^{\alpha\beta}\frac{\partial\phi}{\partial x^\beta}\right) + \rho = 0 \tag{3.23}$$

ρ represents the last two terms of eqn.(3.5). The indices α and β are summed over the coordinates x^1 and x^2.

In vector form, Poisson's equation for an inhomogeneous but isotropic medium can be written as

$$\nabla\cdot(K\nabla\phi) + \tau = 0 \tag{3.24}$$

Poisson's equation can also be expressed in the following tensor form*

---

* See A. D. Michal, ref. 17 page 117

$$\frac{1}{\sqrt{g}} \frac{\partial}{\partial x^\alpha} \left(\sqrt{g}\, g^{\alpha\beta} K \frac{\partial \phi}{\partial x^\beta}\right) + \tau = 0 \qquad (3.25)$$

This equation holds for a three dimensional space as well as for a two dimensional space. It is evidently a scalar equation. The significance of the g's is as follows. In a Euclidean 2-space the distance between two points is given by

$$(ds)^2 = g_{11}(dx^1)^2 + 2g_{12}(dx^1 dx^2) + g_{22}(dx^2)^2 \qquad (3.26)$$

or

$$(ds)^2 = g_{\alpha\beta}\, dx^\alpha\, dx^\beta$$

Referring to Fig. 27 we see that $\sqrt{g_{11}}$ is the length of a unit vector along x^1, that $\sqrt{g_{22}}$ is the length of a unit vector along x^2 and that

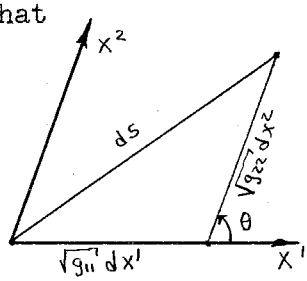

Fig. 27.

$$g_{12} = \sqrt{g_{11} g_{12}} \cos\theta \qquad (3.27)$$

$g_{\alpha\beta}$ is called the Euclidean metric tensor. The determinant of this tensor is (for a 2-space)

$$g = \begin{vmatrix} g_{11} & g_{12} \\ g_{12} & g_{22} \end{vmatrix} = g_{11}g_{22} - (g_{12})^2 \qquad (3.28)$$

The symbol $g^{\alpha\beta}$ used in eqn.(3.25) is the associated contravarient metric tensor. In a Euclidean 2-space its components are:

$$g^{11} = \frac{g_{22}}{g} \qquad g^{12} = g^{21} = -\frac{g_{12}}{g} \qquad g^{22} = \frac{g_{11}}{g} \qquad (3.29)$$

Eqns.(3.23) and (3.25) will be identical provided that

$$f^{\alpha\beta} = \sqrt{g}\, g^{\alpha\beta} K$$

$$\rho = \sqrt{g} \cdot \tau \qquad (3.30)$$

K, τ and the components of the metric tensor can be solved for by means

of these equations. Since $g^{\alpha\beta} = g^{\beta\alpha}$ we see that a necessary condition for this transformation is that $f^{\alpha\beta} = f^{\beta\alpha}$. Another necessary condition is that

$$f^{11}f^{22} - (f^{12})^2 > 0 \tag{3.31}$$

If these conditions are satisfied eqn.(3.23) can be made to represent Poisson's equation for an isotropic medium. One of the five unknown quantities in eqn.(3.30) can be chosen arbitrarily. One possible set of equivalence relationships is:

$$\begin{aligned} g_{11} &= f^{22} \\ g_{22} &= f^{11} \\ g_{12} &= -f^{12} \\ K &= \sqrt{f^{11}f^{22} - (f^{12})^2} \\ \tau &= \frac{\rho}{\sqrt{f^{11}f^{22} - (f^{12})^2}} \end{aligned} \tag{3.32}$$

With the components of the metric tensor given, the isotropic space can be constructed.

As an example consider the equation

$$a\frac{\partial^2\phi}{\partial x^2} + b\frac{\partial^2\phi}{\partial y^2} - 2c\frac{\partial^2\phi}{\partial x \partial y} = 0 \tag{3.33}$$

valid in the region shown in Fig. 28a.

a. Original Space -- Anisotropic

b. Transformed Space -- Isotropic

Fig. 28. Transformation of a Space in Order to Remove Anisotropy

The components of the metric tensor are given by

$$g_{11} = b$$
$$g_{22} = a \qquad (3.34)$$
$$g_{12} = c$$

so that the angle between the axes x and y is given by:

$$\theta = \cos^{-1} \frac{c}{\sqrt{ab}} \qquad (3.35)$$

The transformed isotropic space in which ϕ is a solution of Laplace's equation is shown in Fig. 28b.

3.5 The Separation of Maxwell's Equations into E and H Modes

In the next two sections examples will be given of the solution of Maxwell's equations in a space with axial symmetry. As a preliminary step to these solutions this section will describe the separation of Maxwell's equations into E and H modes for the case when there is no dependence on one of the coordinates in an orthogonal coordinate system.

Maxwell's equations may be written in M.K.S. units as follows for an orthogonal coordinate system.* The physical components of the field vectors are employed.

---

* See Stratton, ref. 18, page 50

$$\frac{1}{h_2h_3}\left[\frac{\partial}{\partial u^2}(h_3E_{(3)}) - \frac{\partial}{\partial u^3}(h_2E_{(2)})\right] + \frac{\partial B(1)}{\partial t} = 0$$

$$\frac{1}{h_1h_3}\left[\frac{\partial}{\partial u^3}(h_1E_{(1)}) - \frac{\partial}{\partial u^1}(h_3E_{(3)})\right] + \frac{\partial B(2)}{\partial t} = 0$$

$$\frac{1}{h_1h_2}\left[\frac{\partial}{\partial u^1}(h_2E_{(2)}) - \frac{\partial}{\partial u^2}(h_1E_{(1)})\right] + \frac{\partial B(3)}{\partial t} = 0$$

$$\frac{1}{h_2h_3}\left[\frac{\partial}{\partial u^2}(h_3H_{(3)}) - \frac{\partial}{\partial u^3}(h_2H_{(2)})\right] - \frac{\partial D(1)}{\partial t} - I_{(1)} = 0$$

$$\frac{1}{h_1h_3}\left[\frac{\partial}{\partial u^3}(h_1H_{(1)}) - \frac{\partial}{\partial u^1}(h_3H_{(3)})\right] - \frac{\partial D(2)}{\partial t} - I_{(2)} = 0 \qquad (3.36)$$

$$\frac{1}{h_1h_2}\left[\frac{\partial}{\partial u^1}(h_2H_{(2)}) - \frac{\partial}{\partial u^2}(h_1H_{(1)})\right] - \frac{\partial D(3)}{\partial t} - I_{(3)} = 0$$

$$\frac{\partial}{\partial u^1}(h_2h_3B_{(1)}) + \frac{\partial}{\partial u^2}(h_1h_3B_{(2)}) + \frac{\partial}{\partial u^3}(h_1h_2B_{(3)}) = 0$$

$$\frac{\partial}{\partial u^1}(h_2h_3D_{(1)}) + \frac{\partial}{\partial u^2}(h_1h_3D_{(2)}) + \frac{\partial}{\partial u^3}(h_1h_2D_{(3)}) = \rho h_1h_2h_3$$

where

$$B_{(1)} = \mu H_{(1)} \qquad D_{(1)} = \varepsilon E_{(1)} \qquad I_{(1)} = \sigma E_{(1)} \qquad (3.37)$$

Substitute covariant components for physical components

$$\begin{aligned} h_\alpha E_{(\alpha)} &= E_\alpha \\ h_\alpha H_{(\alpha)} &= H_\alpha \\ h_2h_3B_{(1)} &= \mu\frac{h_2h_3}{h_1}H_1 \\ h_2h_3D_{(1)} &= \varepsilon\frac{h_2h_3}{h_1}E_1 \\ h_2h_3I_{(1)} &= \sigma\frac{h_2h_3}{h_1}E_1 \end{aligned} \qquad (3.38)$$

Also set $\frac{\partial}{\partial u^3} = 0$. Then the equations fall into two sets.

$$\begin{aligned}
&\frac{\partial E_3}{\partial u^2} + \mu\frac{\partial}{\partial t}\left(\frac{h_2h_3}{h_1} H_1\right) = 0 \\
&-\frac{\partial E_3}{\partial u^1} + \mu\frac{\partial}{\partial t}\left(\frac{h_1h_3}{h_2} H_2\right) = 0 \\
&\frac{\partial H_2}{\partial u^1} - \frac{\partial H_1}{\partial u^2} - \varepsilon\frac{\partial\left(\frac{h_1h_2}{h_3} E_3\right)}{\partial t} - \sigma\frac{h_1h_2}{h_3} E_3 = 0 \\
&\mu\left[\frac{\partial}{\partial u^1}\left(\frac{h_2h_3}{h_1} H_1\right) + \frac{\partial}{\partial u^2}\left(\frac{h_1h_3}{h_2} H_2\right)\right] = 0
\end{aligned} \tag{3.39}$$

$$\begin{aligned}
&\frac{\partial H_3}{\partial u^2} - \varepsilon\frac{\partial\left(\frac{h_2h_3}{h_1} E_1\right)}{\partial t} - \sigma\frac{h_2h_3}{h_1} E_1 = 0 \\
&-\frac{\partial H_3}{\partial u^1} - \varepsilon\frac{\partial\left(\frac{h_1h_3}{h_2} E_2\right)}{\partial t} - \sigma\frac{h_1h_3}{h_2} E_2 = 0 \\
&\frac{\partial E_2}{\partial u^1} - \frac{\partial E_1}{\partial u^2} + \mu\frac{\partial}{\partial t}\left(\frac{h_1h_2}{h_3} H_3\right) = 0 \\
&\varepsilon\left[\frac{\partial}{\partial u^1}\left(\frac{h_2h_3}{h_1} E_1\right) + \frac{\partial}{\partial u^2}\left(\frac{h_1h_3}{h_2} E_2\right)\right] = \rho h_1h_2h_3
\end{aligned} \tag{3.40}$$

Substitute $j\omega$ for $\frac{\partial}{\partial t}$. Then in the first set

$$H_1 = \frac{+j}{\omega\mu}\frac{h_1}{h_2h_3}\frac{\partial E_3}{\partial u^2}$$

and

$$H_2 = \frac{-j}{\omega\mu}\frac{h_2}{h_1h_3}\frac{\partial E_3}{\partial u^1} \tag{3.41}$$

Substitute these equations into the third of eqns.(3.39). The resulting equation is in terms of E_3 alone:

$$\frac{\partial}{\partial u^1}\left(\frac{h_2}{h_1h_3}\frac{\partial E_3}{\partial u^1}\right) + \frac{\partial}{\partial u^2}\left(\frac{h_1}{h_2h_3}\frac{\partial E_3}{\partial u^2}\right) + \frac{h_1h_2}{h_3} E_3\ (\omega^2u\varepsilon - j\omega\mu\sigma) = 0 \tag{3.42}$$

The fourth of eqns.(3.39) becomes an identity. E_3 may be regarded as a scalar field in eqn.(3.42). The second set of equations reduce to an exactly similar form:

$$\frac{\partial}{\partial u^1}\left(\frac{h_2}{h_1h_3}\frac{\partial H_3}{\partial u^1}\right) + \frac{\partial}{\partial u^2}\left(\frac{h_1}{h_2h_3}\frac{\partial H_3}{\partial u^2}\right) + \frac{h_1h_2}{h_3} H_3\cdot(\omega^2\mu\varepsilon - j\omega\mu\sigma) = 0 \tag{3.43}$$

In these equations h_3 may be regarded as a characteristic of the material. By the definition of the h's and eqns.(3.29):

$$\frac{h_2}{h_1} = \frac{h_2^2}{h_1 h_2} = \frac{g_{22}}{\sqrt{g}} = \sqrt{g}\, g^{11} \qquad (3.44)$$

and

$$\frac{h_1}{h_2} = \frac{h_1^2}{h_1 h_2} = \frac{g_{11}}{\sqrt{g}} = \sqrt{g}\, g^{22}$$

With these substitutions eqns.(3.42) and (3.43) become

$$\frac{1}{\sqrt{g}} \frac{\partial}{\partial u^\alpha}\left[\frac{\sqrt{g}\, g^{\alpha\alpha}}{h_3} \frac{\partial \begin{Bmatrix} E_3 \\ H_3 \end{Bmatrix}}{\partial u^\alpha}\right] + \frac{\omega^2 \mu\varepsilon - j\omega\mu\sigma}{h_3} \begin{Bmatrix} E_3 \\ H_3 \end{Bmatrix} = 0 \qquad (3.45)$$

This is exactly Poisson's equation for an inhomogeneous medium* in which $K = \frac{1}{h_3}$ and the components of u^α are orthogonal coordinates. In section 3.2 a general asymmetric net was developed for the solution of Poisson's equation without regard to a particular coordinate system. This method may be applied to the solution of eqn.(3.45). The actual coordinates u^1 and u^2 need not be specified.

If $h_3 = 1$, (i.e. $u^3 = \underset{\sim}{i}$, $\underset{\sim}{j}$, $\underset{\sim}{k}$ or $\underset{\sim}{r}$) then eqn.(3.45) is Poisson's equation for a homogeneous plane space. If the space has axial symmetry and $u^3 = \phi$, the azimuth angle, then $h_3 = \rho$, the distance from the axis.

3.6 Example I: The Conical Line Resonator

The use of networks for the solution of Maxwell's equations has received considerable attention in the past few years. Following G. Kron's publication of the equivalent circuits for the field equations of Maxwell[19] in May, 1944 articles appeared by mem-

---

* Compare with eqn.(3.25) page 71

bers of the General Electric Company giving results of network analyzer studies.[20,21] An outgrowth of this work was the construction of a computing facility at Stanford University[22] for the solution of wave guide and cavity resonator problems. Two calculating boards were constructed at Stanford, one for the solution of problems with plane symmetry and the other for the solution of problems with axial symmetry. Over 1000 coils are used in each network and the operating frequency is about 100 KC. The elements are arranged in a fixed rectangular pattern and have been used principally for the solution of problems with rectangular boundaries.

The Cal Tech Electric Analog Computor has at present eighty coils which is far fewer than the minimum number required for the solution of problems with complex geometrical boundaries. However, these elements may be connected in any desired pattern so that efficient use can be made of the asymmetric net.

Two considerations influenced the choice of the conical line resonator as a subject of investigation. The first is that its cross-sectional boundaries are not rectangular making it a good problem on which to try out the asymmetric net. The second is that its lowest modes are TEM modes whose expression in analytical form is particularly simple.

A cross-sectional view of the resonator is shown in Fig. 31. The conical dimples each have a half-angle of 30°. Since the conductivity of the space in an air-filled cavity is zero, eqn.(3.45) for the H modes becomes:

$$\frac{1}{\sqrt{g}}\left[\frac{\partial}{\partial u^{\alpha}}\left(\frac{\sqrt{g}\, g^{\alpha\alpha}}{\rho}\frac{\partial H_3}{\partial u^{\alpha}}\right)\right] + \frac{\omega^2 \mu \varepsilon}{\rho} H_3 = 0 \qquad (3.46)$$

where ρ is the distance from the axis and $H_3 = \rho H_\phi$. This equation is identical with Poisson's equation for an inhomogeneous plane sheet in which the conductivity $K = \frac{1}{\rho}$ and the density of the inserted currents is given by the second term.

A network representing one half of the cavity is shown in Fig. 29. It is necessary to represent only one-half of the cavity since all normal modes must be either symmetrical or anti-symmetrical with respect to the equatorial plane. These conditions can be imposed by either opening or shorting the network along the center line. The values of the network elements were calculated as follows. Fig. 29 was laid out on a large sheet of graph paper with the radius, a, arbitrarily chosen as 24 divisions. Then the geometrical factors $\frac{\rho \overline{AB}}{\ell_{12}}$* were computed for every branch and the effective areas associated with each node were divided by ρ. The values of the inductors were calculated from

$$L = K_1 \frac{\rho \overline{AB}}{\ell_{12}} \tag{3.47}$$

where K_1 is an arbitrary constant. The capacitors were calculated from

$$C = K_2 \frac{(\text{Area of Cell})}{\rho} \tag{3.48}$$

where K_2 is an arbitrary constant. The value of $\mu\epsilon$ in eqn.(3.46) is equal to $K_1 K_2$. In M.K.S. units $\frac{1}{\sqrt{\mu\epsilon}}$ is the velocity of propagation. K_1 was chosen as 10^{-2} and K_2 was chosen as 10^{-6}. The constants that describe the problem are then:

$$\begin{aligned} a &= 24 \text{ (units)} \\ v_c &= \frac{1}{\sqrt{\mu\epsilon}} = 10^4 \text{ (units)/sec.} \\ \theta_o &= 30^\circ \end{aligned} \tag{3.49}$$

The boundary conditions for H modes along the walls of the cavity

---

* See eqn.(3.16)

are $\frac{\partial H_3}{\partial n} = 0$. This is imposed on the lumped electrical network by opening the circuit at the edges as shown in Fig. 29. The resonant frequencies of the H modes were obtained by exciting the network at an appropriate point with a voltage generator and adjusting the frequency either for a maximum or a minimum input current. This is similar to the way in which the normal modes of beams were excited in Part II. Some insight and knowledge of the problem are required in order to choose the best position for exciting a particular mode.

The boundary conditions for the E modes are that $E_3 = 0$ along the walls of the cavity. This condition can be imposed on the network by grounding the nodes along the edges.

The analytical solution for the TEM modes of a conical line resonator is:*

$$(H_\phi)_n = \frac{A_n \sin(\frac{n\pi r}{2a})}{r \sin\theta} e^{j\omega t} \tag{3.50}$$

where

$$\omega = \frac{n\pi}{2a\sqrt{\mu\epsilon}} \tag{3.51}$$

Since $H_3 = H_\phi r \sin\theta$, H_3 is independent of θ for the TEM modes. A comparison of measured and analytical values of H_3 for the lowest TEM mode is shown in Fig. 30. This mode was excited by connecting a small voltage source near the apex of the cones and adjusting the frequency for a maximum current input. A comparison of measured and exact resonant frequencies for the three lowest TEM modes is given in Table V. The errors in the network frequencies are compared with those calculated in Table II for a transmission line.

---

* See ref. 23, page 412

The field pattern for a higher H mode as measured by the network is shown in Fig. 31. The lines of constant H_3 are parallel to the electric flux lines.

Table V

Comparison of Measured and Analytically Computed Frequencies of the Transmission Line Modes of a Conical Line Resonator

a	Frequency Analytical	Measured	% Error	Length of Radial Cell	Error from Table II
$\lambda/4$	104.2	104.6	+0.4	$\lambda/24$	-0.3%
$\lambda/2$	208.4	206	-1.15	$\lambda/12$	-1.1%
$3\lambda/4$	312.6	297	-5.25	$\lambda/8$	-2.6%

FIG. 29

NETWORK FOR THE "H" MODES OF A CONICAL LINE RESONATOR

INDUCTANCES ARE GIVEN IN HENRYS
CAPACITANCES ARE GIVEN IN mfd.
FOR "E" MODES SHORT ALL BOUNDARY POINTS TO GROUND

$\sqrt{\mu\epsilon} = 10^{-4}$

$a = 24$

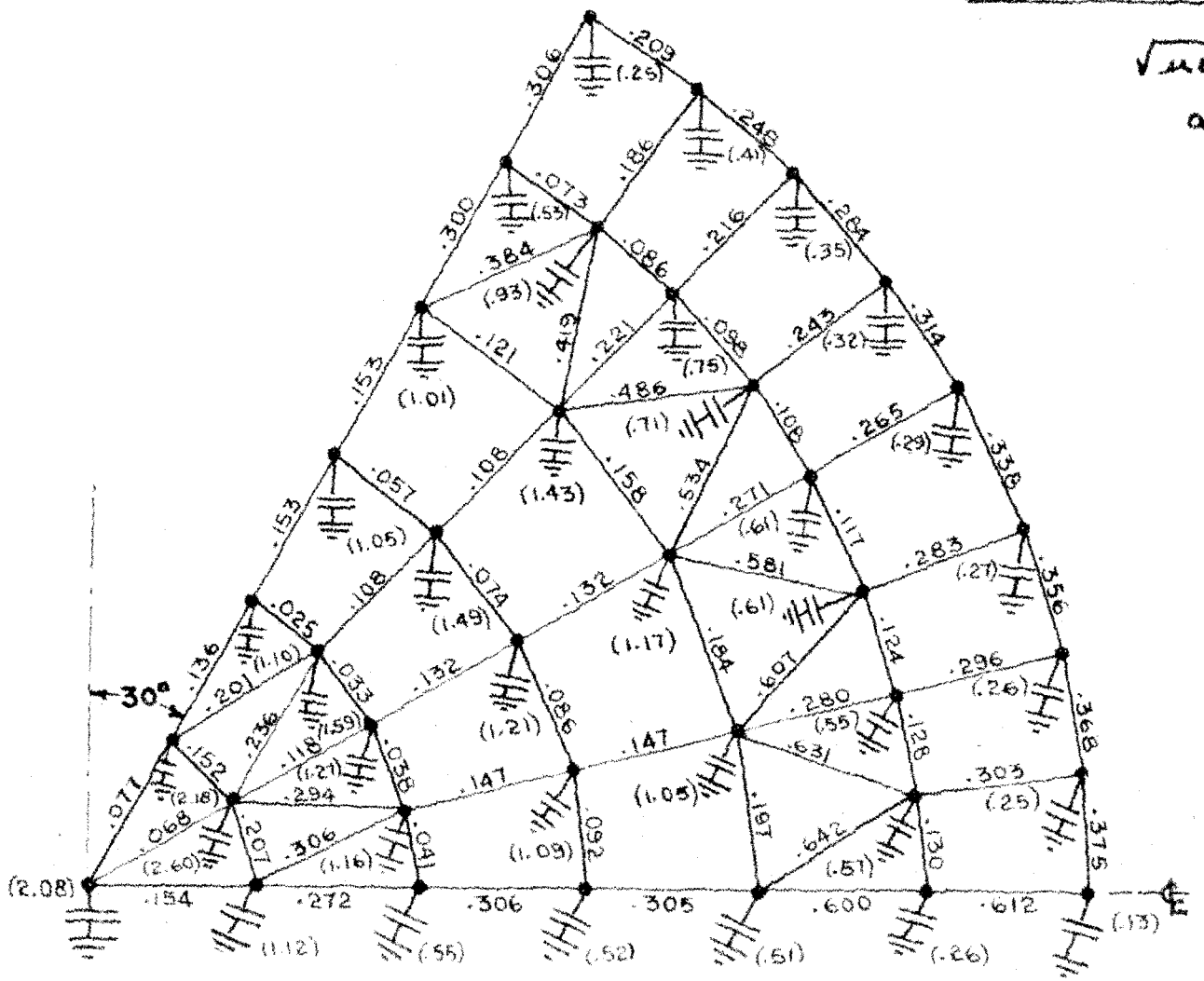

FIG. 29

FIG. 30

COMPUTER SOLUTION OF THE LOWEST MODE OF A CONICAL LINE RESONATOR

MEASURED $\lambda = 3.984a$

ANALYTICAL $\lambda = 4a$

VALVES SHOWN ARE THOSE OF THE COVARIANT MAGNETIC FIELD COMPONENT. $H_3 = \rho H_\phi$

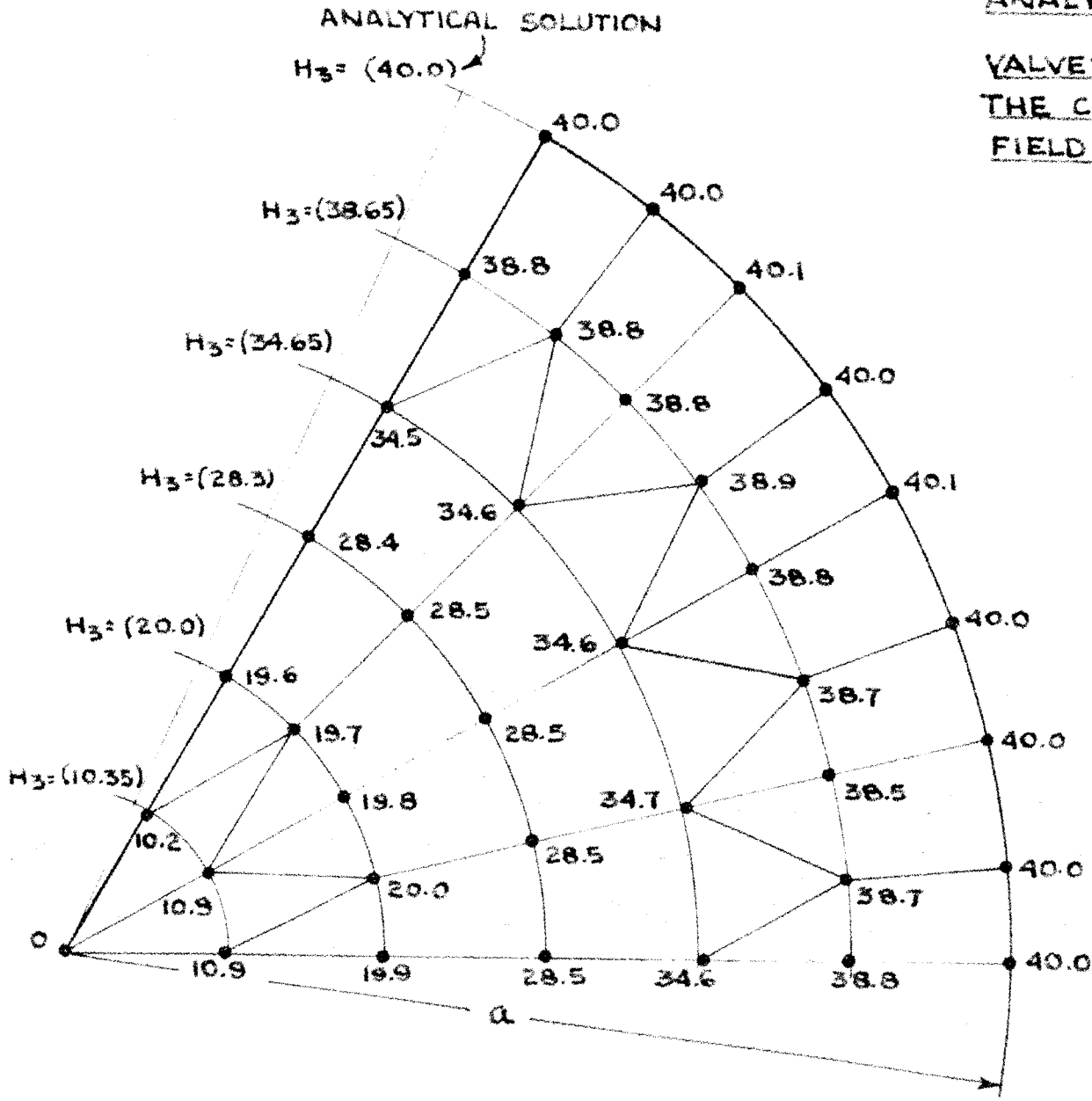

FIG. 31

HIGHER "H" MODE OF A CONICAL LINE RESONATOR

$\lambda = 1.457a$

CONTOURS ARE LINES OF CONSTANT H_3 PARALLEL TO THE ELECTRIC FLUX LINES. CAVITY IS SYMMETRICAL ABOUT EQUATORIAL PLANE.

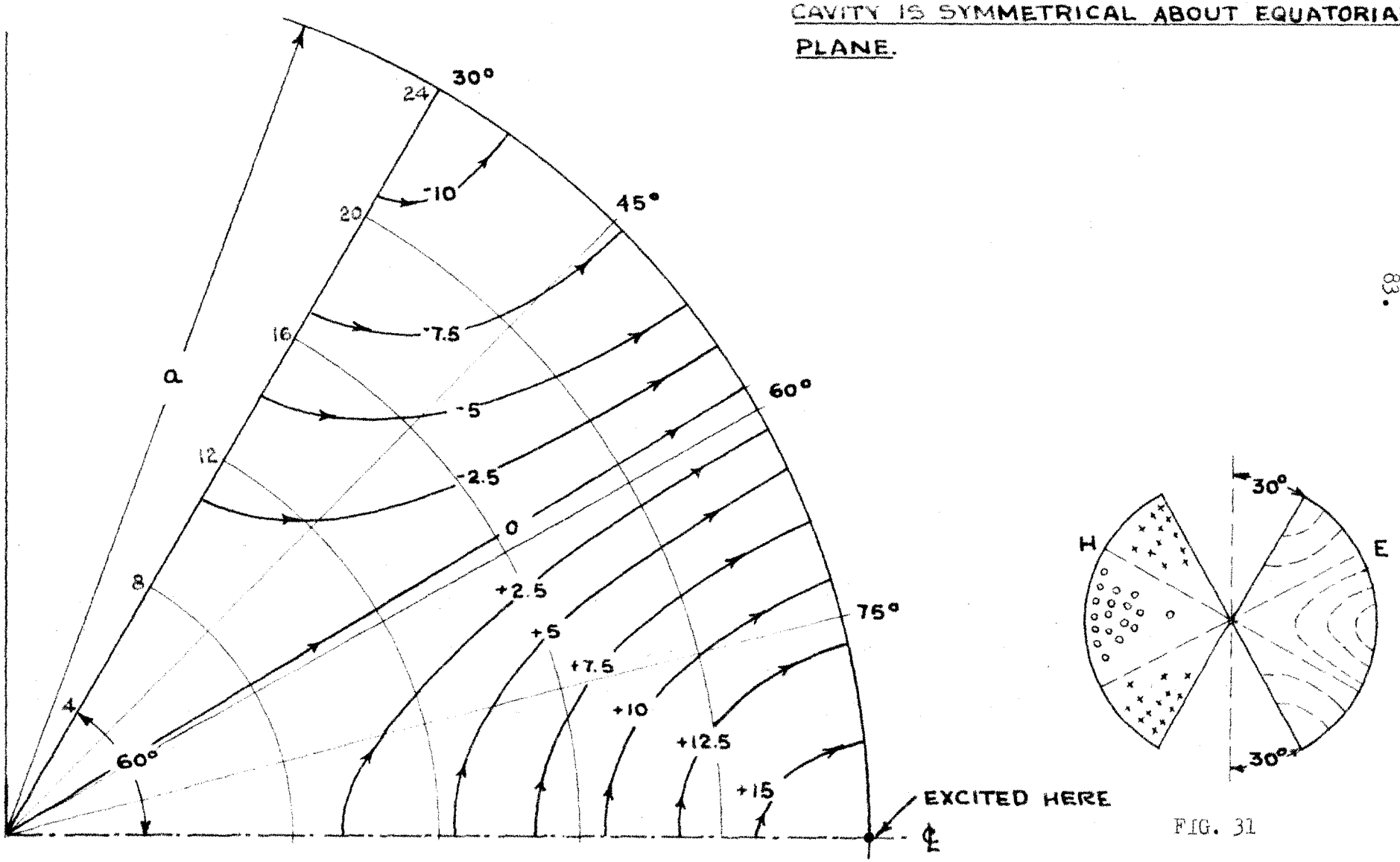

FIG. 31

3.7 Example II The Field of a Spherical Radiator

In this section a network is described that is suitable for the determination of the field near an axially symmetrical radiating body. The problems of radiation are distinguished from those of non-radiating cavities and wave guides in that the whole of space must be represented. For the network solution of such problems it is essential that there exist a method for representing the characteristic resistance of free space. Spherical polar coordinates are the natural coordinate system in which to calculate a radiation problem because at a great distance from the source all field components except H_ϕ and E_θ are negligible. Furthermore the equi-phase surfaces are nearly the spheres, r = constant. For these reasons and also because space would be considerably compressed, a network with r and θ as rectangular Cartesian coordinates would be appropriate. Unfortunately eqn.(3.43) would not be isotropic in such a region. This difficulty is avoided if log r and θ are chosen as coordinates. If

$$\begin{aligned} u^1 &= R = \log r \\ u^2 &= \theta \end{aligned} \tag{3.52}$$

then

$$\begin{aligned} h_1 &= \frac{dr}{dR} = r \\ h_2 &= r \end{aligned} \tag{3.53}$$

and eqn.(3.43) becomes, since $h_3 = r \sin\theta$:

$$\frac{\partial}{\partial R}\left(\frac{1}{r \sin\theta}\frac{\partial H_3}{\partial R}\right) + \frac{\partial}{\partial \theta}\left(\frac{1}{r \sin\theta}\frac{\partial H_3}{\partial \theta}\right) + \frac{r\omega^2\mu\varepsilon H_3}{\sin\theta} = 0 \tag{3.54}$$

This we recognize as Poisson's equation for an isotropic but inhomogeneous sheet in which $K = \frac{1}{r \sin\theta}$ and R and θ are Cartesian coordi-

nates. The boundaries of this sheet for the case of a cylindrical antenna are shown in Fig. 35. The region near the origin is considerably exaggerated in this space as the network will extend to $R = -\infty$ for $r = 0$. However, the values of inductors in the network are proportional to r and hence become vanishingly small for small r. The values of these inductors are, from eqns.(3.54) and (3.16):

$$L = K_1 \, r \sin \theta \, \frac{\overline{AB}}{\lambda_{12}} \tag{3.55}$$

where K_1 is an arbitrary constant. The values of the capacitors connecting the nodes of the network to ground are given by:

$$C = K_2 \, \frac{r}{\sin \theta} \, (\text{Area of Cell}) \tag{3.56}$$

where K_2 is an arbitrary constant. Then, from eqn.(3.54), $\mu\varepsilon$ is equal to $K_1 K_2$. For θ equal to zero or π, L is zero and C is infinite. This means that the network should be shorted to ground at these points.

Except for points near the boundary of the antenna the network should be a rectangular grid. If a constant cell size is kept in both the R and θ directions, the points in space corresponding to the nodes of the network will become farther and farther apart. This is permissible insofar as θ is concerned because the lines R = const. are nearly equiphase lines. The field propagates along radial lines almost as though each ray were independent of neighboring rays. The spreading of points in a radial direction is not permissible and the discussion of section 1.7 on this point is applicable. In order to have reasonably small errors, the maximum radial distance between points in the network should be less than $\lambda/12$.

The network can safely be terminated in the characteristic resis-

tance of space when the radial distance from the origin is about two wavelengths (depending on the type of antenna). For points beyond this the induction field is a small fraction of the radiation field. The only radiating field components are $H_{(\phi)}$ and $E_{(\theta)}$ and their ratio is given by

$$\frac{E(\theta)}{H(\phi)} = \sqrt{\frac{\mu}{\epsilon}} \tag{3.57}$$

The covarient field components are

$$\begin{aligned} H_3 &= h_3 H(\phi) = r \sin\theta \, H(\phi) \\ E_2 &= h_2 E(\theta) = r \, E(\theta) \end{aligned} \tag{3.58}$$

By eqn.(3.40):

$$E_2 = -\frac{1}{j\omega\epsilon} \frac{h_2}{h_1 h_3} \frac{\partial H_3}{\partial u^1} = -\frac{1}{j\omega\epsilon \, r \sin\theta} \frac{\partial H_3}{\partial R} \tag{3.59}$$

In the network the following finite difference approximation is made:

$$\left(\frac{\partial H_3}{\partial R}\right)_{n+\frac{1}{2}} \simeq \frac{(H_3)_{n+1} - (H_3)_n}{\Delta R} = \frac{-j\omega L_{n+\frac{1}{2}} \, I_{n+\frac{1}{2}}}{\Delta R} \tag{3.60}$$

where $I_{n+\frac{1}{2}}$ is the current flowing in the positive R direction.

For the rectangular network:

$$L_R = K_1 \, r \sin\theta \frac{\Delta R}{\Delta\theta} \text{ and } \quad C = K_2 \frac{r}{\sin\theta} \Delta R \Delta\theta \tag{3.61}$$

Eqns.(3.57) through (3.61) and the fact that in the network $\mu\epsilon = K_1 K_2$, yield the following relationship

$$\left(\frac{H_3}{I}\right)_{n+\frac{1}{2}} = \frac{\sin\theta}{\Delta\theta} \sqrt{\frac{K_1}{K_2}} = \sqrt{\frac{L_R}{C}} \tag{3.62}$$

This equation gives the value of the characteristic impedance with which to terminate the network. We notice that the characteristic

impedance depends only on θ and that it is equal to the characteristic impedance of a transmission line made up of the capacitors and the radial inductors in the network. For each value of θ a resistor whose value is given by eqn.(3.62) connects the last node of the network to ground.

The problem chosen for analysis on the analog computor is the calculation of the field of an oscillating sphere. The radius of the sphere was made equal to 1. K_1 was chosen equal to 10^{-1} and K_2 was chosen equal to 2×10^{-6} so that the velocity of propagation,

$$v_c = \frac{1}{\sqrt{u\varepsilon}} = 2236 \ \frac{\text{radii}}{\text{sec}} \qquad (3.63)$$

The network for the solution of this problem is shown in Fig. 32. Since the field is symmetrical with respect to the equatorial plane, only half of the sphere is represented in the network and symmetry conditions are imposed at $\theta = \frac{\pi}{2}$. The network is terminated after 7.5 sections at $r = 8$. The network was excited by a voltage generator at the node on the surface of the sphere nearest the equatorial plane. This corresponds to specifying the total current that crosses the equator of the sphere.

Solutions to the problem are shown in Figs. 33 and 34. The voltage in the network is $H_3 = r \sin\theta \, H(\phi)$. The radiation component of the magnetic field is proportional to r^{-1} while the induction field components are proportional to r^{-2} and the higher negative powers of r. Consequently the voltages in the network approach a constant value asymptotically as r increases. This aids the visual interpretation of the data shown in Figs. 33 and 34.

For the field of Fig. 33 the length of the largest radial cell

is $\lambda/6.2$ almost twice the recommended maximum length. As a result some standing waves are in evidence. These do not appear in Fig. 34, where λ is about twice as large.

The analytical solution with which the computor solution is compared in Fig. 33 is taken from ref. 23, pages 466-474. Only two terms of the solution were calculated as the solution does not converge on the surface of the sphere.

FIG. 32

NETWORK FOR SPHERICAL RADIATOR

INDUCTANCES GIVEN IN HENRYS

CAPACITANCES ( ) GIVEN IN MFD.

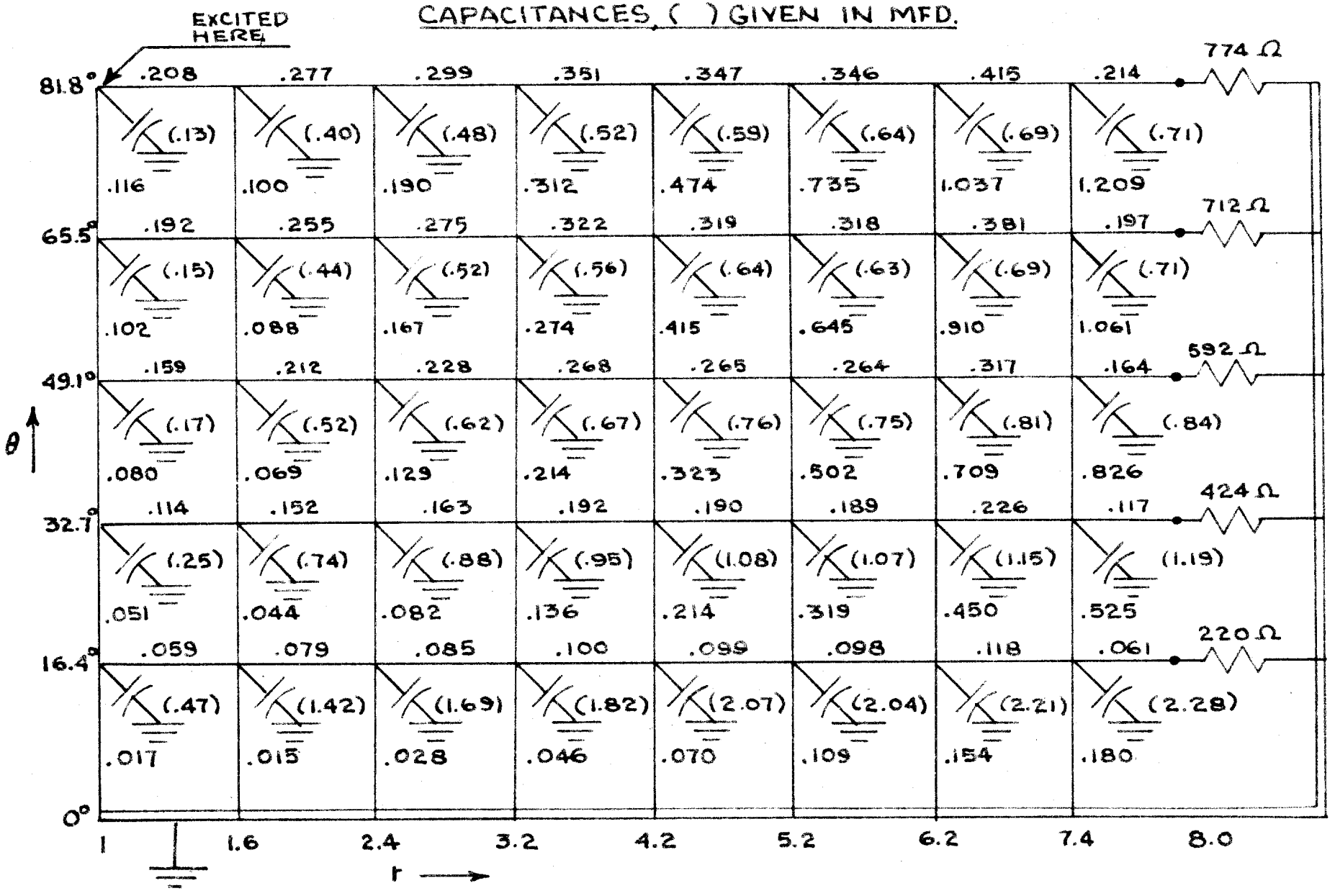

FIG. 33

FIELD OF A SPHERICAL RADIATOR

$\lambda = 7.46\,a$

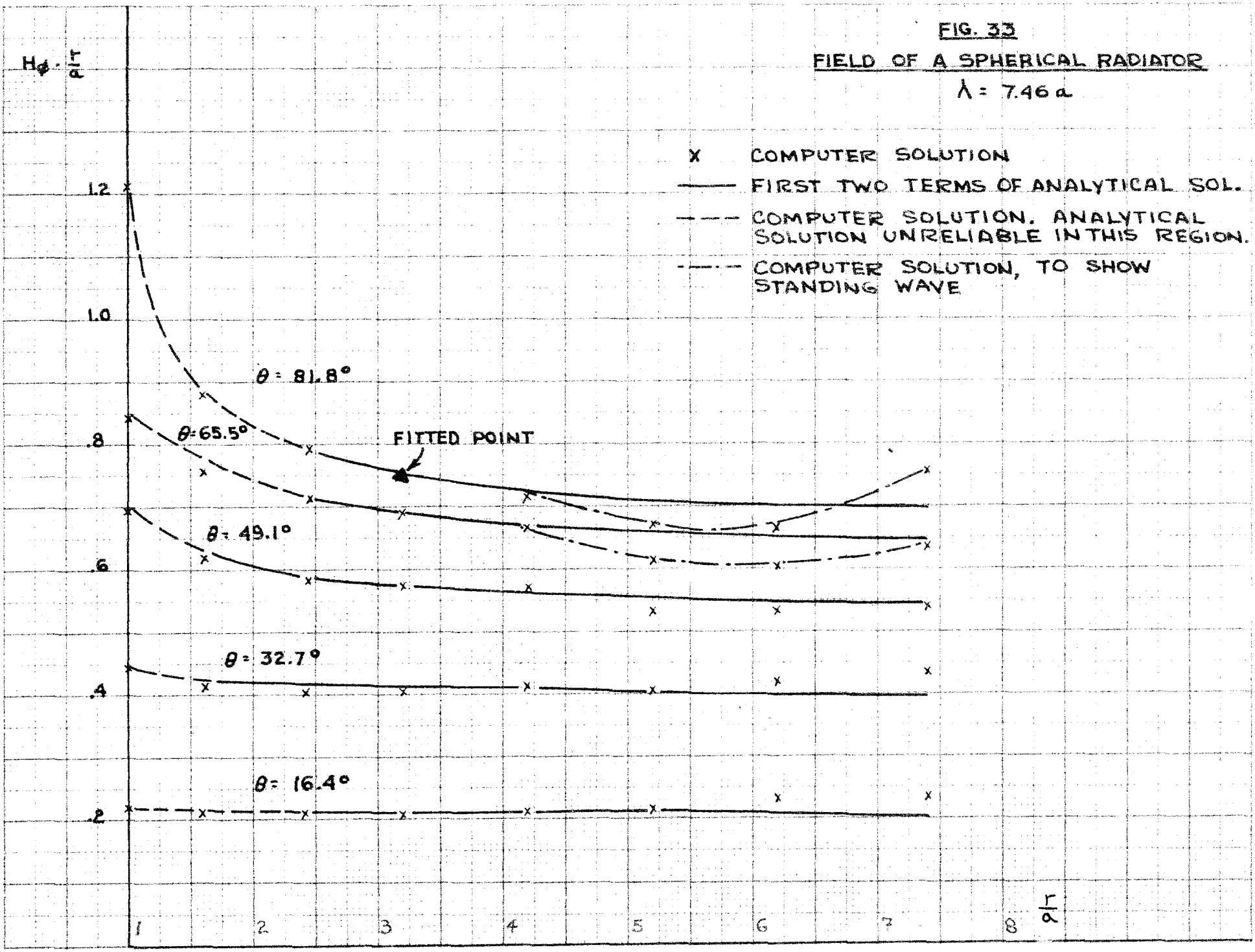

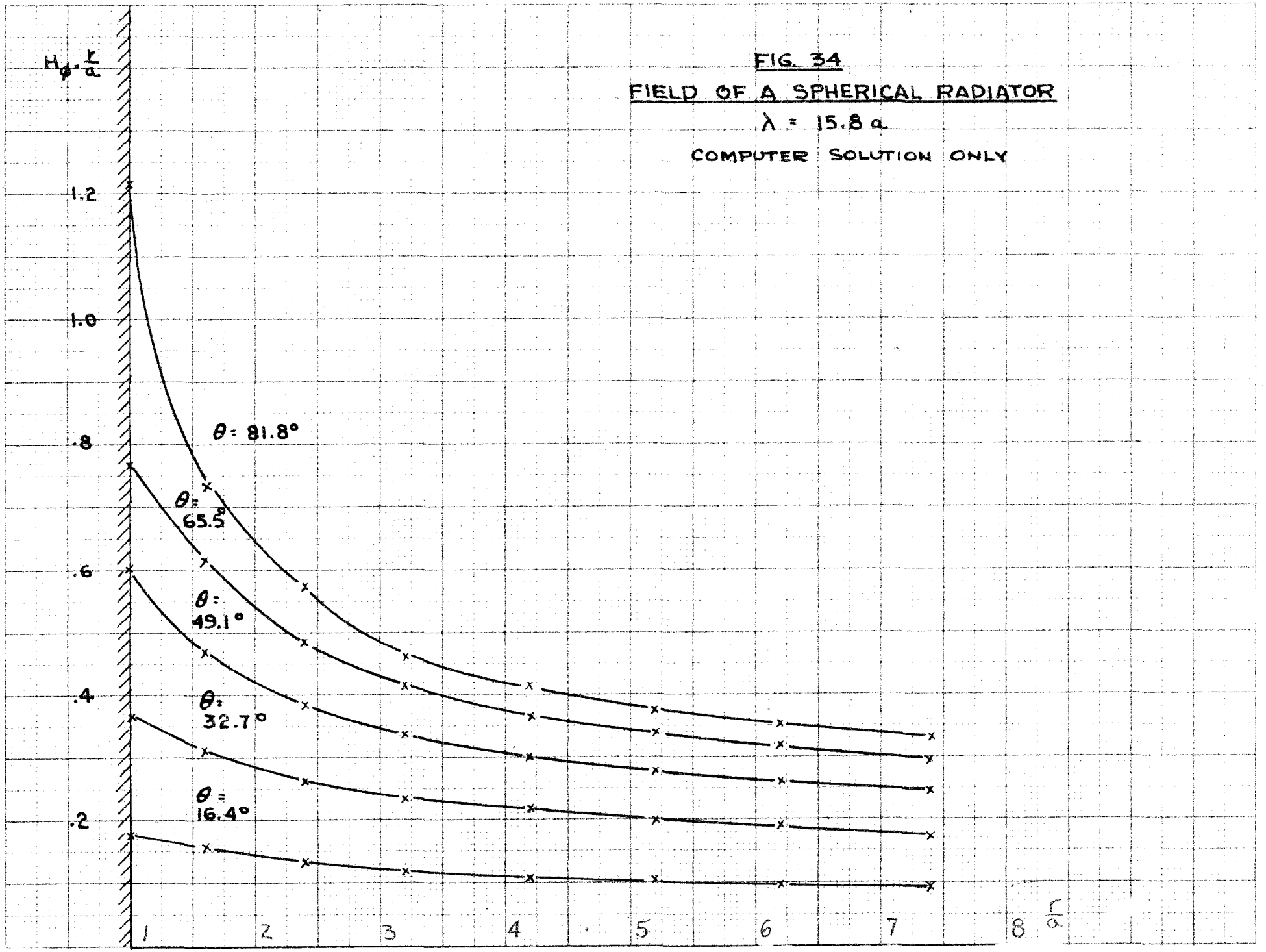
FIG. 34
FIELD OF A SPHERICAL RADIATOR
λ = 15.8 a
COMPUTER SOLUTION ONLY
$H_\phi \cdot \frac{r}{a}$
1.2
1.0
.8
.6
.4
.2
θ = 81.8°
θ = 65.5°
θ = 49.1°
θ = 32.7°
θ = 16.4°
1
2
3
4
5
6
7
8
r/a

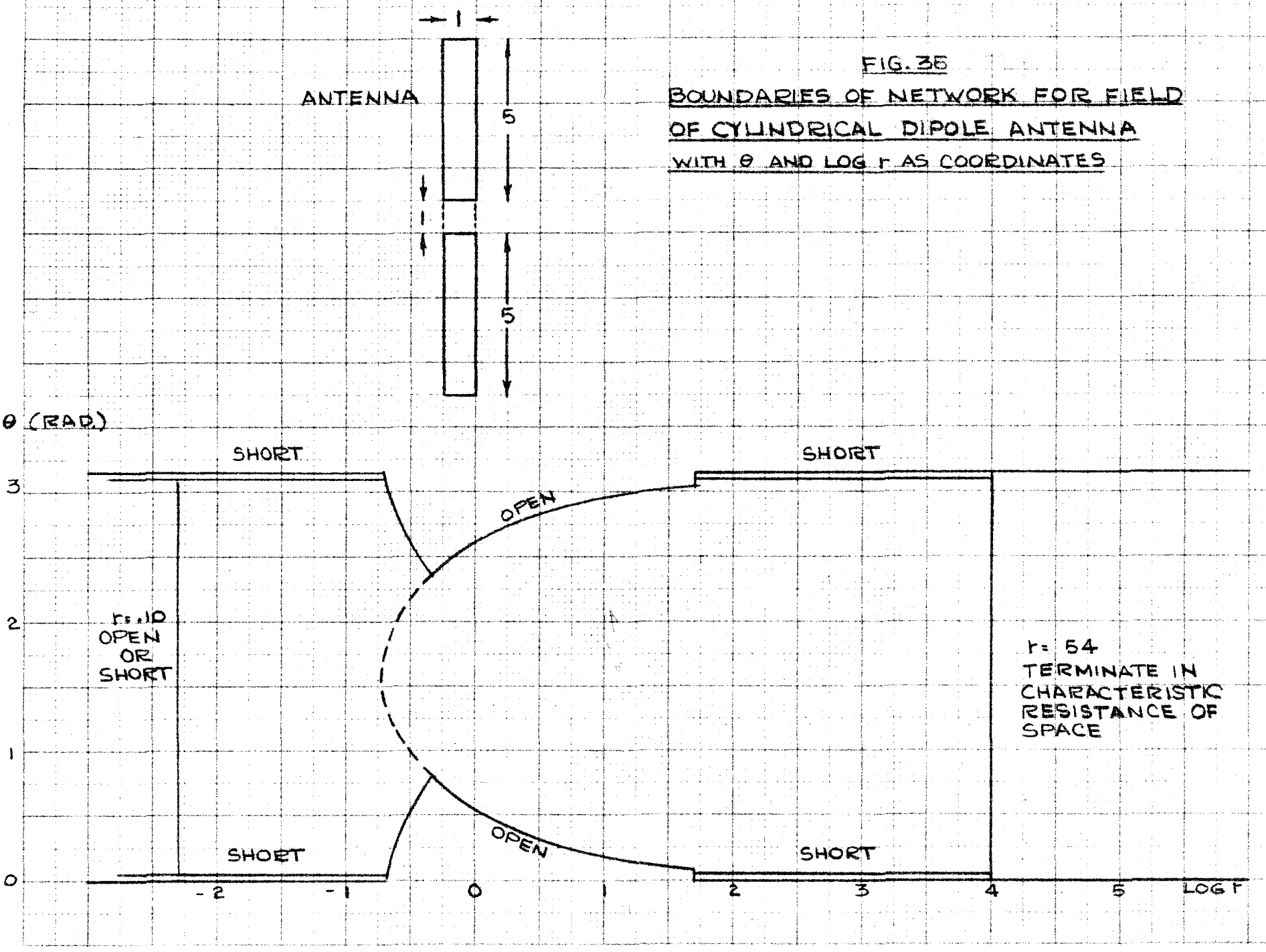

FIG. 35

BOUNDARIES OF NETWORK FOR FIELD OF CYLINDRICAL DIPOLE ANTENNA WITH θ AND LOG r AS COORDINATES

IV ELASTIC PLATE PROBLEMS *

4.1 Two Dimensional Problems in Elasticity

The two dimensional problems of elasticity cannot in general be reduced to the solution of Poisson's equation for a scalar potential function. Exceptions to this statement are the problems of the torsion of a long bar and the deflection of a membrane. If a scalar potential function is introduced, the equations of elasticity become fourth order partial differential equations. In the succeeding sections of this part, the bending of plates will be discussed in terms of such equations. Alternatively the equations of elasticity may be expressed in tensor form.[24] Using this point of view G. Kron has derived the equivalent circuits of the elastic field.[5] His networks for the cases of plane strain and axially symmetrical strain are of particular interest because they are networks that can be solved practically by an analog computor. They consist of two separate networks coupled through mutual inductances. The voltages at the nodes of the two circuits are respectively the components of the elastic displacement vector, while the currents are the components of the stress tensor. When the dilitation, ξ_i^i, is zero the mutual inductances drop out.

One important fact about the equations of elasticity is that they cannot be represented by an asymmetrical electrical network. In both Kron's networks for the elastic field and our networks for the elas-

---

* The material included in this part will also be found in two Analysis Laboratory reports: refs. 26 and 27. The treatment in these reports is more extensive than that given here. The first report includes a discussion of the capacitor analogy and the extension of the dynamic analogy to a skew Cartesian coordinate system. A large amount of experimental data is given in the second report.

tic plate the voltages are components of vectors. The coordinate system in which these vectors are expressed must remain fixed. As a result it becomes somewhat more awkward to represent boundary points along an irregularly shaped edge.

Electrical networks for plates can be derived by writing out the complete finite difference equivalent of the fourth order equation of equilibrium.* This technique has been used in the numerical solution of plate problems[28] and has even been extended to the case of skew Cartesian coordinates.[29] When applied to the derivation of an electrical network, this method leads to the necessity of negative inductances. Such elements can be simulated by capacitors for static deflections but cannot be satisfactorily synthesized for transient and normal mode studies. A further disadvantage is that slopes, moments and shears are not represented in the network.

The dynamic analogy that will be derived here is quite similar to the analogy for the beam derived in Part II. Its only disadvantage is that it requires a large number of expensive, high quality transformers for its realization.

4.2 The Dynamic Analogy for a Constant Thickness Plate

In this section an electrical analogy for the elastic plate will be developed that is similar to that for beams given in Part II. The notation is the same as that in Timoshenko's, Theory of Plates and Shells.[30]

The differential equation for a constant thickness plate is:

---

* See Table I for the finite difference equivalent of $\frac{\partial^4 y}{\partial x^4}$

$$\frac{\partial^4 w}{\partial x^4} + 2\frac{\partial^4 w}{\partial x^2 \partial y^2} + \frac{\partial^4 w}{\partial y^4} = \frac{q}{D} \tag{4.1}$$

which can also be written in the following form:

$$\frac{\partial}{\partial x}\left(\frac{\partial^2}{\partial x^2} + \frac{\partial^2}{\partial y^2}\right)\frac{\partial w}{\partial x} + \frac{\partial}{\partial y}\left(\frac{\partial^2}{\partial x^2} + \frac{\partial^2}{\partial y^2}\right)\frac{\partial w}{\partial y} = \frac{q}{D} \tag{4.2}$$

where w is the deflection normal to the plate, q is the load density and D is the stiffness constant. From Part II the equation for the bending of a uniform elastic beam is:

$$\frac{\partial}{\partial x}\left(\frac{\partial^2}{\partial x^2}\right)\frac{\partial w}{\partial x} = \frac{q}{EI} \tag{4.3}$$

The first term of eqn.(4.2) is the same as the left side of eqn.(4.3) with $\frac{\partial^2}{\partial x^2} + \frac{\partial^2}{\partial y^2}$ replacing $\frac{\partial^2}{\partial x^2}$. In section 2.2 it is shown that the two outside operators are represented by a transformer between two ladder networks, in one of which w is the voltage to ground and in the other $\frac{\partial w}{\partial x} = \theta_x$ is the voltage to ground. $\frac{\partial^2}{\partial x^2}$ is represented by an impedance ladder in the θ circuit.* The network to represent the first term of eqn.(4.2) is shown in Fig. 36. In addition to the impedances Z_x it has impedances Z_{xy} oriented parallel to the y axis to represent the additional term $\frac{\partial^2}{\partial y^2}$. Each row of transformers are interconnected by the impedances Z_{xy} to form a two-dimensional grid.

The second term of eqn.(4.2) is represented by a second network, entirely similar to that of Fig. 36. The primaries of its transformers, which are oriented parallel to the y axis, are joined at the nodes of the w circuit with the x transformers, so that a two-dimensional grid of transformer primary windings is formed. Thus

---

* See Fig. 8.

there exist three separate two-dimensional grids which are only interconnected magnetically and in which the voltages to ground are respectively w, $\theta_x = \frac{\partial w}{\partial x}$ and $\theta_y = \frac{\partial w}{\partial y}$. Plan views of these networks are shown in Figs. 37a, 37b and 37c. In Fig. 38 they are superimposed to show the geometrical relationship of the nodes and currents of the three networks. This superposition is useful for analytical investigations, while the clarity of the separate views recommend this technique to the solution of problems on the analog computor.

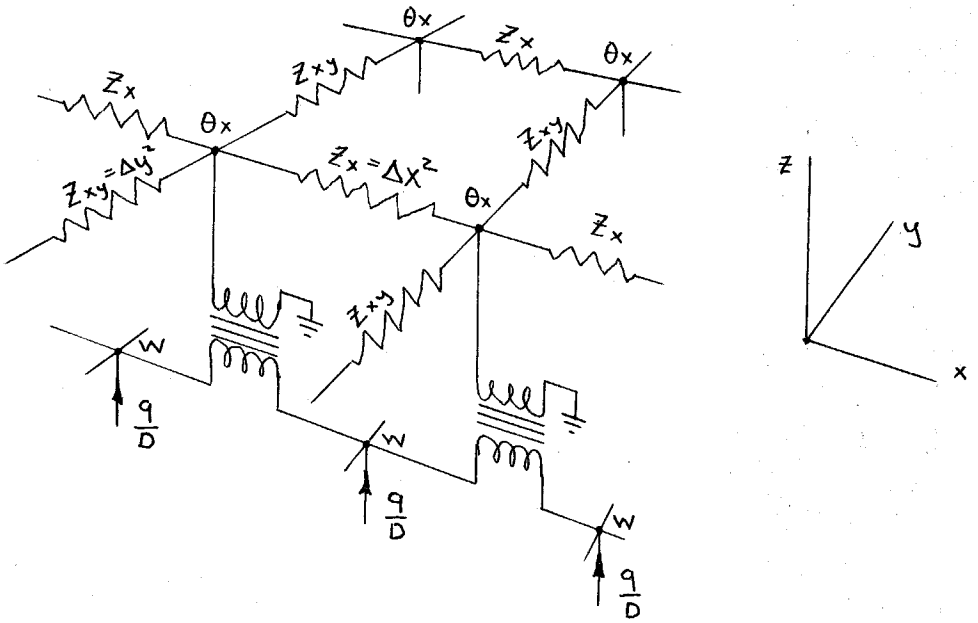

Fig. 36 Dynamic Analog for 1st Term of Eqn.(4.2)

4.3 The Dynamic Analogy for a Variable Thickness Plate

The equations given for the bending moments in ref. 30, page 88, are, with the substitutions $\theta_x = \frac{\partial w}{\partial x}$ and $\theta_y = \frac{\partial w}{\partial y}$:

ν = Poisson's ratio

$$M_x = -D\left(\frac{\partial \theta_x}{\partial x} + \nu \frac{\partial \theta_y}{\partial y}\right) \qquad (4.4)$$

$$M_y = -D\left(\frac{\partial \theta_y}{\partial y} + \nu \frac{\partial \theta_x}{\partial x}\right) \qquad (4.5)$$

$$M_{yx} = -D(1-\nu)\frac{\partial \theta_x}{\partial y} = -D(1-\nu)\frac{\partial \theta_y}{\partial x} \qquad (4.6)$$

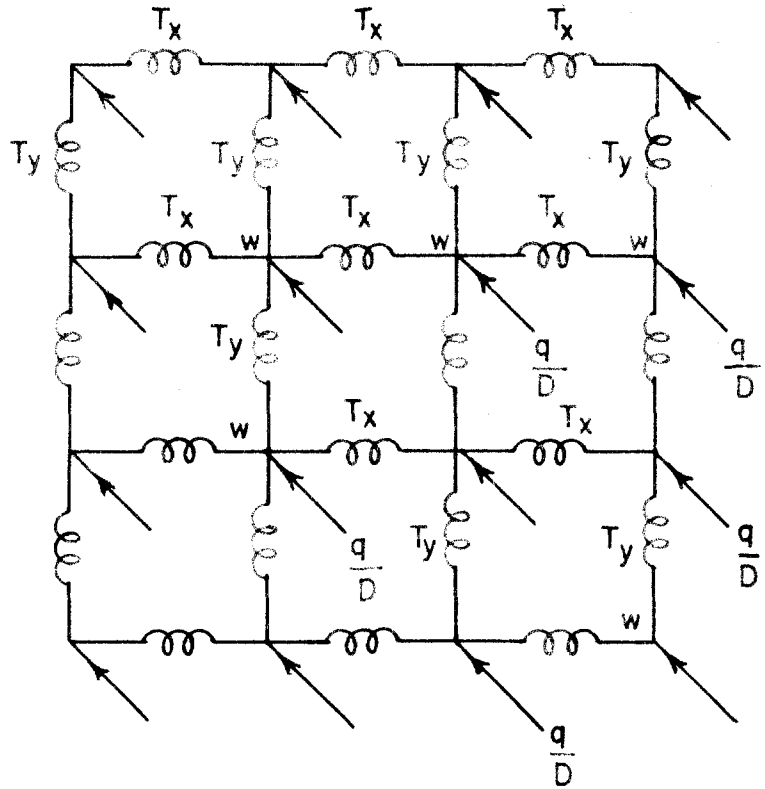

(a) W CIRCUIT

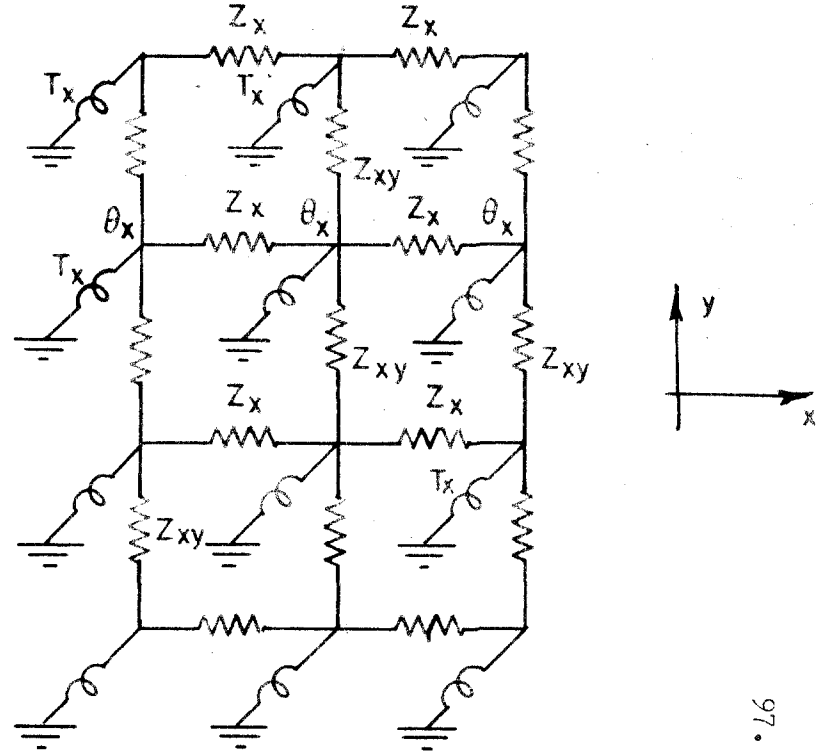

(b) θ_x CIRCUIT

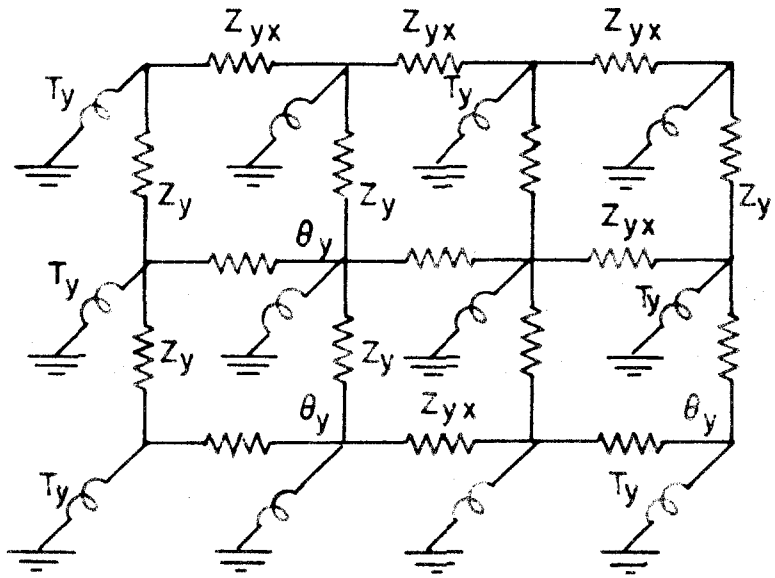

(c) θ_y CIRCUIT

FIG. 37 DYNAMIC ANALOGY FOR A CONSTANT THICKNESS PLATE.

$$Z_x = \Delta x^2$$

$$Z_{xy} = \Delta y^2$$

$$Z_y = \Delta y^2$$

$$Z_{yx} = \Delta x^2$$

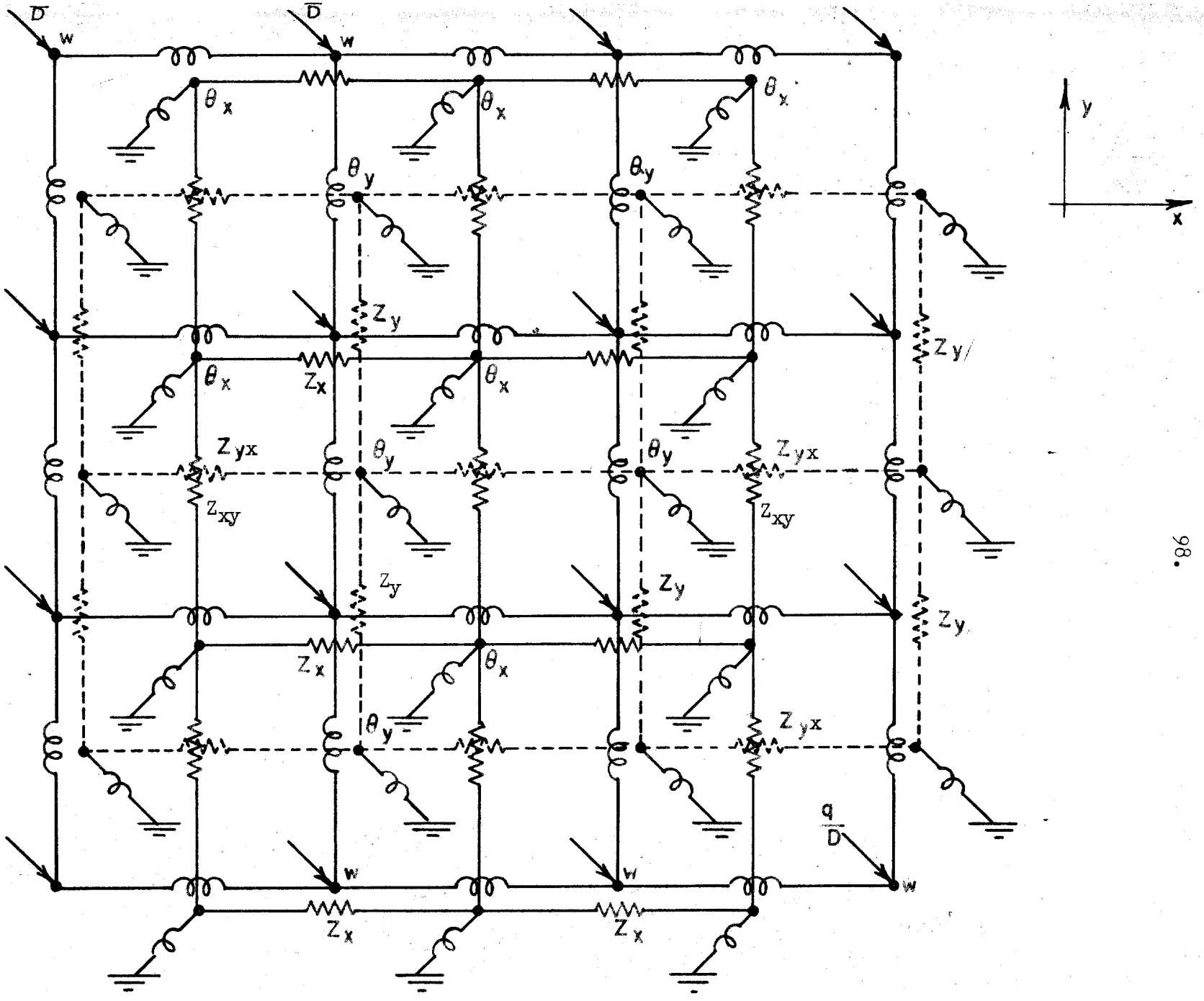

FIG. 38 DYNAMIC ANALOGY FOR A CONSTANT THICKNESS PLATE. SUPERIMPOSED VIEW TO SHOW GEOMETRICAL RELATIONSHIPS

The shears are given by

$$Q_x = \frac{\partial M_x}{\partial x} + \frac{\partial M_{yx}}{\partial y} \tag{4.7}$$

$$Q_y = \frac{\partial M_y}{\partial y} + \frac{\partial M_{yx}}{\partial x} \tag{4.8}$$

The static equilibrium of the plate requires that

$$\frac{\partial Q_x}{\partial x} + \frac{\partial Q_y}{\partial y} + q = 0 \tag{4.9}$$

Combining eqns.(4.4) through (4.9) where D need not be constant, the equation of the plate may be written as:

$$\frac{\partial}{\partial x}\left\{\frac{\partial}{\partial x}\left[D\left(\frac{\partial \theta_x}{\partial x} + \nu \frac{\partial \theta_y}{\partial y}\right)\right] + \frac{\partial}{\partial y}\left[D(1-\nu)\,\frac{\partial \theta_x}{\partial y}\right]\right\}$$

$$+ \frac{\partial}{\partial y}\left\{\frac{\partial}{\partial y}\left[D\left(\frac{\partial \theta_y}{\partial y} + \nu \frac{\partial \theta_x}{\partial x}\right)\right] + \frac{\partial}{\partial x}\left[D(1-\nu)\,\frac{\partial \theta_y}{\partial x}\right]\right\} = q \tag{4.10}$$

Fung[31] has shown that this equation which is based on the assumption that the strain varies linearly from the top to the bottom surfaces of the plate, is inaccurate. He has derived an expression based on a power series expansion in the thickness of the plate including terms up to the third order. His expression contains additional terms of the same order as those in eqn.(4.10). For a constant thickness plate his expression reduces to eqn.(4.1). We shall not use his equations because of their increased complexity.

The only terms of eqn.(4.10) that cannot be represented by the network of Figs. 37 and 38 are those involving $\nu \frac{\partial \theta_y}{\partial y}$ and $\nu \frac{\partial \theta_x}{\partial x}$. The other terms can be represented by the network with

$$Z_x' = \frac{\Delta x^2}{D} \qquad Z_{xy} = \frac{\Delta y^2}{D(1-\nu)}$$

$$Z_y' = \frac{\Delta y^2}{D} \qquad Z_{yx} = \frac{\Delta x^2}{D(1-\nu)}$$

The terms $\nu\frac{\partial\theta_y}{\partial y}$ and $\nu\frac{\partial\theta_x}{\partial x}$ represent a mutual coupling between the θ_x and θ_y circuits. In Fig. 38 it will be seen that the Z_x and Z_y branches cross each other and that their currents are defined at the same geometrical point. A mutual admittance between the two branches is required where

$$Y_m = + \frac{\nu D}{\Delta x \Delta y}$$

In a physical circuit mutual admittances can be converted into mutual impedances. Z_x and Z_y are also modified as follows:

$$\begin{aligned} Z_x &= \frac{1}{1-\nu^2}\frac{\Delta x^2}{D} \\ Z_y &= \frac{1}{1-\nu^2}\frac{\Delta y^2}{D} \\ Z_m &= -\frac{\nu}{1-\nu^2}\frac{\Delta x \Delta y}{D} \\ Z_{xy} &= \frac{1}{1-\nu}\frac{\Delta y^2}{D} \\ Z_{yx} &= \frac{1}{1-\nu}\frac{\Delta x^2}{D} \end{aligned} \qquad (4.11)$$

Fig. 39 shows the network for a variable thickness plate. In this network the currents in the slope circuits are proportional to the moments as defined in eqns.(4.4), (4.5) and (4.6) and the currents in the w circuit are proportional to the shears:

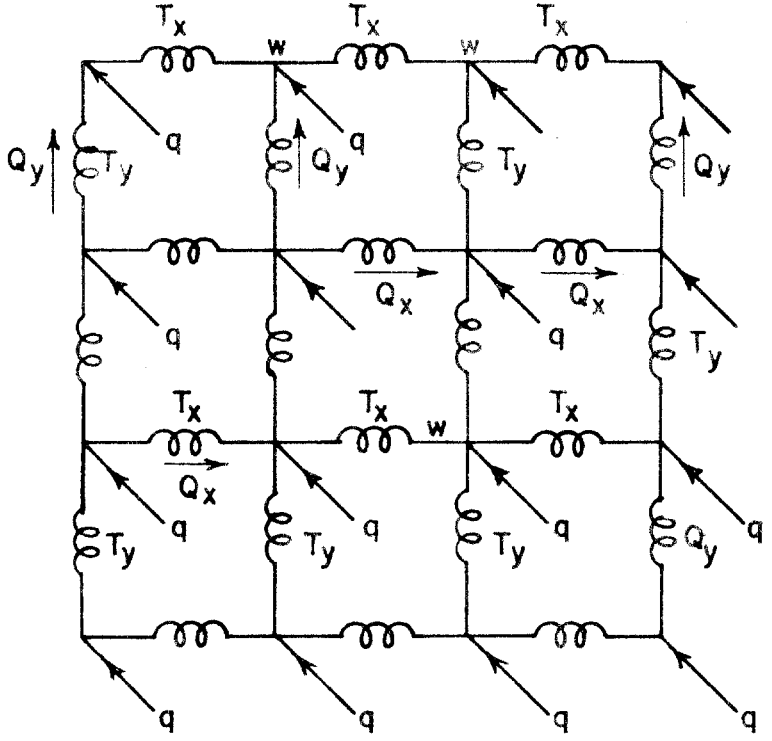

(a) W CIRCUIT

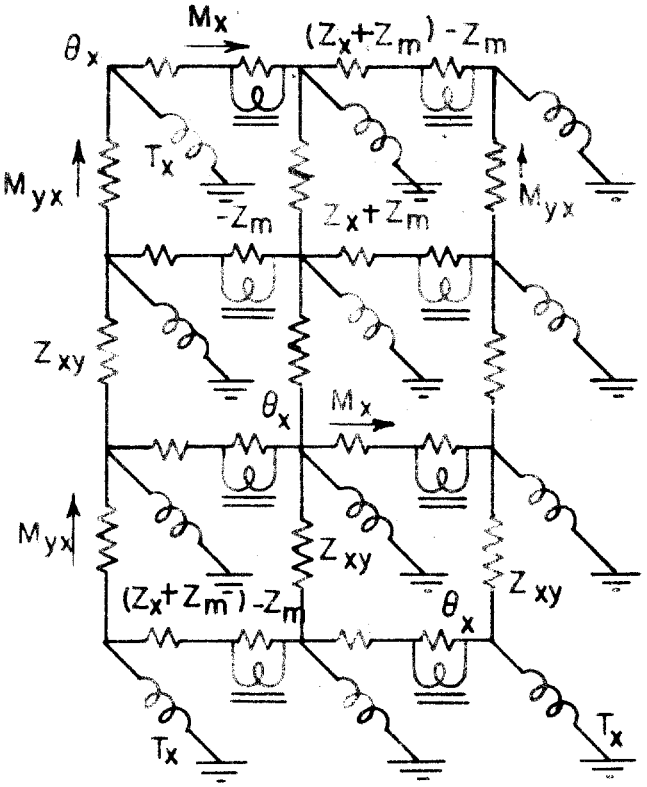

(b) θ_x CIRCUIT

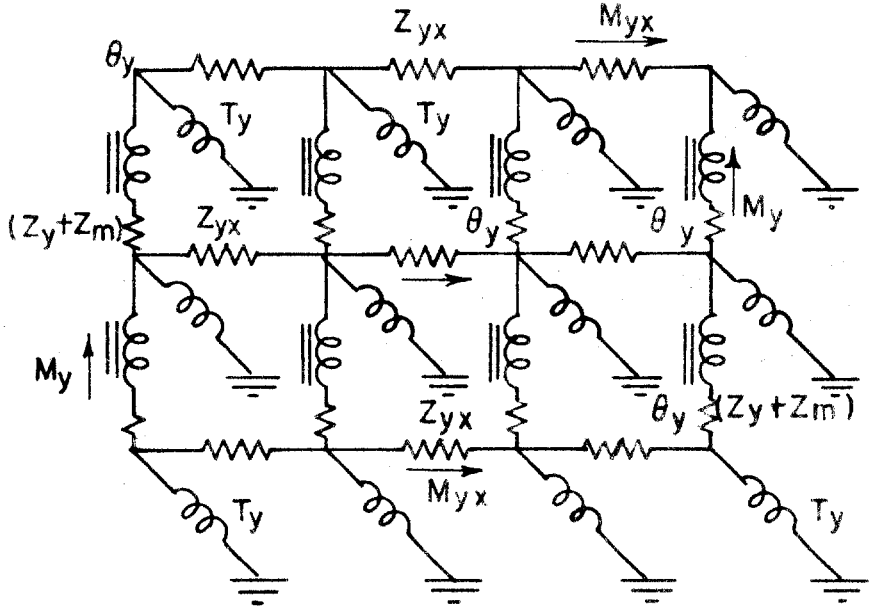

(c) θ_y CIRCUIT

FIG. 39 DYNAMIC ANALOGY FOR A VARIABLE THICKNESS PLATE

$$Z_x = \frac{1}{1-\nu^2}\,\frac{\Delta x^2}{D}$$

$$Z_y = \frac{1}{1-\nu^2}\,\frac{\Delta y^2}{D}$$

$$Z_m = -\frac{\nu}{1-\nu^2}\,\frac{\Delta x \Delta y}{D}$$

$$Z_{xy} = \frac{1}{1-\nu}\,\frac{\Delta y^2}{D}$$

$$Z_{yx} = \frac{1}{1-\nu}\,\frac{\Delta x^2}{D}$$

$$\begin{aligned}
&\text{Current in } Z_x = \frac{M_x}{\Delta x} \\
&\text{Current in } Z_y = \frac{M_y}{\Delta y} \\
&\text{Current in } Z_{xy} = \frac{M_{yx}}{\Delta y} \\
&\text{Current in } Z_{yx} = \frac{M_{yx}}{\Delta x} \\
&\text{Current in x branch of w circuit} = \frac{Q_x}{\Delta x} \\
&\text{Current in y branch of w circuit} = \frac{Q_y}{\Delta y}
\end{aligned} \tag{4.12}$$

The fact that the currents in the various branches of the network have a physical significance for the plate is very fortunate. It permits the direct measurement of the moments and shears. It simplifies the problem of the representation of the boundary conditions at a free edge. The identity between the plate and its electrical analogy is so complete that it eventually becomes unnecessary, as shall be seen, to justify every manipulation performed with the network in the representation of boundary points.

4.4 The Method of Representing Boundary Points

The boundary conditions at a clamped edge are that $w = 0$ and $\frac{\partial w}{\partial n} = 0$ where n is the normal to the edge.

The boundary conditions at a simply supported edge are that $w = 0$ and $M_n = -D\left[\frac{\partial^2 w}{\partial n^2} + \upsilon\frac{\partial^2 w}{\partial t^2}\right] = 0$.

The boundary conditions at a free edge are that $M_n = 0$ and $Q_n + \frac{\partial M_{tn}}{\partial t} = 0$.

It will be noted that the boundary conditions are paired in such a way that one condition from each of the following two groups applies:

$$
\begin{array}{lll}
1^{st} \text{ group} & w = 0 & (a) \\
 & Q_n + \frac{\partial M_{tn}}{\partial t} = 0 & (b) \\
2^{nd} \text{ group} & \frac{\partial w}{\partial n} = 0 & (c) \\
 & M_n = 0 & (d)
\end{array}
\qquad (4.13)
$$

The combination (b), (c) applies to a line of symmetry, with the further derived condition that M_{tn}, the twisting moment, is equal to zero. For the dynamic analogy the 1^{st} group of conditions apply to the w circuit while the 2^{nd} group of conditions apply to the slope circuits. Hence, we may expect that the representation of boundary points will conform with physical intuition.

There are two ways of looking at the boundary conditions at the edges of a plate. The conditions given above are the mathematical consequences of physical situations which are mechanically quite simple. For example, the boundary conditions at a free edge express the facts that there are no constraints, that no load is applied at points beyond the edge and that the stiffness constant becomes zero for points beyond the edge. In this simple form, however, the conditions are not useful for the analytical solution of the problem.

As we have seen there is a one-to-one correlation between nearly every property of an elastic plate and its dynamic electrical analogy. Deflections, slopes, moments and shears can be measured in the network. An important property of the variable thickness network is that the value of each impedance depends only on the local value of the stiffness constant and the cell size. Another important property is that the grouping of the boundary conditions corresponds with the division into deflection and slope circuits. The fact that there are three circuits and only two groups of equations can, in most

cases, be explained by the fact that the two conditions imply a third appropriate to the additional circuit.

Because of these correlations the analogy may be looked upon as though it were the plate. For example, the boundary condition at a free edge can be imposed by allowing the local value of the stiffness constant (and the corresponding impedances) to vanish. We shall see that this procedure leads to results that agree with the conventional conditions in simple cases and we shall therefore gain confidence for its application to more difficult cases that cannot be calculated analytically. In this way the rectangular network can be applied to plates of any shape whatsoever.

4.5 Boundary Conditions for Rectangular Plates

The analogy developed in section 4.2 can be used only for constant thickness plates with a combination of simply supported and clamped edges.

If the edge x = const. is clamped the constraints are that $w = 0$ and $\frac{\partial w}{\partial x} = 0$ along the edge. As a consequence of the first constraint $\frac{\partial w}{\partial y}$ is also equal to zero along the edge. These conditions can be imposed on the network by grounding the deflection and slope networks at the point where they cross the boundary. If the boundary does not coincide with a node of a circuit, a part of the impedance element is retained proportional to the remaining value of its "impedance square". This is illustrated in Fig. 40.

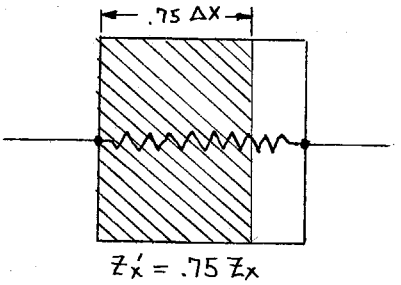

Fig. 40 Impedance Square

If the edge x = const. is simply supported the conditions are:

$$w = 0$$
$$M_x = -D\left(\frac{\partial^2 w}{\partial x^2} + \nu \frac{\partial^2 w}{\partial y^2}\right) = 0 \tag{4.14}$$

As a consequency of the first condition

$$\frac{\partial w}{\partial y} = 0 \qquad \text{and} \qquad \frac{\partial^2 w}{\partial y^2} = 0 \tag{4.15}$$

so that

$$\frac{\partial^2 w}{\partial x^2} = 0 \tag{4.16}$$

In the circuit developed in section 4.2 and illustrated in Fig. 37 the current in the impedance elements Z_x is proportional to $\frac{\partial^2 w}{\partial x^2}$. Consequently, a Z_x branch that crosses a simply supported edge is left open. The w and θ_y circuits are grounded where they cross a simply supported edge. Fig. 41 shows the method of representing simply supported and clamped edges when they coincide with nodes of the w circuit.

The conditions at a free edge cannot be satisfied with this network. To represent a free edge, the analogy for a variable thickness plate must be used, even though the plate may be uniform.

The boundary conditions at clamped and at simply supported edges

are imposed in the same way for the variable thickness network as for the constant thickness plate illustrated in Fig. 41.

For a free edge along x = a the conventional conditions are

$$M_x = 0$$
$$Q_x + \frac{\partial M_{yx}}{\partial y} = 0 \qquad (4.17)$$

The physical conditions along a free edge are the absence of any constraints and the vanishing of the stiffness constant for points beyond the edge. Applying these physical conditions to the circuit of Fig. 42 we reason that:

$(Z_y)_6$, $(Z_x)_6$, $(Z_{yx})_5$ and $(Z_{xy})_5$ must vanish $(=\infty)$

Consequently there can be no current in the y branches of the w circuit along x = 6, and these branches can be left out. Since there is no load at x = 6 no current can flow through the x branches of the deflection circuit at x = 5. This means that no current flows into the nodes of the θ_x circuit through the transformer secondaries. Consequently no current flows in $(Z_x)_4$ and these impedances can be left out.

Half of the impedance square for $(Z_y)_4$ is empty so that the impedance of this branch should be doubled. Furthermore, since there is no current in $(Z_x)_4$, the mutual impedance between the two circuits can be omitted. (This is not the same thing as omitting the mutual admittance, a condition that would be appropriate if $(Z_x)_4$ had been shorted.) The resulting circuit for the free edge is shown in Fig. 43.

Since the load vanishes for points beyond the edge the average load density at the edge is one-half the load density for points inside the plate. Consequently the load current for points on the edge should be reduced by one-half.

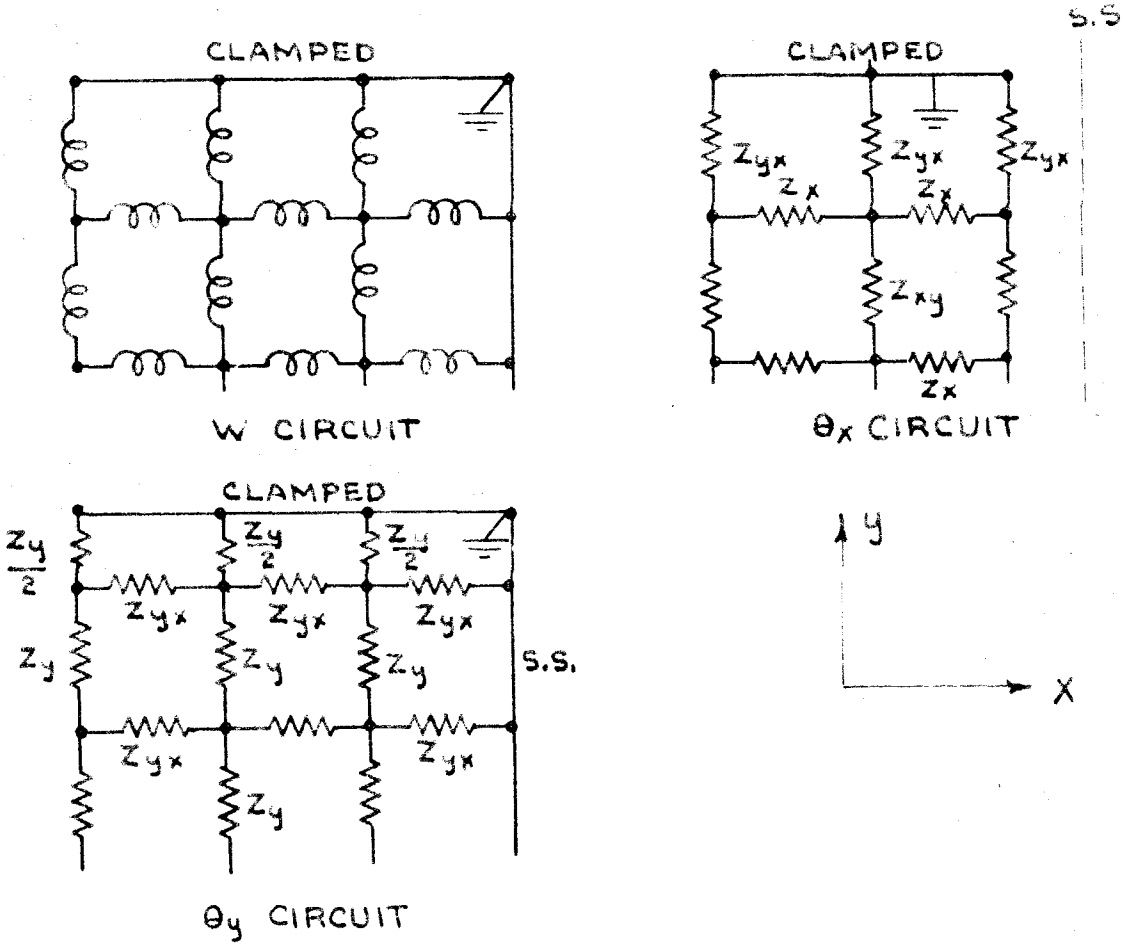

FIG. 41 CLAMPED AND SIMPLY SUPPORTED EDGES FOR A CONSTANT THICKNESS PLATE.

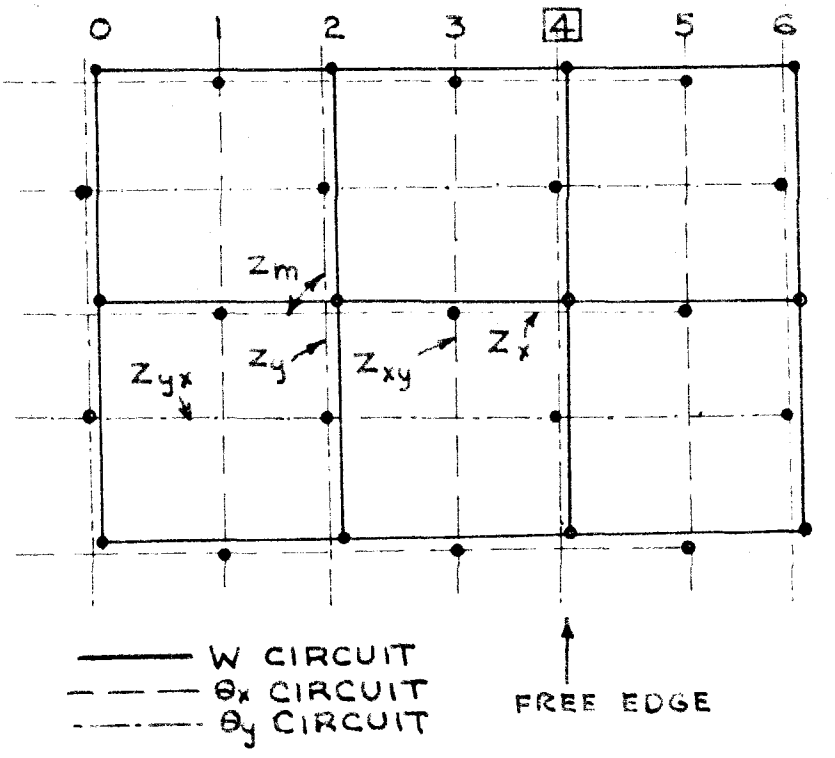

FIG. 42 GEOMETRICAL RELATIONSHIP OF NETWORKS NEAR A FREE EDGE

It will now be shown that the network of Fig. 43 also satisfies the mathematical boundary conditions given in eqn.(4.17). Fig. 44 shows the location of the points where the moments are defined in the neighborhood of a boundary point (4,4). The quantities M_{x64}, M_{yx55}, and M_{yx53} are fictitious. By eliminating them from the boundary condition equations a single equation is obtained that the real moments must satisfy. In terms of the moments the differential equation is

$$\frac{\partial^2 M_x}{\partial x^2} + 2\frac{\partial^2 M_{yx}}{\partial x \partial y} + \frac{\partial^2 M_y}{\partial y^2} = q \tag{4.18}$$

and the boundary condition equations are

$$\begin{aligned} M_x &= 0 \\ \frac{\partial M_x}{\partial x} + 2\frac{\partial M_{yx}}{\partial y} &= 0 \end{aligned} \qquad \text{at } x = 4 \tag{4.19}$$

The finite difference equivalent of eqn.(4.18) is:

$$\frac{M_{x64} - 2M_{x44} + M_{x24}}{\Delta x^2} + 2\left[\frac{M_{yx55} - M_{yx53} + M_{yx33} - M_{yx35}}{\Delta x \Delta y}\right] + \frac{M_{y46} - 2M_{y44} + M_{y42}}{\Delta y^2} = q_{44} \tag{4.20}$$

The finite difference equivalents of eqn.(4.19) are:

$$M_{x44} = 0 \tag{4.21}$$

and

$$\frac{M_{x64} - M_{x24}}{2\Delta x} + \frac{M_{yx55} + M_{yx35} - M_{yx33} - M_{yx53}}{\Delta y} = 0 \tag{4.22}$$

Multiply eqn.(4.22) by $\frac{2}{\Delta x}$

$$\frac{M_{x64} - M_{x24}}{\Delta x^2} + 2\left[\frac{M_{yx55} + M_{yx35} - M_{yx33} - M_{yx53}}{\Delta x \Delta y}\right] = 0 \tag{4.23}$$

Subtract eqn.(4.23) from eqn.(4.20). Then, utilizing eqn.(4.21) we obtain:

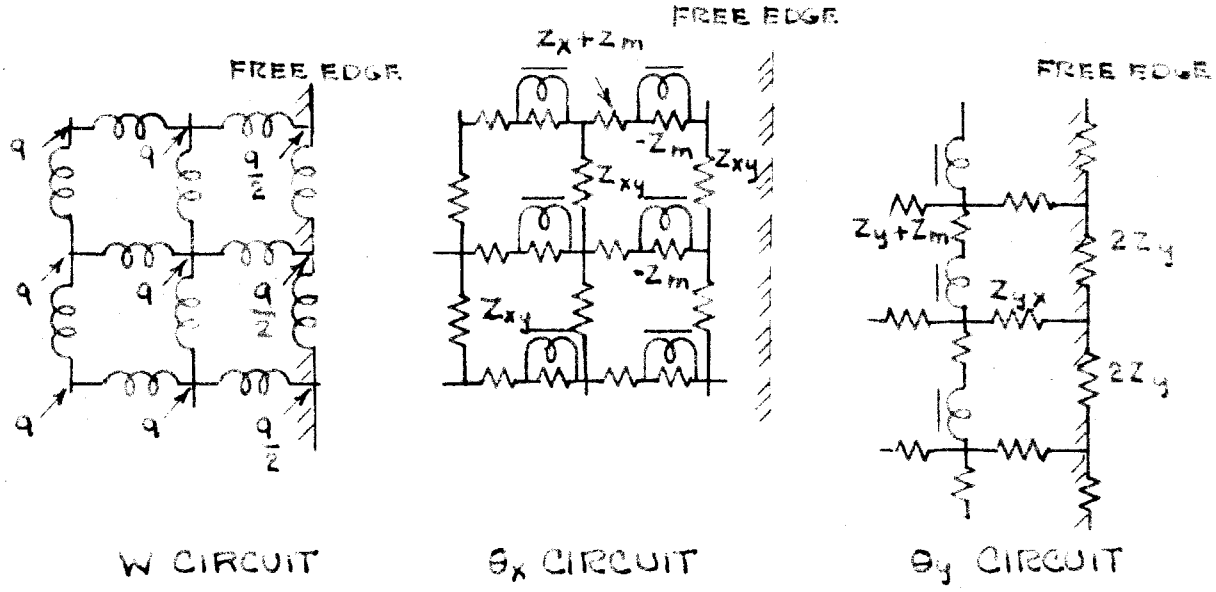

FIG. 43 CIRCUITS TO REPRESENT FREE EDGE

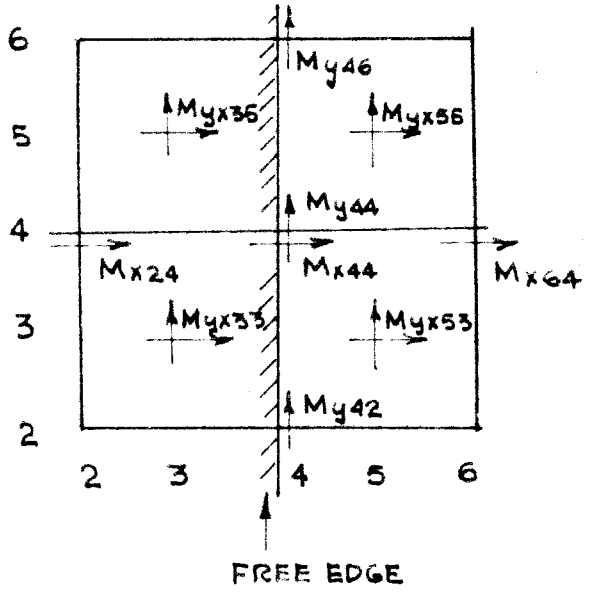

FIG. 44 GEOMETRICAL DISTRIBUTION OF MOMENTS NEAR A FREE EDGE

$$\frac{M_{x24}}{\Delta x^2} + 2\,\frac{M_{yx33} - M_{yx35}}{\Delta x \Delta y} + \frac{M_{y46} - 2M_{y44} + M_{y42}}{2\Delta y^2} = \frac{q_{44}}{2} \qquad (4.24)$$

This equation is satisfied by the network of Fig. 43. It indicates that the impedance in the M_y circuit should be doubled at the edge and that load current at the edge should be halved. Since $M_x = 0$:

$$(M_y)_{y=4} = -D(1-\nu^2)\,\frac{\partial \theta_y}{\partial y} \qquad (4.25)$$

so that

$$(Z_y)_{x=4} = -2\Delta y\,\frac{\theta_{y45} - \theta_{y43}}{M_{y44}} = \frac{2\Delta y^2}{(1-\nu^2)\,D} = 2Z_y \qquad (4.26)$$

Thus the circuit of Fig. 43 is verified in every detail.

4.6 Boundary Conditions for an Edge not Parallel to a Coordinate Axis

By employing the physical reasoning of the previous section it is possible to obtain boundary conditions for an edge not parallel to either of the coordinate axes. It becomes more difficult to check the resulting configurations with the conventional mathematical boundary conditions.

It is necessary to decide what should be done with impedance elements that cross or lie close to the boundary. The transformer primaries that constitute the w circuit do not involve the stiffness constant and consequently will not be changed or eliminated when a free edge is crossed. All that happens is that no load currents enter its nodes beyond the edge. For a clamped or simply supported edge the deflection is constrained to zero at the edge and the transformer being considered as a distributed coil is grounded where it crosses the boundary. The part extending beyond the edge is not elim-

inated. A case in point is a continuous plate with multiple interior supports. Along such edges the only effect on the electrical circuit is that the w circuit is grounded where it crosses them.

Along clamped edges the slope circuits are also grounded where they cross the edge, the impedance elements being considered as distributed along the length of their branches. A difficulty arises in that the transformer secondaries cannot be so distributed and if they fall on or beyond the clamped edge they are grounded. The primaries of such transformers consequently behave as though they were shorted and as a result the deflection is made zero at a short distance from the edge. This situation caused no appreciable inaccuracy in the cantilever beam analogy at points two or three cells distant from the clamped end.

Some impedance elements in the slope circuits may run near but not cross a clamped edge, so that their impedance squares, (Fig. 45), cross the edge. In such cases it is probably correct to allow the impedance elements their full value.

At free and at simply supported edges the stiffness constant is zero for points beyond the edge. Fig. 45 shows four possible relationships of an "impedance square" with such an edge.

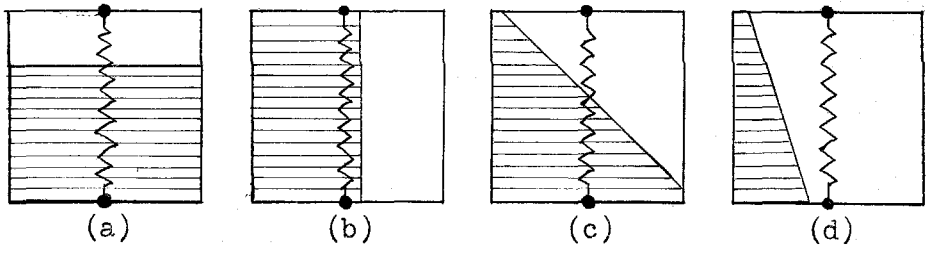

Fig. 45 Impedance Squares and an Edge where D Vanishes in Each Case

If it is assumed in each case that the appropriate value of the stiffness constant is the average value over the square, then the admittance of each element will be proportional to the area of the square inside the plate. Case (b) has already been met in connection with the free edge and we will shortly meet case (c). The load current inserted at a node of the deflection circuit will also, if it is physically distributed, be multiplied by the effective per unit area of its square.

It has been mentioned that when the current in the Z_x or Z_y branch is zero, any mutual impedance associated with it is zero. In like manner when such an element is shorted (at a clamped edge) any mutual admittance associated with it is zero. As an example consider the impedances of eqn.(4.11). If the current in Z_x is zero then $Z_y = \frac{1}{1-\nu^2}\frac{\Delta y^2}{D}$ but if Z_x is shorted $Z_y = \frac{\Delta y^2}{D}$.

We now have a set of simple rules for handling any type of boundary situation. The question of the validity of these rules cannot be entirely answered by an analysis of the electrical network and must await the results of experimentation.

The example of a free edge crossing diagonally through the nodes of the deflection circuit will now be analyzed. Consider the rotation of axes shown in Fig. 46

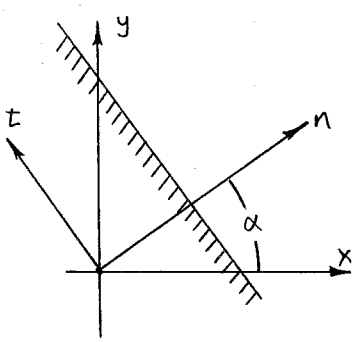

$$x = n\cos\alpha - t\sin\alpha$$

$$y = n\sin\alpha + t\cos\alpha$$

$$\frac{\partial}{\partial n} = \frac{\partial}{\partial x}\cos\alpha + \frac{\partial}{\partial y}\sin\alpha \qquad (4.27)$$

$$\frac{\partial}{\partial t} = -\frac{\partial}{\partial x}\sin\alpha + \frac{\partial}{\partial y}\cos\alpha$$

Fig. 46. Rotation of Axes

The boundary conditions along a free edge, n = const., are

$$M_n = -D\left(\frac{\partial^2 w}{\partial n^2} + \nu \frac{\partial^2 w}{\partial t^2}\right) = 0$$
$$Q_n + \frac{\partial M_{tn}}{\partial t} = 0 \qquad (4.28)$$

Carrying out the transformation one obtains for the particular case of $\alpha = \frac{\pi}{4}$:

$$M_n = \tfrac{1}{2}(M_x + M_y) + M_{yx}$$
$$M_{tn} = \tfrac{1}{2}(M_y - M_x) \qquad (4.29)$$
$$Q_n = \frac{1}{\sqrt{2}}\left[\frac{\partial M_x}{\partial x} + \frac{\partial M_y}{\partial y} + \frac{\partial M_{yx}}{\partial x} + \frac{\partial M_{yx}}{\partial y}\right]$$

so that the boundary conditions at a free diagonal edge are:

$$M_x + M_y + 2M_{yx} = 0$$
$$\frac{\partial M_x}{\partial x} + \frac{\partial M_y}{\partial y} + \frac{\partial M_{yx}}{\partial x} + \frac{\partial M_{yx}}{\partial y} + \frac{1}{\sqrt{2}}\left(\frac{\partial M_y}{\partial t} - \frac{\partial M_x}{\partial t}\right) = 0 \qquad (4.30)$$

We now turn to a determination of the network configuration from physical reasoning. In Fig. 47 all impedances in the slope circuits which lie wholly outside the plate must vanish. Therefore there is no current in the transformers of the w circuit lying outside the plate except in those that are connected to nodes lying on the boundary. Furthermore, since there is no load current at node (6,4), for example, the current in $(T_y)_{63}$ is the negative of the current in $(T_x)_{54}$. The impedances of the slope circuits that cross the boundary are given twice the normal value.

The current flowing in $(T_x)_{54}$ is $\frac{1}{2}\left[\frac{M_{x44}}{\Delta x^2} + \frac{M_{yx53}}{\Delta x \Delta y}\right]$ while the current flowing in $(T_y)_{63}$ is $\frac{1}{2}\left[\frac{M_{y62}}{\Delta y^2} + \frac{M_{yx53}}{\Delta x \Delta y}\right]$.

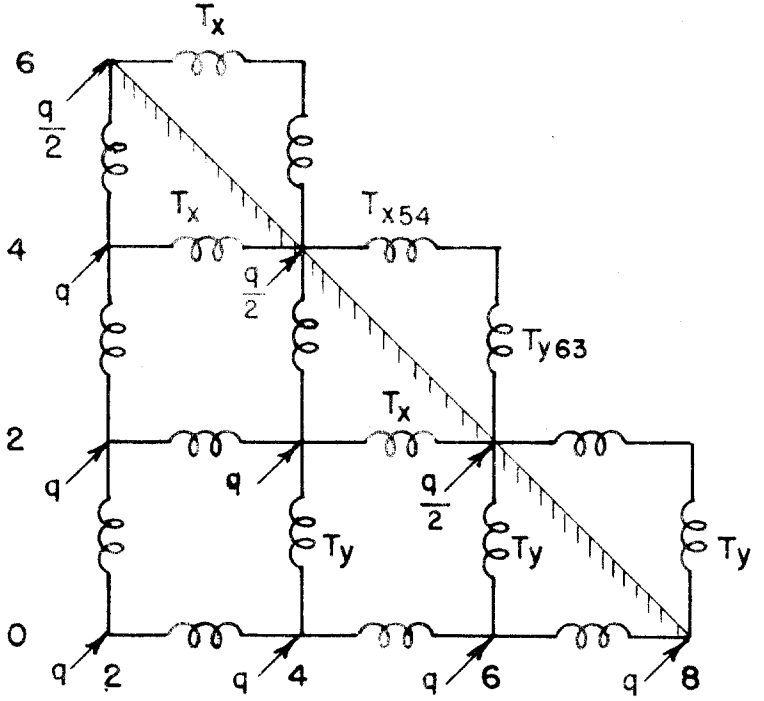

(a) W CIRCUIT

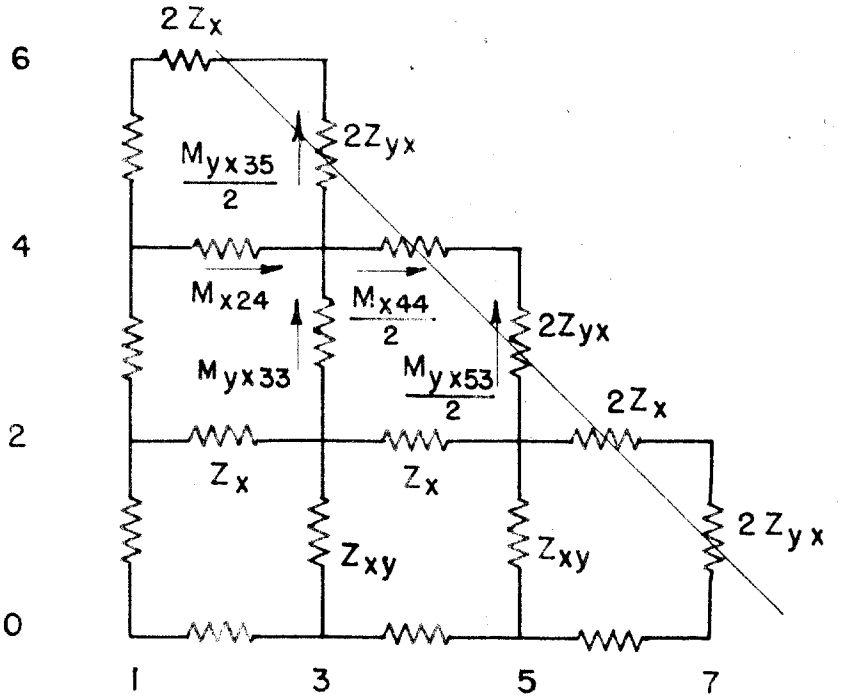

(b) θ_x CIRCUIT

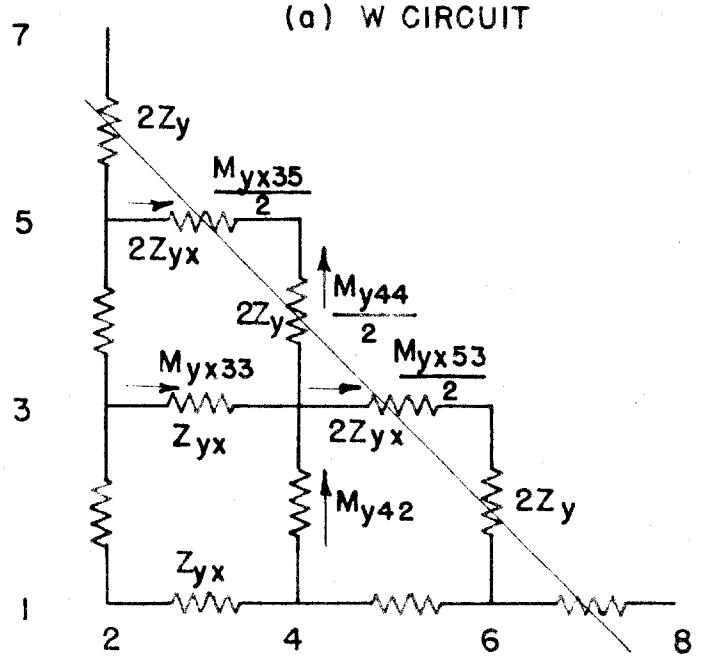

(c) θ_y CIRCUIT

FIG. 47 DYNAMIC NETWORK AND A FREE DIAGONAL EDGE. TRANSFORMER SECONDARIES IN THE SLOPE CIRCUITS ARE SUPPRESSED

Hence:

$$(i_T)_{54} + (i_T)_{63} = \tfrac{1}{2}\left(\frac{M_{x44}}{\Delta x^2} + 2\,\frac{M_{yx53}}{\Delta x \Delta y} + \frac{M_{y62}}{\Delta y^2}\right) = 0 \qquad (4.31)$$

For the case of a diagonal edge $\Delta x = \Delta y$ so that

$$M_{x44} + M_{y62} + 2M_{yx53} = 0 \qquad (4.32)$$

Sum the currents entering the node (4,4):

$$\left[\frac{M_{x24}}{\Delta x^2} - \frac{M_{x44}}{2\Delta x^2} + \frac{M_{yx33}}{\Delta x \Delta y} - \frac{M_{yx35}}{2\Delta x \Delta y}\right] - \left[\frac{M_{x44}}{2\Delta x^2} + \frac{M_{yx53}}{2\Delta x \Delta y}\right]$$
$$+\left[\frac{M_{y42}}{\Delta y^2} - \frac{M_{y44}}{2\Delta y^2} + \frac{M_{yx33}}{\Delta x \Delta y} - \frac{M_{yx53}}{2\Delta x \Delta y}\right] - \left[\frac{M_{y44}}{2\Delta x^2} + \frac{M_{yx35}}{\Delta x \Delta y}\right] = \frac{q_{44}}{2} \qquad (4.33)$$

Collect the terms and let $\Delta x = \Delta y = \lambda$:

$$M_{x24} - M_{x44} + M_{y42} - M_{y44} + 2M_{yx33} - M_{yx35} - M_{yx53} = \frac{q_{44}\lambda^2}{2} \qquad (4.34)$$

Comparing the first of eqns.(4.30) and (4.32) for the point (5,3) we see that this boundary condition is almost but not quite satisfied by the network. Subtracting the two conditions:

$$M_{x53} - M_{x44} + M_{y53} - M_{y62} \simeq 2\Delta t\left(\frac{\partial M_{tn}}{\partial t}\right)_{53} = 0 \qquad (4.35)$$

If the cell size or the tangential variation of the twisting moment is small this approximation is good.

To verify eqn.(4.34) write the finite difference equivalent of the second of eqns.(4.30) for the point (4,4):

$$\frac{M_{x64} - M_{x24}}{2\lambda} + \frac{M_{y46} - M_{y42}}{2\lambda} + \frac{M_{y55} - M_{y33}}{\lambda}$$
$$+ \frac{1}{8\lambda}\left(M_{y62} - M_{y26} - M_{x62} + M_{x26}\right) = 0 \qquad (4.36)$$

Multiply by $2/\lambda$ and subtract this equation from eqn.(4.20), the

finite difference equivalent of the differential equation for the point (4,4). The result is:

$$M_{x24} - M_{x44} + M_{y42} - M_{y44} + 2M_{yx33} - M_{yx53} - M_{yx35}$$

$$+ \frac{1}{4}(M_{y26} - M_{y62} + M_{y62} - M_{y26}) = \frac{\lambda^2 q_{44}}{2} \qquad (4.37)$$

Eqns.(4.34) and (4.37) are identical except for the term in brackets which represents the tangential derivative of twisting moment. The twisting moment creates discrepancies for both boundary conditions at a free diagonal edge. Not only are the missing terms not represented in the network derived by physical reasoning but also there is no simple way of including them.

As the reader can judge, the verification of the boundary conditions for other than a diagonal edge is very difficult.

4.7 Example I: Symmetrically Loaded Clamped Rectangular Plates

The networks that have been developed for the elastic plate have been applied to the solution of some simple and moderately difficult problems with the intention of demonstrating the feasibility of solving plate problems with an electric analog computor. The number of cells that can be represented on the Cal Tech Electric Analog Computor is at present limited by the number of high quality transformers that are available. Two such transformers are required for every cell and there are at present 25 such transformers available in the computor. The errors in our solutions due to an insufficient number of cells are very appreciable. It was known before this investigation was undertaken that this would be the case and one of the

purposes of the investigation was to determine the minimum number of cells necessary for the satisfactory solution of general plate problems. It is estimated that a four-fold increase in the number of cells is necessary for the adequate solution of problems having a complexity equal to that of the problems investigated in this report and a tenfold increase for the adequate solution of more complex problems involving irregular shapes or multiple spans.

The coordinates used in the static deflection of a clamped plate are shown in Fig. 48. The constant thickness analogy developed in section 4.2 can be used for this problem and the network that was set up is shown in Fig. 49. Since only symmetrical loads were considered it was necessary to represent only one quarter of the plate. Symmetry conditions* were imposed along the interior edges.

The impedances in the slope circuits are resistances for static loading tests. Since the transformer leakage and magnetizing impedances are reactive they will have less effect in this case than they will when the slope circuit impedances are inductances. The load currents were fed into the nodes of the deflection circuit by connecting each node to a voltage source through a resistor of large value.

The deflections for uniformly loaded clamped plates of two different shapes are given in Figs. 50 and 51. The deflections at the center of each plate were also obtained analytically** and are plotted in these figures for comparison. The computor solution for the deflection at the center of the square plate was low by 10.4% and the

---

* See eqn.(4.13) conditions (b) and (c).

** See ref. 30, page 228, Table 30.

solution for the deflection of the plate of Fig. 51 was low by 8.3%. The computor solutions for symmetrical point loads are tabulated in Table VI, for a clamped square plate.

In addition to these tests the normal mode frequencies and mode shapes were calculated. The errors in the mode shapes were small but the errors in frequency were high and tended to be larger for the higher modes. This is in contrast with the results obtained with the beam network analogy and indicates that the number of cells was insufficient.

TABLE VI

Results for Symmetrical Point Loading of a Square Clamped Plate

D = .500 a = b = 8 applied load = 2.00

Point loads were applied at the points listed and simultaneously at the image points in the other three quadrants. From this table the deflections for any distributed symmetrical loading can be obtained by superposition. See Fig. 48 for coordinates.

Load applied at		$(\frac{7}{2},\frac{7}{2})$	$(\frac{5}{2},\frac{5}{2})$	$(\frac{3}{2},\frac{3}{2})$	$(\frac{5}{2},\frac{3}{2})$	$(\frac{7}{2},\frac{3}{2})$	$(\frac{7}{2},\frac{5}{2})$	$(\frac{3}{2},\frac{5}{2})$	$(\frac{5}{2},\frac{7}{2})$	$(\frac{3}{2},\frac{7}{2})$
Deflection Measured at										
x	y									
$\frac{7}{2}$	$\frac{3}{2}$	1.34	.86	.229	.605	1.12	1.29	.351	.900	.392
$\frac{5}{2}$	$\frac{3}{2}$	.944	.77	.307	.726	.602	.850	.362	.740	.353
$\frac{3}{2}$	$\frac{3}{2}$	.402	.37	.439	.309	.231	.355	.303	.357	.231
$\frac{7}{2}$	$\frac{5}{2}$	3.22	1.78	.353	.844	1.27	2.79	.725	2.10	.890
$\frac{5}{2}$	$\frac{5}{2}$	2.22	1.67	.363	.762	.842	1.76	.754	1.76	.837
$\frac{3}{2}$	$\frac{5}{2}$	.943	.77	.307	.363	.353	.730	.720	.845	.603
$\frac{7}{2}$	$\frac{7}{2}$	4.89	2.13	.391	.900	1.27	3.04	.887	3.04	1.26
$\frac{5}{2}$	$\frac{7}{2}$	3.22	1.78	.352	.737	.894	2.11	.834	2.79	1.27
$\frac{3}{2}$	$\frac{7}{2}$	1.33	.855	.230	.353	.391	.894	.598	1.27	1.12

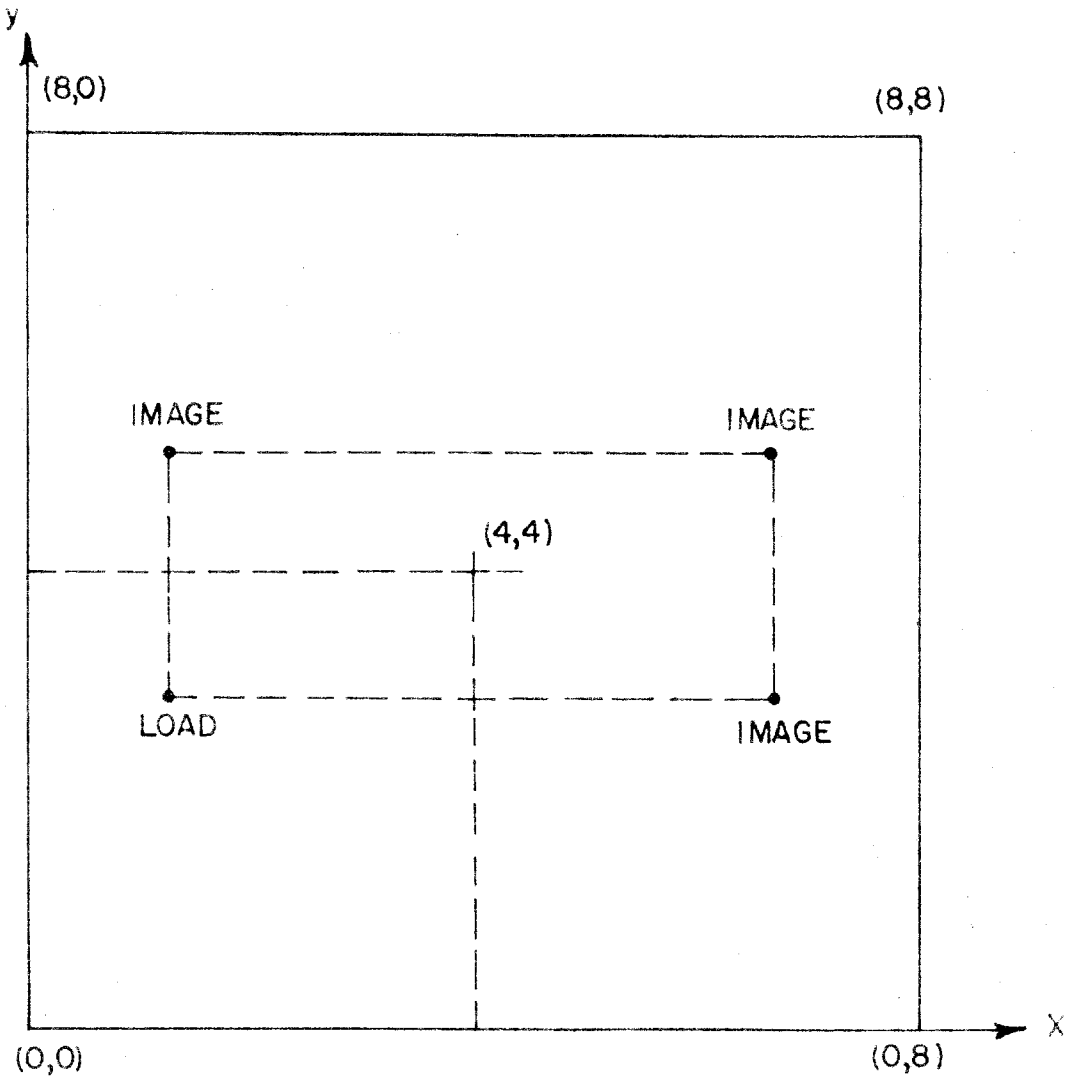

FIG.48 COORDINATES USED IN STATIC DEFLECTION OF A CLAMPED PLATE, SHOWING APPLICATION OF SYMMETRIC POINT LOADS.

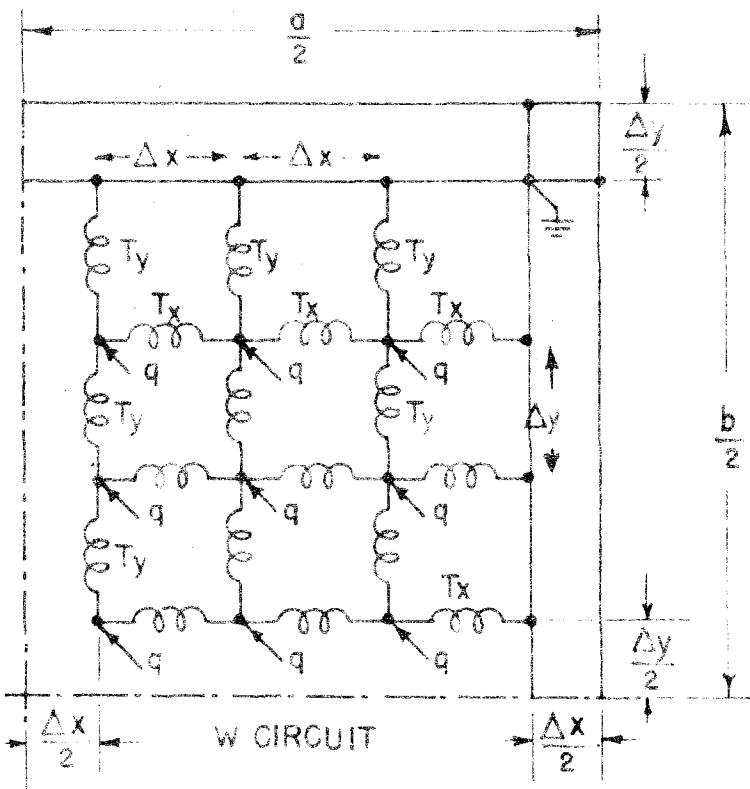

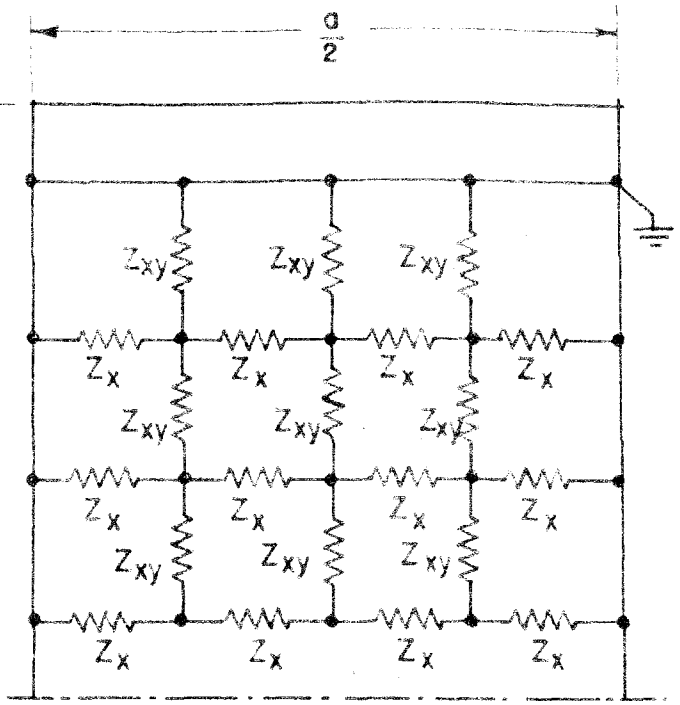

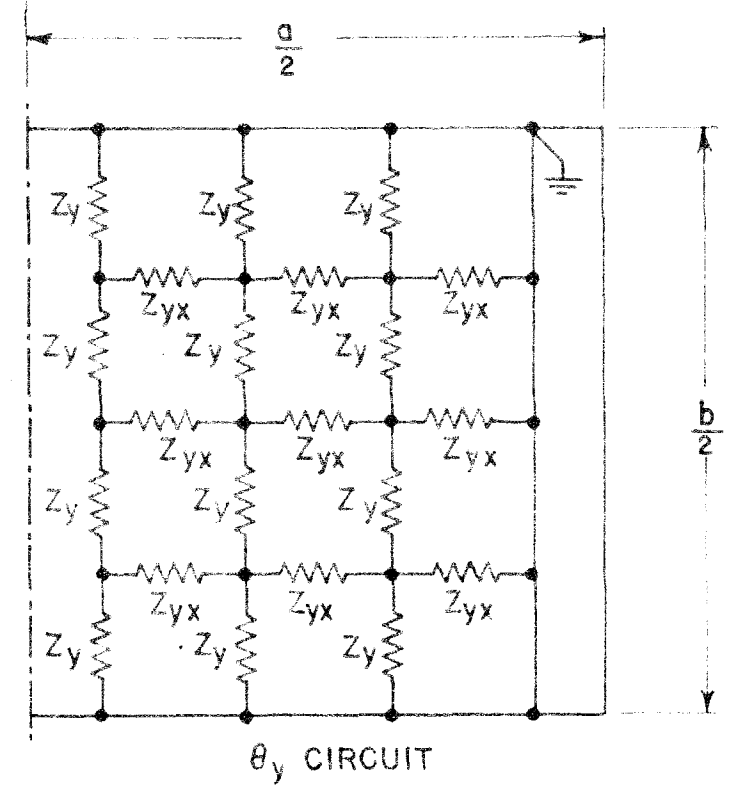

FIG. 49 NETWORK FOR A SYMMETRICALLY LOADED CLAMPED RECTANGULAR PLATE.

$$Z_x = \frac{\Delta x^2}{D} \qquad Z_{xy} = \frac{\Delta y^2}{D}$$

$$Z_y = \frac{\Delta y^2}{D} \qquad Z_{yx} = \frac{\Delta x^2}{D}$$

TRANSFORMER SECONDARIES NOT SHOWN.

FIG.50

STATIC DEFLECTION OF A UNIFORMLY LOADED CLAMPED SQUARE PLATE

D=.500 q=1.00 a=8

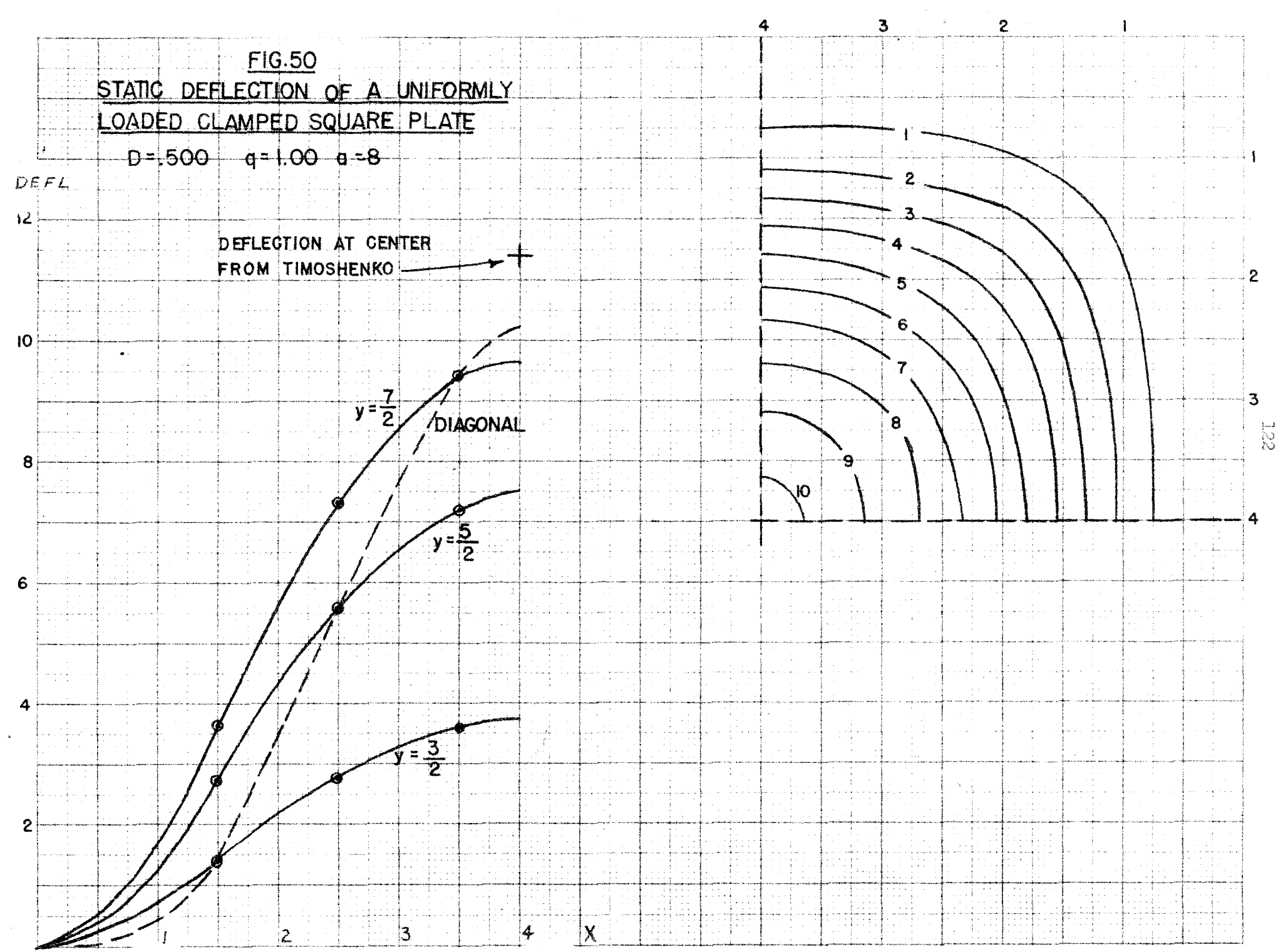

FIG. 51

STATIC DEFLECTION OF A UNIFORMLY LOADED CLAMPED RECTANGULAR PLATE

D = .500 q = 1.00 q = 8 b = 16

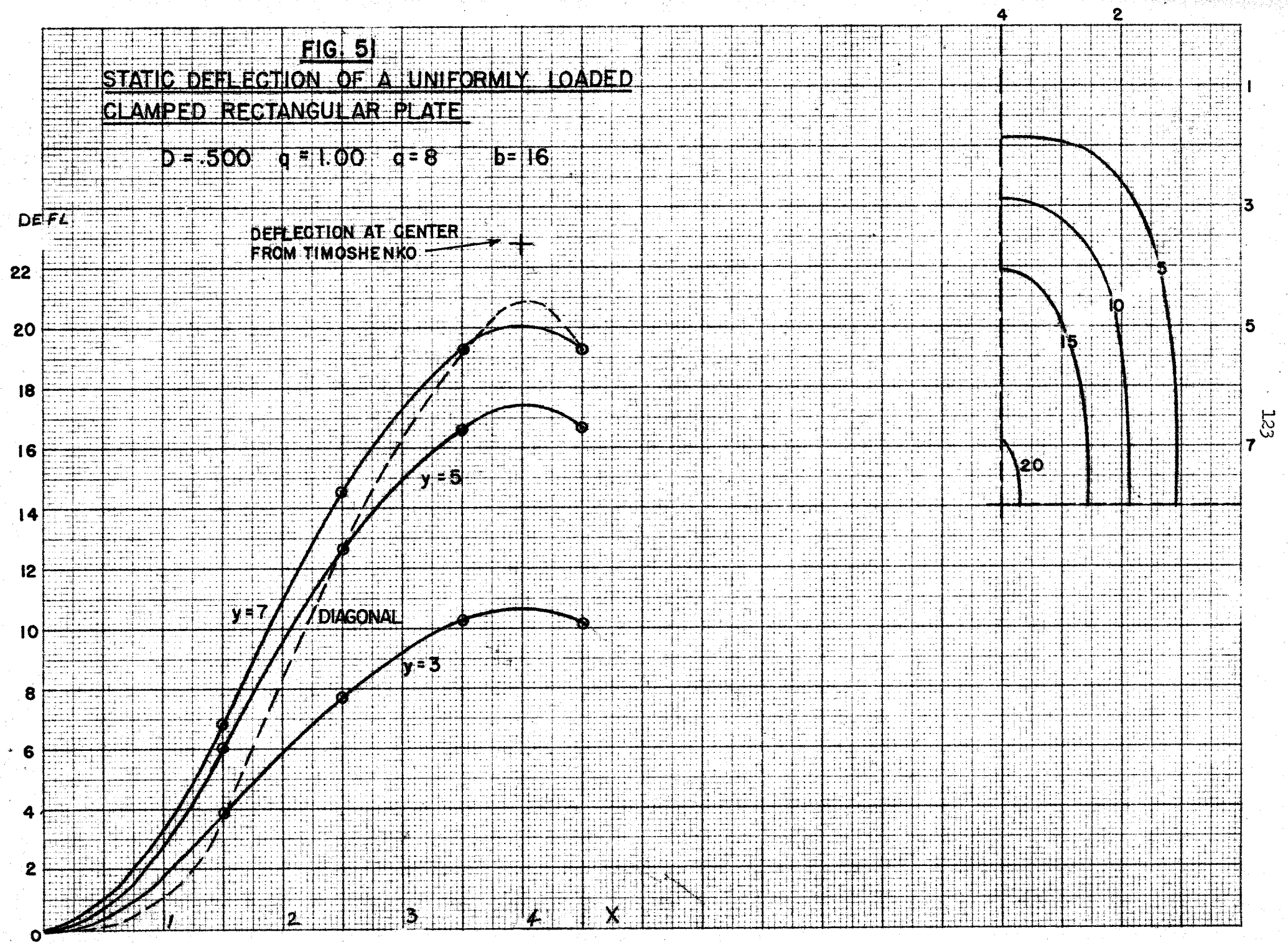

4.8 Example II The Normal Modes of a Cantilever Square Plate

For this problem it was necessary to use the variable thickness analogy derived in section 4.3. The electrical network for the plate is shown in Fig. 52 and the constants of the plate and the values of the electrical impedances are shown in Table VII. Eight of the twelve nodes of the deflection circuit lie along free edges so that the accuracy of the solution is very much dependent upon the correct representation of boundary conditions. The impedances in Table VII were derived according to the principles of section 4.5. These impedances must be inductances for the study of normal modes. Capacitances were connected to each node of the deflection circuit whose value was equal to the average mass density for the cell surrounding the node. Any convenient value for the density of the plate can be chosen since the frequency of vibration is expressed in terms of the constants of the plate. The only quantity that cannot be varied in comparing results for two different square cantilever plates is Poisson's ratio. The normal modes were excited by connecting a voltage source to one of the nodes of the deflection circuit and adjusting the frequency of the source for a minimum current input.

The results for the first five normal modes are plotted in Figs. 53 through 57. The contours of deflection were obtained from the curves plotted on the left side of each figure. These results have not previously been obtained by any method of computation.

The cantilever plate was also subjected to a uniform static load along the overhanging edge and to point loads at each of the nodes in the deflection circuit. For these tests resistances were substituted for the inductances in the slope circuits. The results of

the uniform edge loading test are given in Table VIII where bending and twisting moments are given as well as deflections. The results of the point loading test are given in Table IX. Both of these tests provide internal checks on the accuracy of the solution since symmetry with respect to the center line of the plate is required. In addition two values of twisting moment are provided, each being independently measured in one of the slope circuits.

W CIRCUIT

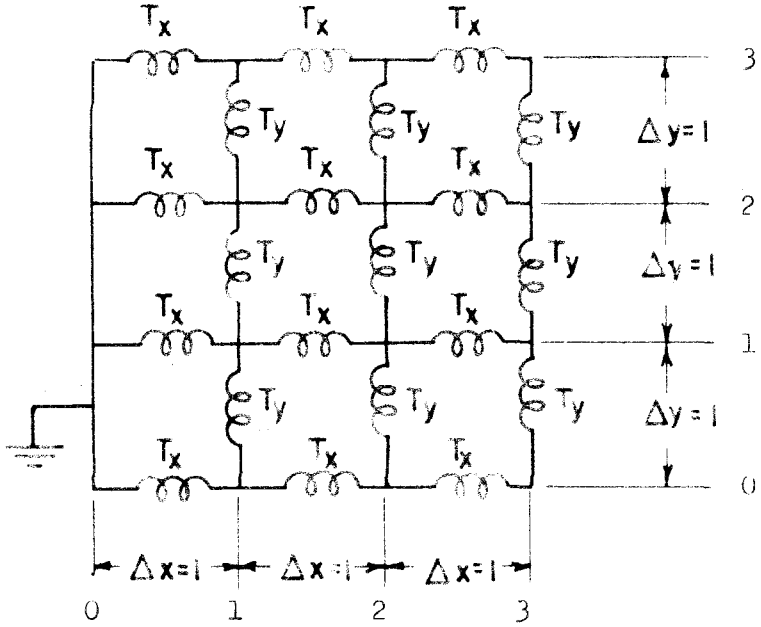

θ_x CIRCUIT

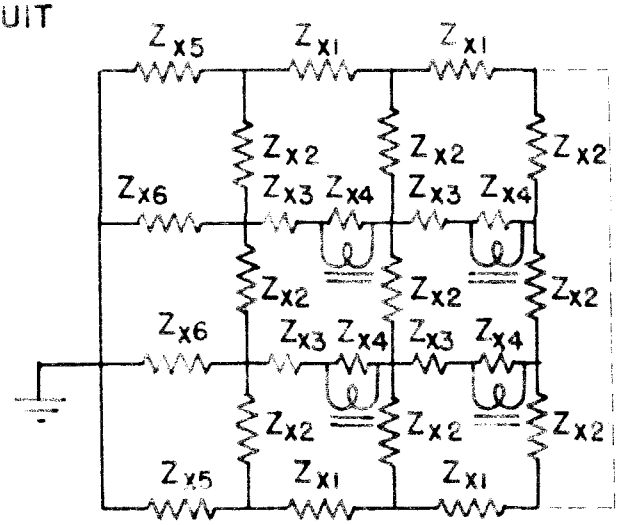

θ_y CIRCUIT

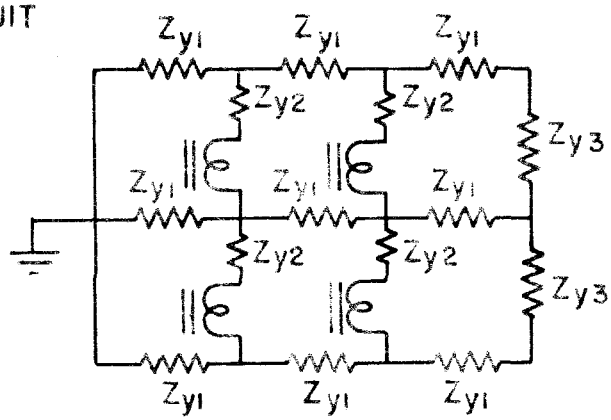

FIG. 52 NETWORK FOR THE SOLUTION OF THE RECTANGULAR CANTILEVER PLATE PROBLEM.

TABLE VII

Data for the Electrical Analogy of the Rectangular Cantilever Plate.

$\Delta x = 1$ $\Delta y = 1$ $\nu = .30$ $D = .500$

$$Z_{x1} = \frac{2\,\Delta x^2}{D\,(1-\nu^2)} = \frac{2.25}{D}$$

$$Z_{x2} = \frac{\Delta y^2}{D\,(1-\nu)} = \frac{1.43}{D}$$

$$Z_{x3} = \frac{\Delta x^2}{D\,(1-\nu^2)} - \frac{\nu\,\Delta x \Delta y}{D\,(1-\nu^2)} = \frac{.77}{D}$$

$$Z_{x4} = \frac{\nu \Delta x \Delta y}{D\,(1-\nu^2)} = \frac{.33}{D}$$

$$Z_{x5} = \frac{\Delta x^2}{D\,(1-\nu^2)} = \frac{1.125}{D}$$

$$Z_{x6} = \frac{\Delta x^2}{2D} = \frac{.50}{D}$$

$$Z_{y1} = \frac{\Delta x^2}{D\,(1-\nu)} = \frac{1.43}{D}$$

$$Z_{y2} = \frac{\Delta y^2}{D\,(1-\nu^2)} - \frac{\nu \Delta x \Delta y}{D\,(1-\nu^2)} = \frac{.77}{D}$$

$$Z_{y3} = \frac{2\Delta y^2}{D\,(1-\nu^2)} = \frac{2.25}{D}$$

TABLE VIII

Results for Uniform Edge Load

Loads - 1.000 were applied at (3,1) and (3,2)
Loads - 0.500 were applied at (3,0) and (3,3)

This represents a uniform edge load equal to 1.000 per unit length of edge.

Deflections and Slopes								
x	y	w	x	y	$\theta_x = \frac{\partial w}{\partial x}$	x	y	$\theta_y = \frac{\partial w}{\partial y}$
1	0	2.95	0.5	0	2.97	1	0.5	.460
2	0	10.3	1.5	0	7.36	2	0.5	.455
3	0	19.8	2.5	0	9.53	3	0.5	.348
1	1	3.38	0.5	1	3.30	1	1.5	.008
2	1	10.8	1.5	1	7.35	2	1.5	.009
3	1	20.25	2.5	1	9.42	3	1.5	.008
1	2	3.38	0.5	2	3.31	1	2.5	- .454
2	2	10.8	1.5	2	7.35	2	2.5	- .462
3	2	20.25	2.5	2	9.43	3	2.5	- .353
1	3	2.95	0.5	3	2.96			
2	3	10.3	1.5	3	7.36			
3	3	19.9	2.5	3	9.52			

Moments

Two values of the twisting moments are given. They were measured independently in the network. The sign of the moments was not measured.

Bending Moments								Twisting Moments			
x	y	M_x	M_y	x	y	M_x	M_y	x	y	M_{yx} meas. in θ_x circuit	M_{yx} meas. in θ_y circuit
.25	0	2.614	0	.25	2	3.35	0	.5	.5	.119	.159
1.00	0	1.964	0	1.00	2	2.05	.43	1.5	.5	.022	.009
2.00	0	.986	0	2.00	2	1.016	.104	2.5	.5	.045	.040
.25	1	3.24	0	.25	3	2.614	0	.5	1.5	.004	.004
1.00	1	2.07	.420	1.00	3	1.960	0	1.5	1.5	.002	.001
2.00	1	1.014	.102	2.00	3	.992	0	2.5	1.5	.001	.003
3.00	0	0	0	3.00	2	0	.154	.5	2.5	.122	.154
3.00	1	0	.154	3.00	3	0	0	1.5	2.5	.023	.006
								2.5	2.5	.050	.038

TABLE IX

Results for Point Loading of a Square Cantilever Plate.

Applied Load = 2.000

Load applied at	(1,0)	(2,0)	(3,0)	(1,1)	(2,1)	(3,1)	(3,2)
Deflection measured at							
(1,0)	1.83	2.63	3.28	.880	1.65	2.30	1.48
(2,0)	2.62	7.10	10.1	1.74	4.85	7.75	5.65
(3,0)	3.25	10.00	18.8	2.54	8.00	14.40	11.0
(1,1)	.88	1.73	2.58	.975	1.67	2.41	2.11
(2,1)	1.63	4.81	7.95	1.65	4.78	7.70	6.80
(3,1)	2.29	7.70	14.4	2.40	7.65	14.40	12.60
(1,2)	.380	1.03	1.77	.625	1.35	2.11	2.41
(2,2)	.940	3.21	5.90	1.34	4.00	6.80	7.65
(3,2)	1.48	5.60	11.0	2.10	6.80	12.70	14.40
(1,3)	.064	.391	.855	.38	.940	1.47	2.30
(2,3)	.392	1.91	4.05	1.03	3.24	5.65	7.70
(3,3)	.845	4.00	8.55	1.75	5.90	11.0	14.40

FIG. 53

LOWEST MODE

OF A SQUARE CANTILEVER PLATE

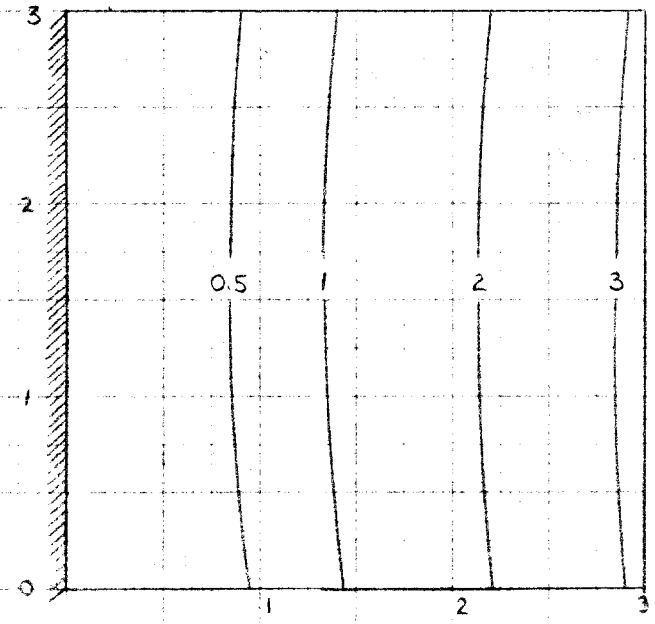

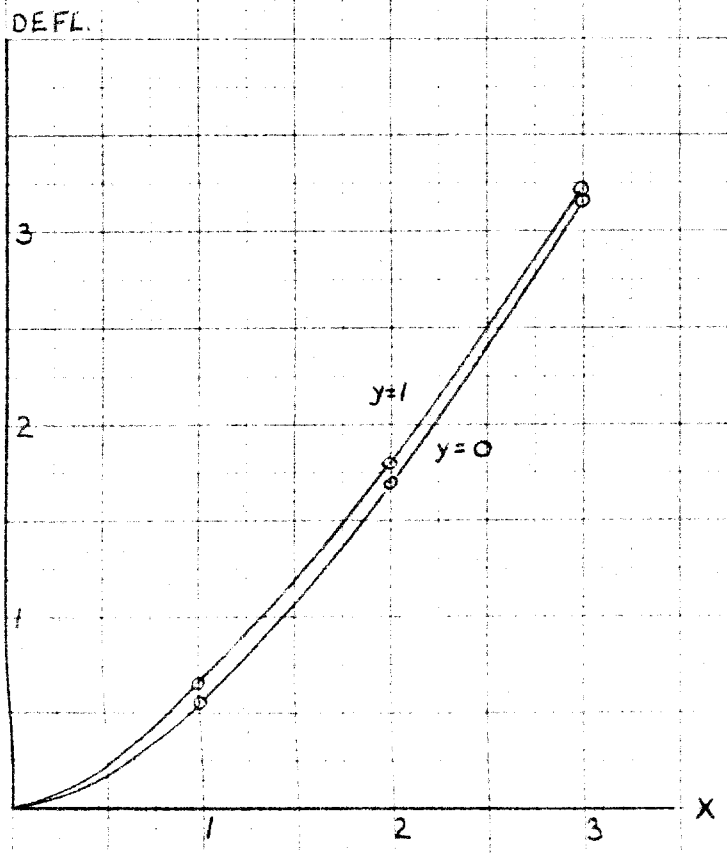

$$\text{FREQ} = 1.77 \frac{1}{a^2}\sqrt{\frac{D}{m}}$$

FIG 54

2 nd MODE

OF A SQUARE CANTILEVER PLATE

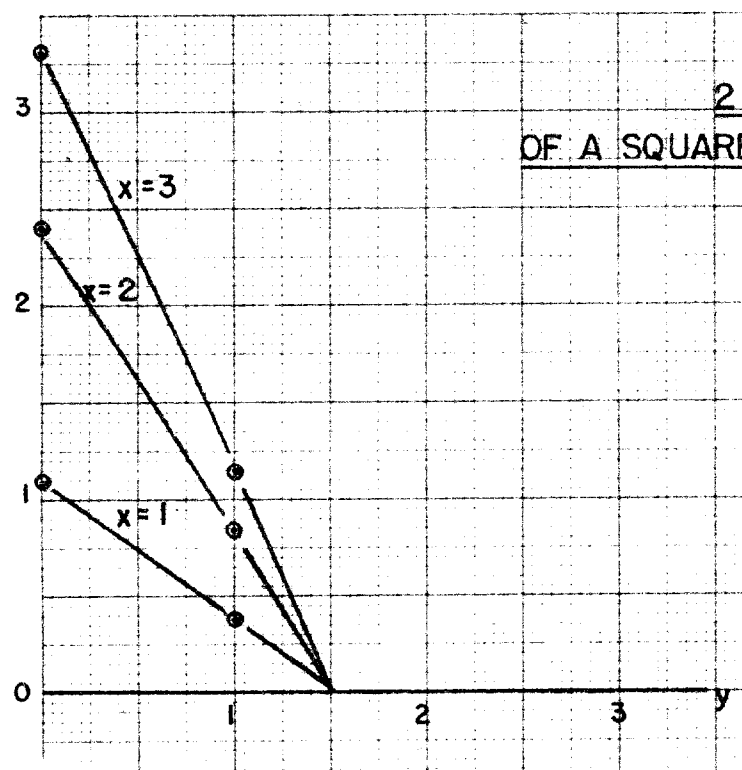

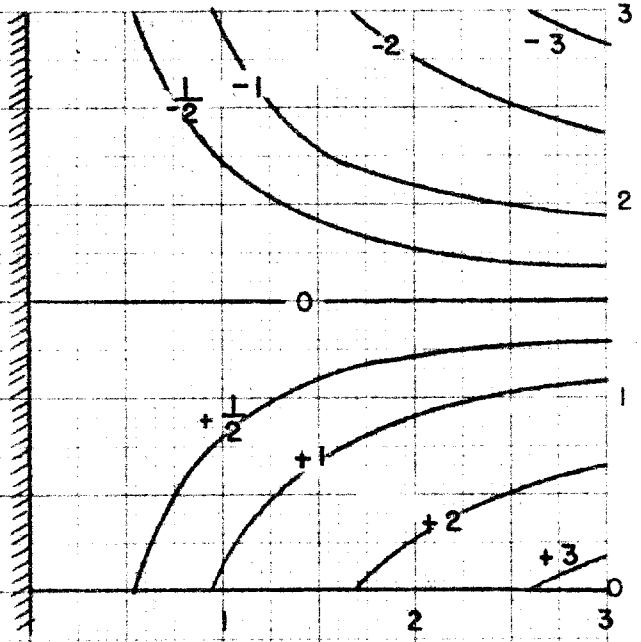

FREQ. = $3.98 \frac{1}{a^2}\sqrt{\frac{D}{m}}$

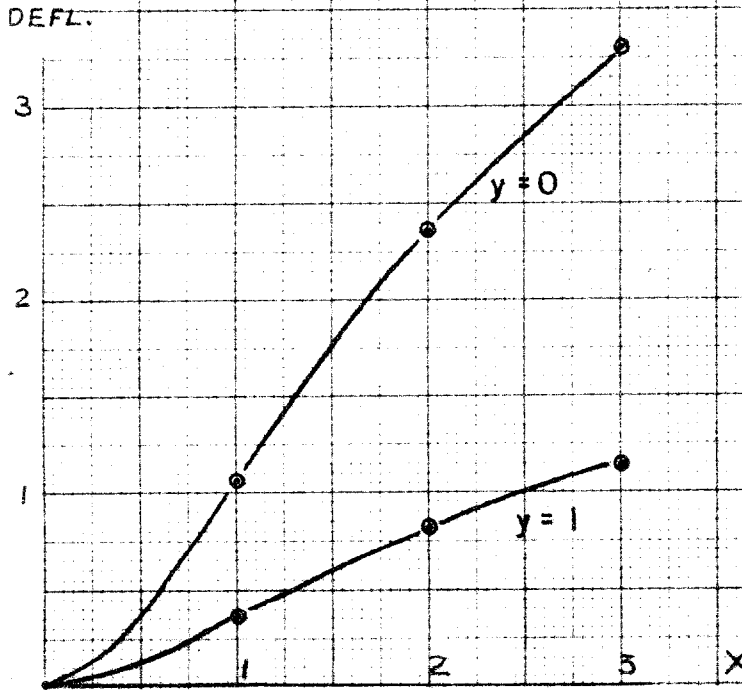

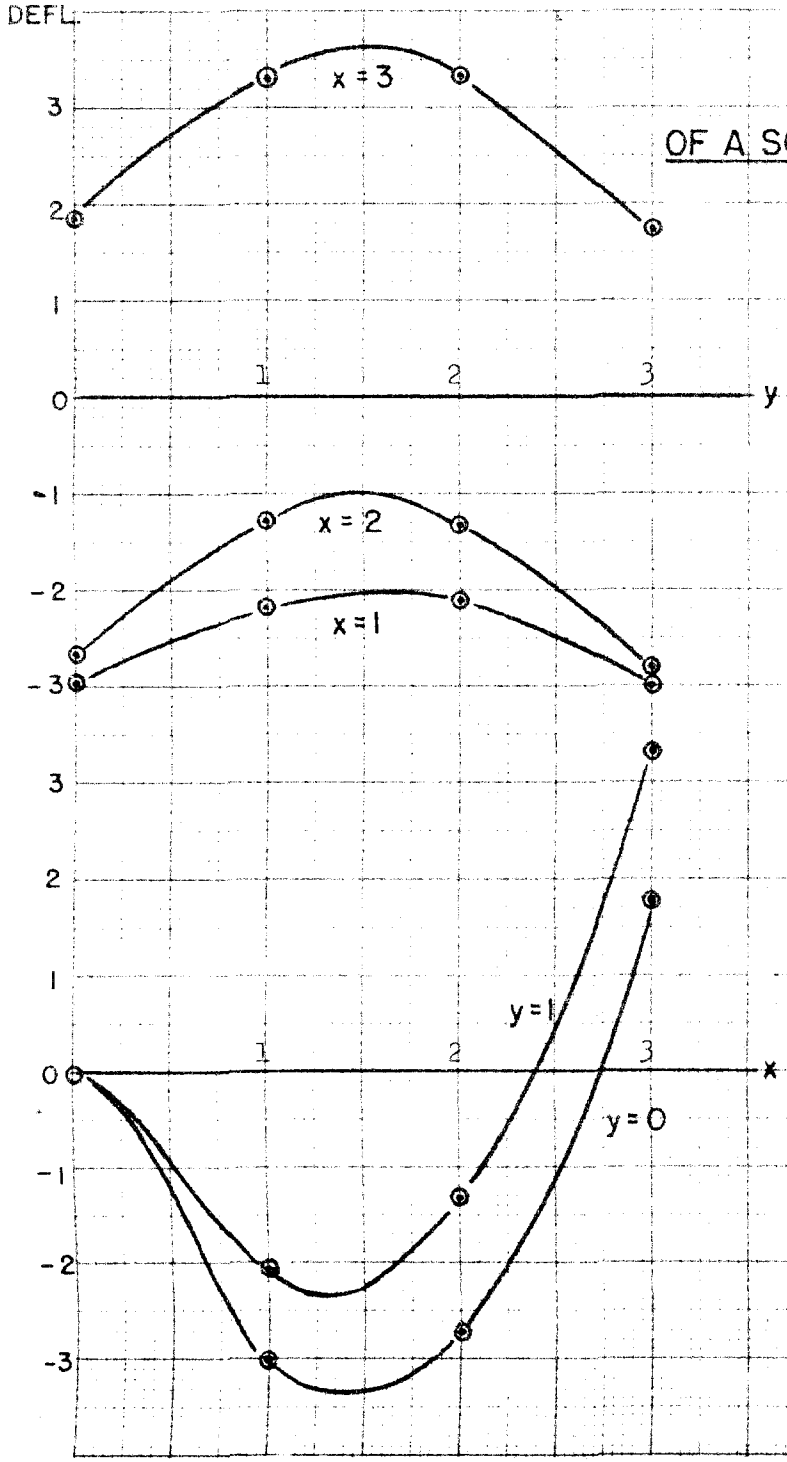

FIG. 55
3rd MODE
OF A SQUARE CANTILEVER PLATE

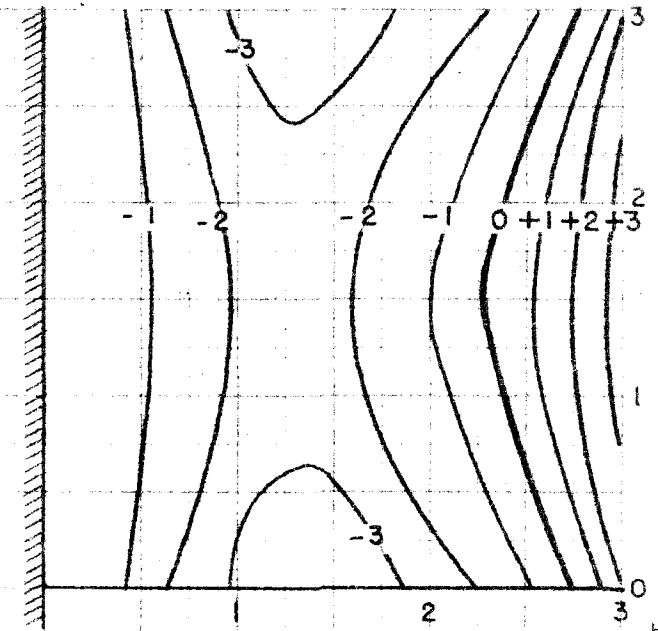

FREQ. = $7.81 \frac{1}{a^2} \sqrt{\frac{D}{m}}$

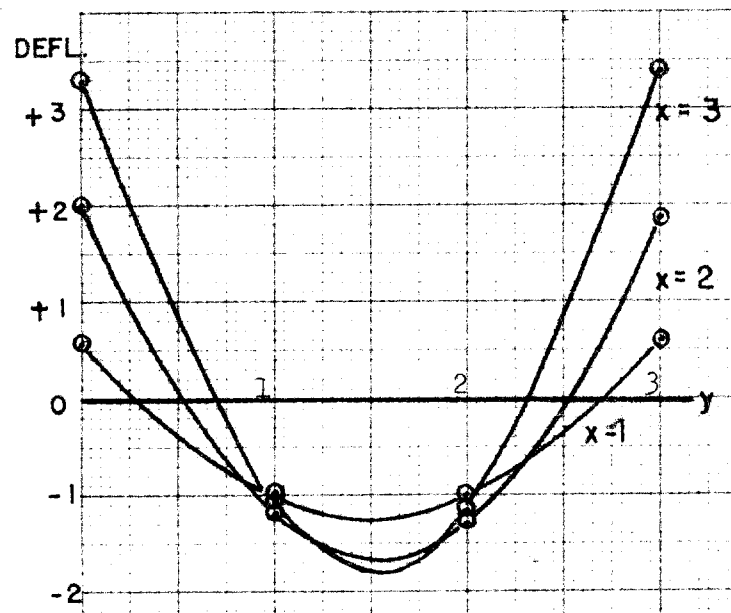

FIG. 56
4th MODE
OF A SQUARE CANTILEVER PLATE

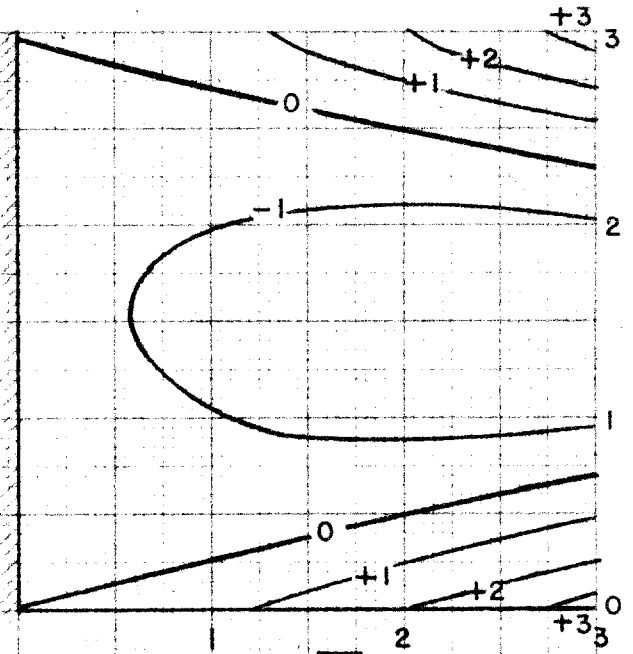

$$\text{FREQ.} = 10.10 \frac{1}{a^2} \sqrt{\frac{D}{m}}$$

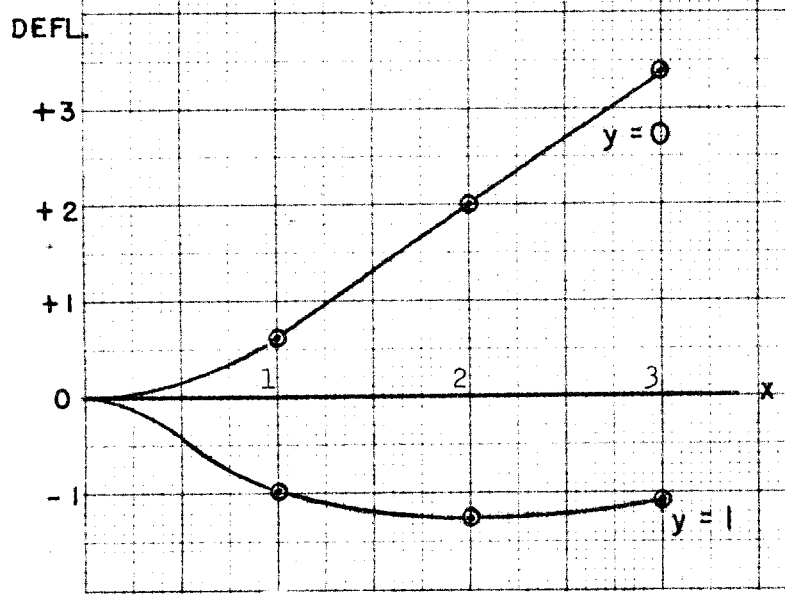

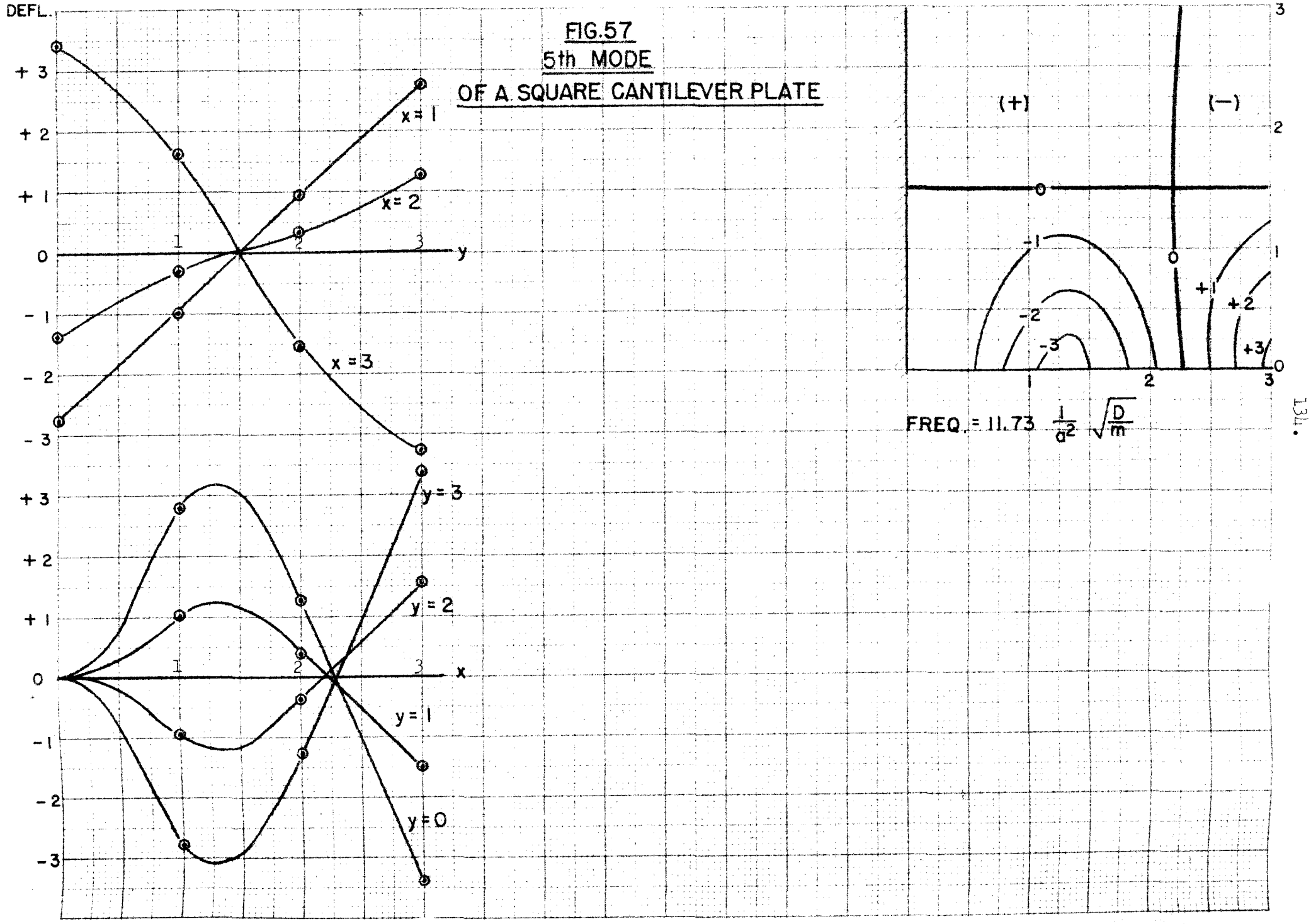

FIG.57
5th MODE
OF A SQUARE CANTILEVER PLATE

FREQ. = 11.73 $\frac{1}{a^2}\sqrt{\frac{D}{m}}$

V NOTES ON THE DESIGN OF A NETWORK ANALYZER FOR THE SOLUTION OF PARTIAL DIFFERENTIAL EQUATIONS

The Cal Tech Electric Analog Computor was conceived as a general purpose computor within the limitation that an analog computor is only useful for the solution of problems for which an electrical analogy exists. It was recognized that there are many important problems in which there are a large number of degrees of freedom and so the computor was designed to eventually include one hundred each of resistors, inductors and capacitors as well as a large number of transformers. At present the computor includes eighty of each of the passive impedance elements and twenty-five transformers. For the solution of non-linear problems and the analysis of control systems, a large number of special electronic devices including amplifiers, multipliers and function generators were also provided for.[32] All elements were designed to operate accurately in the frequency range from ten cycles to one thousand cycles per second.

The requirements of a computor that could be described as a general partial differential equation analyzer are not met by the Cal Tech Electric Analog Computor. The one important fact is that such an analyzer requires an enormous number of passive impedance elements. This has been borne out by the examples that have been included in this thesis. With the eighty inductors available a total of forty nodes can be represented in the solution of a plane potential problem, while with the few transformers available a total of twelve nodes can be represented in the solution of an elastic plate problem. In spite of these limitations a variety of problems can be solved with an accuracy that is surprising to a person unacquainted with the finite differ-

ence technique.

An estimate can be formed as to the number of elements that would be necessary for the solution of different kinds of problems. Problems with one space coordinate can be adequately solved with the number of elements now available in the computor which is, moreover, admirably suited to the solution of non-linear one dimensional problems because of its large stock of non-linear devices. The radiation problems described in section 3.7 probably require more elements than any other type of plane potential problem. It was shown that twelve cells per radial wave length is a minimum requirement and that the representation of two wave lengths will usually be adequate. For radiators that are unsymmetrical with respect to their equatorial plane it would be desirable to have 25 cells in the θ direction. Hence a total of 625 cells or 1250 inductors would be adequate for the solution of this type of problem. In section 4.7 the opinion was formed that most elastic plate problems can be solved with 120 cells. For such a network 240 high quality transformers and 480 inductors would be required. As a tentative estimate one is forced to the conclusion that a network analyzer for the solution of partial differential equations would require approximately 1000 inductors, 1000 resistors, 500 capacitors and 250 high quality transformers.

The methods of construction employed in the present Cal Tech computor could not be used in the design of a partial differential equation computor. In the present computor the quality of the elements was not sacrificed to their cost and the limitation of physically available space was not a serious problem. The passive elements are located in racks, — thirty elements to a 4' x 6' rack — and are

interconnected by means of plug-boards. The inductors cost approximately one hundred dollars each. A partial differential equation computor constructed along these lines would be unreasonably expensive and physically immense.

A precedent exists for the type of computor that has been envisioned. This is the Network Analyzer constructed at Stanford University for the solution of Electromagnetic Field Problems.[22] Although this network analyzer is a special purpose computor the economics of its construction are very impressive. The rectangular network consisting of over 1000 coils with fixed values of inductance was constructed for $2,000. The cylindrical network with 1300 coils in twelve standard sizes from 200 to 2400 uh was constructed for $6,500. These economies were achieved by using air-core coils consisting of only a few turns of wire, by using standard 350 uufd trimmer condensers variable from 50 to 500 uufd and by operating the network in a range of frequencies from 20KC to 300 KC. The network so constructed is somewhat rigid in its possible applications and the exceptionally high frequency introduces problems that it would be desirable to avoid. However, the economies achieved recommend this type of construction to a very serious consideration.

It is certain that some modification of the method of interconnecting the Stanford computor must be adopted in the design of a partial differential equation computor. In the Stanford Computor the electrical elements are physically located in the same way that they are drawn in the circuit diagrams. The coils are wound on forms which fit into clips located at adjacent nodes. The result is an unusually compact design.

The type of partial differential equation computor envisioned here would be considerably more flexible than that constructed at Stanford. Besides solving plane potential problems it should be able to solve the two dimensional problems of elasticity and elastic plate problems. It should also be applicable to the solution of a certain number of non-linear problems including compressible flow problems and non-linear heat flow problems. The inclusion of elasticity problems requires the use of a large number of essentially perfect transformers which cannot be constructed to operate at high frequencies. The maximum frequency for the efficient operation of these transformers will determine the operating frequency of the computor.

The measurement technique on a very high frequency computor must necessarily be crude in order to eliminate parasitic capacitances. Such a limitation is unfavorable for the rapid solution of problems. The metering system in the present Cal Tech Computor includes push-button relays by which any element in the computor can instantly be metered by a single operator. This is a very desirable feature but may be impractical in a computor with a very large number of elements.

The elements in the proposed computor should be variable but should be small in size and relatively inexpensive. Instead of building up elements out of fixed impedances that are set by tap switches, as is done at present, it will probably be expedient to use continuously variable elements that are calibrated every time that they are adjusted. A system for the routine calibration of elements could be devised easily. This provision would reduce the bulk of the elements and also reduce their total cost. It is easy to see how continuously variable resistors and capacitors can be constructed but the

design of continuously variable inductors is a more difficult problem. The design of high quality transformers and coils that are both small in size and inexpensive are the major problems that must be solved in the design of a computor for the solution of partial differential equations. The systems of interconnection, metering and current input are important secondary problems.

The operating frequency range that represents the best compromise is probably included between 1000 and 20,000 cps.

REFERENCES

1. Gabriel Kron, "Equivalent Circuits of Compressible and Incompressible Fluid Flow Fields", J. Aer. Sc., (April, 1945), Vol. 12 p. 221-231

2. G. D. McCann and C. H. Wilts, "Application of Electric Analog Computors to Heat Transfer and Fluid Flow Problems", J. Applied Mech., (To be published in 1949)

3. G. Kron, "Electrical Circuit Models of the Schroedinger Equations", Phys. Rev., (Jan., 1945), Vol. 67, p. 39-43

4. G. K. Carter and G. Kron, "AC Network Analyzer Study of the Schroedinger Equation", Phys. Rev., (Jan., 1945), Vol. 67 p. 44-49

5. G. Kron, "Equivalent Circuits of the Elastic Field", J. Applied Mech., (Sept., 1944), Vol. 66, p. A-149 - A-161

6. R. V. Southwell, "Relaxation Methods in Theoretical Physics", (1946), Oxford, the Clarendon Press

7. W. C. Johnson and R. E. Alley Jr., "An Electrical Analogy Method for the Solution of Differential Equations", (June, 1948), Dept. of E. E., Princeton University, ONR Tech. Report No. 3

8. W. Smythe, "Static and Dynamic Electricity", (1939), McGraw-Hill p. 366

9. G. D. McCann and R. H. MacNeal, "Beam Vibration Analysis with the Electric Analog Computor", J. Applied Mech., (To be published in 1949)

10. G. Kron, "Tensorial Analysis and Equivalent Circuits of Elastic Structures", J. Franklin Inst., (Dec., 1944), Vol. 238, No. 6

11. S. T. Jennings, "The Solution of the Aircraft Wing Flutter Problem by Means of Electric Circuit Analysis", (1947), Ph. D. Thesis, Ohio State Univ.

12. Lord Rayleigh, "Theory of Sound", (1945), Dover reprint

13. R. D. Mindlin, F. W. Stubner, and H. L. Cooper,"Response of Damped Elastic Systems to Transient Disturbances", Proc. Soc. for Exp. Stress Analysis, (No date), Vol. 5, No. 2

14. G. D. McCann and E. L. Harder, "A Large-scale General Purpose Electric Analog Computor", Trans. AIEE, (April, 1948), Vol. 67, p.

15. H. W. Emmons, "The Numerical Solution of Partial Differential Equations", Quart. App. Math., (1944), Vol. 2, p. 173-195

16. G. Kron, "Numerical Solution of Ordinary and Partial Differential Equations by Means of Equivalent Circuits", J. App. Phys., (March, 1945), Vol. 16, p. 172-186

17. A. D. Michal, "Matrix and Tensor Calculus", (1947), Wiley

18. J. A. Stratton, "Electromagnetic Theory", (1941), McGraw-Hill

19. G. Kron, "Equivalent Circuits of the Field Equations of Maxwell", IRE, (May, 1944), Vol. 32, p. 289-299

20. Whinnery, Concordia, Ridgway and Kron, "Network Analyzer Studies of Electromagnetic Cavity Resonators", IRE, (June, 1944), Vol. 32, p. 360-367

21. J. R. Whinnery and S. Ramo, "A New Approach to the Solution of High Frequency Field Problems", IRE, (May, 1944), Vol. 32, p. 284-288

22. Spangenberg, Walters and Schott, "Electrical Network Analyzers for the Solution of Electromagnetic Field Problems", (1948), Tech. Report, Stanford University

23. S. Ramo and J. R. Whinnery, "Fields and Waves in Modern Radio", (1944), Wiley

24. I. S. Sokolnikoff and R. D. Spect, "Mathematical Theory of Elasticity", (1946), McGraw-Hill

25. G. K. Carter, "Numerical and Network Analyzer Solution of the Equivalent Circuits for the Elastic Field", J. App. Mech., (Sept., 1944), Vol. 66, p A-162 - A-167

26. R. H. MacNeal, "Electrical Analogies for Elastic Plates", (Feb., 1949), CIT Anal. Lab. Tech. Report

27. R. H. MacNeal, "Electric Analog Computor Solutions of Elastic Plate Problems", (Feb., 1949), CIT Anal. Lab. Tech. Report

28. M. V. Barton, "Finite Difference Equations for the Analysis of Thin Rectangular Plates with Combinations of Fixed and Free Edges", (Aug., 1948), Univ. of Texas, Def. Res. Lab. CF. 1005 DRL 175

29. V. P. Jensen, "Analyses of Skew Slabs", Univ. of Illinois Bulletin, (Sept., 1941), Vol. XXXIX No. 3

30. S. Timoshenko, "Theory of Plates and Shells", (1940), McGraw-Hill

31. Y. C. Fung, "Elastostatic and Aeroelastic Problems Relating to Thin Wings of High-speed Airplanes", (1948), Ph. D. Thesis, CIT

32. G. D. McCann, C. H. Wilts and B. Locanthi, "Electronic Techniques Applied to Analog Methods of Computation", IRE, (To be published in 1949)